

CELLULOSE SUPPORTED  
POLY(AMIDOXIME) Cu/Pd NANOPARTICLES  
FOR AZA-MICHAEL AND SUZUKI-MIYAURA  
REACTIONS

TAHNIM SULTANA

UMP

Master of Science

UNIVERSITI MALAYSIA PAHANG

## UNIVERSITI MALAYSIA PAHANG

### DECLARATION OF THESIS AND COPYRIGHT

Author's Full Name : TAHNIM SULTANA

Date of Birth : 02/01/1988

Title : Cellulose supported Poly(amidoxime) Cu/Pd nanoparticles for Suzuki-Miyaura and Aza-Michael reactions

Academic Session : 2015-2017

I declare that this thesis is classified as:

- CONFIDENTIAL (Contains confidential information under the Official Secret Act 1997)\*
- RESTRICTED (Contains restricted information as specified by the organization where research was done)\*
- OPEN ACCESS I agree that my thesis to be published as online open access (Full Text)

I acknowledge that Universiti Malaysia Pahang reserves the following rights:

1. The Thesis is the Property of Universiti Malaysia Pahang
2. The Library of Universiti Malaysia Pahang has the right to make copies of the thesis for the purpose of research only.
3. The Library has the right to make copies of the thesis for academic exchange.

Certified by:



(Student's Signature)

MSK 15002  
New IC/Passport Number  
Date:

(Supervisor's Signature)

Dr Shaheen Sarkar  
Name of Supervisor  
Date:

## SUPERVISOR'S DECLARATION

We hereby declare that we have checked this thesis and in our opinion, this thesis is adequate in terms of scope and quality for the award of the degree of Master of Science in Advanced Materials.

---

(Supervisor's Signature)

Full Name : DR SHAHEEN M. SARKAR

Position : ASSISTANT PROFESSOR

Date :

---

(Co-supervisor's Signature)

Full Name : DR. MOHD HASBI BIN AB RAHIM

Position : ASSOCIATE PROFESSOR

Date :

### STUDENT'S DECLARATION

I hereby declare that the work in this thesis is based on my original work except for quotations and citations which have been duly acknowledged. I also declare that it has not been previously or concurrently submitted for any other degree at Universiti Malaysia Pahang or any other institutions.



---

(Student's Signature)

Full Name : TAHNIM SULTANA

ID Number : MSK 15002

Date :



UMP

CELLULOSE SUPPORTED POLY(AMIDOXIME) Cu/Pd  
NANOPARTICLES FOR AZA-MICHAEL AND SUZUKI-MIYAUURA  
REACTIONS

The logo of the University of Malaysia Pahang (UMP) is a shield-shaped emblem. It features a central white vertical band with a yellow diamond at the top. The shield is divided into four quadrants by this central band and a horizontal line. The top-left and bottom-right quadrants are light blue, while the top-right and bottom-left quadrants are a darker blue. A stylized, glowing ring in shades of blue and green encircles the top portion of the shield.

TAHNIM SULTANA

Thesis submitted in fulfillment of the requirements  
for the award of the degree of  
Master of Science

UMP

Faculty of Sciences & Technology  
UNIVERSITI MALAYSIA PAHANG

May 2018

## ACKNOWLEDGEMENT

Sokor Alhamdulillah. Finally, I make myself able to submit this dissertation. It is fulfilling only because of the guideline and support of several individuals. Their cordial contribution and assistance help me to complete this journey of research.

First and foremost, I would like to express my deepest gratitude to my respected supervisor Assistant Professor Dr. Shaheen Sarkar, for his excellent guideline, knowledge, support, and patience which provide me the suitable way to conduct my research. I would also like to devote my appreciation to Professor Lutfor Rahman, my co-supervisor for all his help and wise advice during the research. My sincere thanks to Dr. Mohd Hasbi Ab Rahim, my co-supervisor for all his guidelines and supports.

I would like to convey my gratitude to the Dean of Faculty of Industrial Sciences and Technology (FIST) Professor Jamil Ismail.

My highly appreciation to all the technical staff of central lab mainly scientific officer Nor Hafizah Bt Zainal Abidin for providing all NMR supports and also the technical staff of FIST.

I would also provide special thanks to Haniza Binti Abdullah and Anida Binti Abdullah, office staff of FIST for providing all the information timely and support me for the all undesirable moments.

Truly any research cannot be conducted without sufficient financial support. So, I would like to thank Malaysian Ministry of Education under the fundamental Research Grant Scheme (RDU 140343) for funding the research and support me financially to conduct research with total concentration.

My sincere thanks to my group mates Tapan Kumar Biswas, Siti Hazar Mohamad Ros, Amina Yasin, Bablu Hira Mandal, Youvraj Aralapura and Shahrul Islam.

Most importantly I would like to thank to all the Bangladeshi families of UMP, Nadia Refat, Taslima Sarkar, Ayesha Noor Urmee, my friends Alaa, Ain, Hasneeza Liza, Puranjan Mishra and Bincylv Vijayan and a special thanks to Tarnima Warda Andalib and Zainab Yousif, for all the intense support and care.

Last but not least I would like to apologize for all of my intentional and unintentional inconveniences during this period but truly I appreciate all who contributed towards the success of my study.

Tahnim Sultana

## ABSTRAK

Kajian ini berkaitan dengan penggunaan mangkin logam heterogen berasaskan selulosa bagi tindak balas Aza-Michael dan Suzuki-Miyaura. Kajian sebelum ini banyak berkisar kepada penggunaan mangkin homogen kerana aktiviti dan keterpilihan pemangkinan yang tinggi. Namun demikian, pemisahan produk dengan mangkin selepas tindak balas serta potensi penggunaan semula mangkin adalah sukar dan terhad. Maka, mangkin heterogen seperti silika, logam oksida, polimer organik, grafin dan bahan komposit berasaskan bio telah digunakan untuk mengatasi masalah ini. Dalam masa yang sama, aspek ekonomi serta persekitaran yang mampan dalam tindakbalas bermangkin gandingan-silang seperti penggunaan bahan kurang berbahaya serta mampan masih belum memenuhi kriteria yang dikehendaki. Oleh itu, penggunaan bahan komposit berasaskan bio adalah salah satu kaedah utama bagi menyokong inisiatif ini seterusnya menyelesaikan isu berkenaan kelemahan sistem mangkin homogen tanpa mengurangkan keberkesanan mangkin. Oleh itu, bahan selulosa yang boleh diperolehi dengan mudah dalam kuantiti yang banyak dan murah serta mempunyai kestabilan mekanikal dan kimia yang tinggi, boleh terurai, tidak bertoksik dan mudah dimanipulasi dengan kaedah kimia mempunyai potensi yang tinggi sebagai bahan sokongan mangkin heterogen. Dalam kajian ini, selulosa berasaskan sisa teras jagung yang ditambah logam Pd atau Cu digunakan untuk tindak balas gandingan-silang. Selulosa diekstrak daripada sisa jagung-cob dan diubahsuai menjasi poli(acrylonitrile) dan kemudian poli(amidoxime) chelating ligan, diikuti oleh rawatan dengan  $\text{CuSO}_4 \cdot 5\text{H}_2\text{O}$  dan  $(\text{NH}_4)_2\text{PdCl}_4$  untuk menjadi poli berwarna biru (amidoxime) Cu(II) dan poli berwarna coklat(amidoxime) Pd(II) kompleks. Kedua-dua rawatan dengan hidrazin hidrat memberikan nanopartikel tembaga (CuN@PA) dan nanopartikel palladium (PdNs@PA). Pencirian dan perubahan struktur morfologi dikaji dengan menggunakan kaedah spektroskopi seperti FTIR, FESEM-EDX, TEM, XPS, XRD, UV-Vis, TGA dan ICP-AES. CuN@PA ( $6.8 \pm 2$  nm) yang berwarna coklat gelap membantu tindak balas Aza-Michael amina alifatik dengan olefin secara efisien dan selektif bagi membolehkan produk alkyl sepadan sehingga 96% takat suhu bilik. Manakala, PdNs@PA ( $2.8 \pm 6$  nm) menunjukkan prestasi pemangkinan yang tinggi bagi tindakbalas gandingan-silang Suzuki- Miyaura aryl halida dengan asid organoboronik untuk memberikan produk biaryl yang sama sehingga 95% dengan jumlah perolehan yang tinggi (TON) 16250 dan kekerapan perolehan (TOF)  $5416\text{h}^{-1}$ . Dalam kedua-dua tindak balas ini, mangkin heterogen logam nanopartikel menggunakan selulosa sabagai bahan sokongan boleh diguna beberapa kali tindakbalas tanpa menghilangkanan keupayaan pemangkinan. Hasil kajian ini membuktikan bahawa bahan selulosa berasaskan sisa teras jagung boleh digunakan sebagai bahan sokongan mangkin yang sesuai bagi tindakbalas Suzuki- Miyaura dan Aza-Michael seterusnya menyokong penggunaan teknologi hijau dalam kelestarian pembangunan teknologi terkini.

## ABSTRACT

This research is mainly focused on the utility of cellulose supported heterogeneous metal catalyst for Aza-Michael and Suzuki-Miyaura reactions. Such reactions are generally conducted by homogeneous catalyst, but the untidy reactions, difficulties in separation of product from reaction mixture, removal and reuse of homogeneous catalyst lies as the limitations. Thus, heterogeneous catalysts with different types supports, such as silica gel, metal oxide, organic polymers, graphene and various hybrid inorganic materials have been employed to overcome these issues. Nowadays researchers have developed many economic and environmental sustainable catalytic protocols to develop the process of cross-coupling reactions in green perspective but till now it is difficult to meet the criteria of being safely reusable, non-toxic, chemically sustainable, and organic synthesis catalyst. The development of bio-based materials and composites could be considered as a promising solution of these demerits both in terms of environmental and performances aspects. From this point of view, natural biopolymers (cellulose) could be considered as more acceptable solid support material because it has some promising qualities as widely abundance in nature, bio-degradability, high chemical and mechanical stability, easily chemically modified, bio-renewability, non-toxicity, cheap and environmental friendly. Therefore, cellulose can act as a suitable candidate as solid support for heterogeneous catalytic system. On focusing to this target firstly, cellulose was extracted from waste corn-cob and chemically modified by poly(acrylonitrile). Then resulting polymeric functional group was converted into suitable poly(amidoxime) chelating ligand, followed by treatment with metal (Cu/Pd) salt to afford the related cellulose supported heterogeneous poly(amidoxime) metal complexes. Both complexes were treated with hydrazine hydrate to produce nano-sized cellulose supported poly(amidoxime) copper nanoparticles (**CuN@PA**) and palladium nanoparticles (**PdNs@PA**). The characterization and morphological changes were confined by using several spectroscopic techniques such as fourier transform infrared spectroscopy (FTIR), field emission scanning electron microscopy (FE-SEM), transmission electron microscopy (TEM), energy dispersive x-ray spectroscopy (EDX), x-ray photoelectron spectroscopy (XPS), x-ray powder diffraction (XRD), ultraviolet-visible spectrophotometry (UV-vis), thermogravimetric analysis (TGA) and inductively coupled plasma atomic emission spectroscopy (ICP-AES) analyses. The dark brown coloured **CuN@PA** (size-  $6.8 \pm 2$  nm) was efficiently catalyzed Aza-Michael reaction of aliphatic amines with different olefins to afford the corresponding alkylated products up to 96% at room temperature. Whereas **PdNs@PA** (size-  $2.8 \pm 6$  nm) showed high catalytic performance towards Suzuki-Miyaura cross-coupling reaction of aryl halides with organoboronic acids to give the corresponding biaryl products up to 95% yield with high turnover number (TON) 16250 and turnover frequency (TOF)  $5416 \text{ h}^{-1}$ . In both reactions, the cellulose supported nanoparticles were easy to recover and reused several times without a significant loss of their activity. Thus, a bio-based and effective cellulose supported heterogeneous metal catalyst was prepared from completely waste material (corn-cob) and applied efficiently to two popular reaction, Aza-Michael and Suzuki-Miyaura reactions. This cellulose supported metal catalyst would be a great achievement not only in the green industrial aspect but also a variety of natural products can be synthesized by using heterogeneous catalyzed key step reaction.



## TABLE OF CONTENTS

<b>DECLARATION</b>	
<b>TITLE PAGE</b>	
<b>ACKNOWLEDGEMENT</b>	<b>ii</b>
<b>ABSTRAK</b>	<b>iii</b>
<b>ABSTRACT</b>	<b>iv</b>
<b>TABLE OF CONTENTS</b>	<b>v</b>
<b>LIST OF FIGURES</b>	<b>x</b>
<b>LIST OF TABLES</b>	<b>xiii</b>
<b>LIST OF SYMBOLS</b>	<b>xiv</b>
<b>LIST OF ABBREVIATIONS</b>	<b>xv</b>
<b>CHAPTER 1            INTRODUCTION</b>	
1.1    Background	1
1.2    Pd-nanoparticles as Catalyst	3
1.3    Cu-nanoparticle as Catalyst	4
1.4    Problem Statement	8
1.5    Research Objectives	9
1.6    Research Scopes	10
1.7    Thesis Outline	11
<b>CHAPTER 2            LITERATURE REVIEW</b>	
2.1    Introduction	12
2.2    Cu catalyzed reactions	13
2.3    Pd-Catalyzed Reaction	14

2.4	Use of Supports for Catalyst	14
2.5	Suzuki-Miyaura Cross-Coupling Reactions using Pd Catalyst	15
2.5.1	Suzuki-Miyaura Cross-Coupling Reactions using Homogeneous Pd Catalyst	16
2.5.2	Suzuki-Miyaura Cross-Coupling Reactions using Heterogeneous Pd Catalyst	17
2.5.3	Suzuki-Miyaura Cross-Coupling Reactions using Supported Pd Catalyst	19
2.5.4	Suzuki-Miyaura Cross-Coupling Reactions using Cellulose Supported Pd Catalyst	20
2.6	Aza-Michael Reaction	21
2.6.1	Aza-Michael using Homogeneous Catalyst	22
2.6.2	Aza-Michael Reactions using Heterogeneous Cu Catalyst	23
2.6.3	Aza-Michael Reactions using Supported Cu Catalyst	24
2.5.4	Aza-Michael Reactions using Cellulose Supported Cu Catalyst	25
2.7	Conclusion	25
 <b>CHAPTER 3 MATERIALS AND METHODS</b>		
3.1	Introduction	27
3.2	General Information	27
3.3	Research Methodology	28
3.4	Characterization of Catalyst Nanoparticles	28
3.4.1	Fourier Transform Infrared Spectroscopy (FTIR)	28
3.4.2	Field Emission Scanning Electron Microscope	

and Energy Dispersive X-Ray (FESEM-EDX)	29
3.4.3 X-Ray Diffraction (XRD) Analysis	29
3.5 Preparation of Catalyst	30
3.5.1 Extraction of Cellulose from waste corn-cob	30
3.5.2 Synthesis of Poly(acrylonitrile) <b>1</b>	30
3.5.3 Synthesis of Poly(amidoxime) ligand <b>2</b>	31
3.5.4 Preparation of the Poly(amidoxime) Cu(II) Complex <b>3</b>	32
3.5.5 Preparation of the Poly(amidoxime) Cu-nanoparticles ( <b>CuNs@PA</b> )	33
3.5.6 Preparation of the Poly(amidoxime) Pd(II) Complex <b>4</b>	33
3.5.7 Preparation of the Poly(amidoxime) Pd-nanoparticles ( <b>PdNs@PA</b> )	34
3.6 General procedure for Aza-Michael Addition Reaction	34
3.7 Recycling of the <b>CuNs@PA</b>	35
3.8 General Procedure for Suzuki-Miyaura Reaction	35
3.9 Recycling of the <b>PdNs@PA</b>	36
3.10 Calculation of Yield and Mole Percent	36
 <b>CHAPTER 4: RESULT AND DISSCUSSION</b>	
4.1 Introduction	37
4.2 Synthesis and characterization of <b>CuNs@PA</b>	37
4.2.1 Fourier Transform Infrared Spectroscopy (FTIR)	
Analysis of poly(amidoxime) Cu complex <b>3</b>	38
4.2.2 Field Emission Scanning Electron Microscopy (FE-SEM)	

Images of Ligand <b>2</b> , Cu(II) Complex <b>3</b>	40
4.2.3 Energy-Dispersive X-Ray Spectroscopy (EDX) of Cu(II) Complex <b>3</b>	41
4.2.4 High-Resolution Transmission Electron Microscopy (HR-TEM) Images of Cu(II) complex <b>3</b> and <b>CuNP@PA</b>	42
4.2.5 X-Ray Powder Diffraction (XRD) of Cu(II) Complex <b>3</b> , Fresh and Reused <b>CuNP@PA</b>	44
4.2.6 X-Ray Photoelectron Spectroscopy (XPS) of Poly(amidoxime) Cu(II) Complex <b>3</b> and <b>CuNP@PA</b>	44
4.3 Aza-Michael addition reaction	46
4.4 The recyclability of the <b>CuNs@PA</b> catalyst	49
4.5 NMR Analysis of Aza-Michael products	51
4.6 Preparation and Characterization of <b>PdNs@PA</b>	55
4.6.1 Fourier Transform Infrared Spectroscopy (FTIR) Analysis of Cellulose and Modified Celluloses	56
4.6.2 Field Emission Scanning Electron Microscopy (FE-SEM) Images Analysis of Corn-Cob Cellulose, Modified Celluloses	57
4.6.3 Energy-Dispersive X-Ray Spectroscopy (EDX) of Pd(II) Complex <b>4</b>	58
4.6.4 Transmission Electron Microscopy (TEM) Images of Fresh and 4th Reused of Poly(amidoxime) Pd(II) Complex <b>4</b>	59
4.6.5 X-Ray Powder Diffraction (XRD) of poly(amidoxime) <b>2</b> and <b>PdNs@PA</b> catalyst	59
4.6.6 X-Ray Photoelectron Spectroscopy (XPS) of Fresh	

	and Reused Poly(amidoxime) Pd(II) Complex <b>4</b>	60
4.7	<b>PdNs@PA</b> Catalyzed Suzuki-Miyaura cross-coupling reaction	61
4.8	Recycling of <b>PdNs@PA</b>	66
4.9	NMR Analysis of Suzuki-Miyaura Reaction Products	68

## **CHAPTER 5: CONCLUSIONS AND RECOMMENDATIONS**

5.1	Conclusions	73
5.2	Future Directions	74

<b>REFERENCES</b>		75
-------------------	--	----

<b>APPENDICES</b>		83
-------------------	--	----

Appendix A1:  $^1\text{H}$  and  $^{13}\text{C}$  NMR Spectra of Aza-Michael Products

Appendix A2:  $^1\text{H}$  and  $^{13}\text{C}$  NMR Spectra Suzuki-Miyaura Products

<b>PUBLICATIONS</b>		111
---------------------	--	-----

**UMP**

## LIST OF FIGURES

Figure 1.1	Preparation of Pd-nanocatalysts by supercritical fluid deposition	3
Figure 1.2	Preparation of polystyrene anchored Pd(II) azo-complex	4
Figure 1.3	CuO-nanoparticle catalysed C-S cross-coupling of thiols with iodobenzene	4
Figure 1.4	Synthesis of nano-Fe <sub>3</sub> O <sub>4</sub> -DOPA-Cu catalyst (nano-FeDOPACu)	5
Figure 1.5	A general Suzuki-Miyaura reaction	6
Figure 1.6	Synthesis of Losartan	6
Figure 1.7	Selective mono coupling reaction	6
Figure 1.8	Aza-Michael reaction	7
Figure 1.9	Synthesis of anti-cancer drug 5- Fluorouracil	7
Figure 1.10	Ring formation reaction of 1-aminoadamantane with Michael acceptors	8
Figure 2.1	Mechanism of Suzuki-Miyaura Reaction	16
Figure 2.2	Suzuki-Miyaura reaction of Palladium-Imidazol-2-ylidene catalyst	17
Figure 2.3	Suzuki-Miyaura reaction of bidentate ligand based Pd-catalyst	17
Figure 2.4	Suzuki-Miyaura Reaction of Pd(IPr)(cinnamyl)Cl catalyst	18
Figure 2.5	Suzuki-Miyaura reaction of Pd (OAc) <sub>2</sub> catalyst	18
Figure 2.6	Poly styrene anchored-Pd(II) catalyzed Suzuki-Miyaura coupling	19
Figure 2.7	Ionic liquid Pd catalyzed Suzuki-Miyaura coupling	20
Figure 2.8	Cell-Pd(0) catalyzed Suzuki-Miyaura coupling	20
Figure 2.9	TiO <sub>2</sub> -Cellulose supported Pd catalyzed Suzuki-Miyaura coupling	21
Figure 2.10	Mechanism of Aza-Michael addition reaction	21
Figure 2.11	Aza-Michael reaction of homogenous Bi(NO <sub>3</sub> ) <sub>3</sub> catalyst	22
Figure 2.12	Aza-Michael reaction of homogenous boric acid catalyst	22
Figure 2.13	Aza-Michael Reactions of amines with $\alpha,\beta$ -unsaturated compound using Copper(II) acetylacetonate [Cu (acac) <sub>2</sub> ]	23
Figure 2.14	Aza-Michael reaction using the MOF-199 catalyst	24
Figure 2.15	PANI-Cu catalyzed aza-Michael reaction	24
Figure 2.16	Aza-Michael reaction of N-substituted imidazoles using PS-imCuI catalyst	24
Figure 2.17	Cell-Cu(0) catalyzed aza-Michael reaction	25

Figure 3.1	Research methodology flow chart	28
Figure 3.2	Synthesis of poly(acrylonitrile) <b>1</b>	31
Figure 3.3	Synthesis of poly(amidoxime) <b>2</b>	32
Figure 3.4	Synthesis of poly(amidoxime) Cu(II) complex <b>3</b>	32
Figure 3.5	Synthesis of poly(amidoxime) <b>CuNs@PA</b>	33
Figure 3.6	Synthesis of poly(amidoxime) Pd(II) complex <b>4</b>	33
Figure 3.7	Synthesis of poly(amidoxime) <b>PdNs@PA</b>	34
Figure 4.1	Synthesis of waste corn-cob cellulose-supported <b>CuNs@PA</b>	38
Figure 4.2	FTIR spectra of cellulose and modified cellulose	39
Figure 4.3	(a) Photo image of waste corn-cob, (b) Photo image of <b>2</b> , (c) Photo image of <b>3</b> , (d) Photo image of <b>CuNs@PA</b>	40
Figure 4.4	SEM images of (a) cellulose, (b) cellulose supported poly(acrylonitrile) <b>1</b> , (c) poly(amidoxime) ligand <b>2</b> , and (d) poly(amidoxime) copper complex <b>3</b>	41
Figure 4.5	EDX image of poly(amidoxime) Cu(II) complex <b>3</b>	42
Figure 4.6	(a) TEM image of Cu(II) complex <b>3</b> and (b) <b>CuNs@PA</b>	43
Figure 4.7	Size distribution of the <b>CuNP@PA</b> (the sizes were determined for 100 nanoparticles selected randomly)	43
Figure 4.8	XRD pattern of (a) fresh <b>CuN@PA</b> and (b) reused <b>CuN@PA</b>	44
Figure 4.9	(a) full XPS of fresh poly(amidoxime) Cu(II) complex <b>3</b> , (b) narrow scan XPS of fresh poly(amidoxime) Cu(II) complex <b>3</b> and (c) <b>CuNs@PA</b>	45
Figure 4.10	UV-Vis of poly(amidoxime) <b>2</b> and poly(amidoxime) Cu(II) complex <b>3</b>	46
Figure 4.11	Aza-Michael addition reaction of amines	48
Figure 4.12	Preparation of multi-alkylated products	49
Figure 4.13	XPS image of 4 <sup>th</sup> reused of <b>CuNs@PA</b>	50
Figure 4.14	TEM image of 4 <sup>th</sup> reused of <b>CuNs@PA</b>	51
Figure 4.15	Synthesis of <b>PdNs@PA</b>	55
Figure 4.16	FTIR spectra of the (a) corn-cob cellulose, (b) Poly(acrylonitrile) <b>1</b> (corn-g-PAN), (c) poly(amidoxime) chelating ligand <b>2</b> and (d) poly(amidoxime) Pd(II) complex <b>4</b>	56
Figure 4.17	SEM images of (a) poly(amidoxime) ligand <b>2</b> , and (b) poly(amidoxime) Pd(II) complex <b>4</b> respectively	58

Figure 4.18	EDX spectrum of poly(amidoxime) Pd(II) complex <b>4</b>	58
Figure 4.19	(a) TEM image of <b>PdNs@PA</b> and (b) 4 <sup>th</sup> reused of <b>PdNs@PA</b>	59
Figure 4.20	XRD of Pd(II) complex <b>4</b> and <b>PdNs@PA</b>	60
Figure 4.21	XPS of poly(amidoxime) Pd(II) complex <b>4</b> and <b>PdNs@PA</b>	61
Figure 4.22	Suzuki-Miyaura reaction of aryl iodide	63
Figure 4.23	Suzuki-Miyaura reaction of aryl bromide	64
Figure 4.24	Suzuki-Miyaura reaction of aryl chloride	65
Figure 4.25	Recycling of <b>PdNs@PA</b> for Suzuki-Miyaura Reaction	66
Figure 4.26	Hot filtration of Suzuki-Miyaura reaction	67
Figure 4.27	High TON and TOF in the Suzuki-Miyaura reaction	67

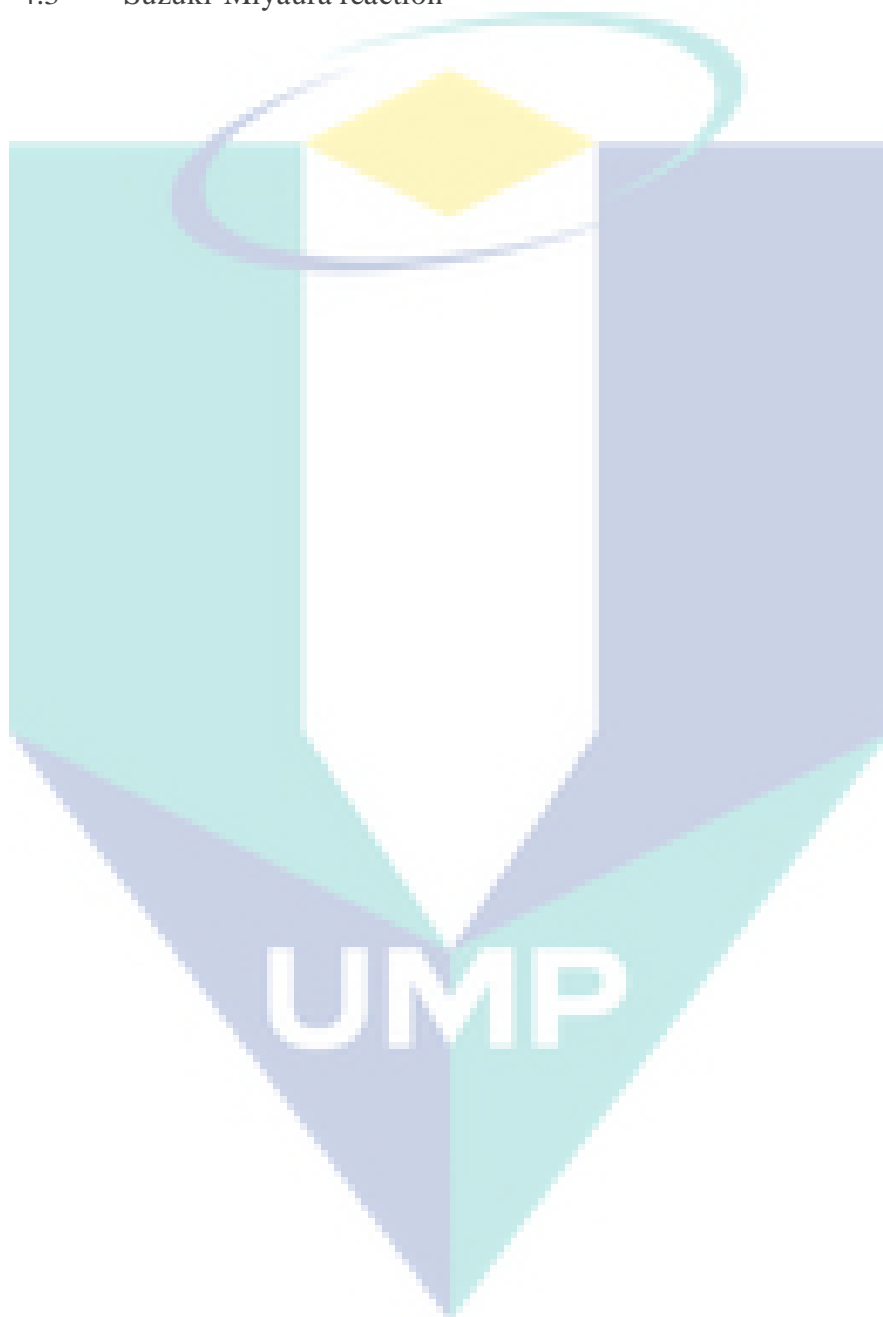


UMP

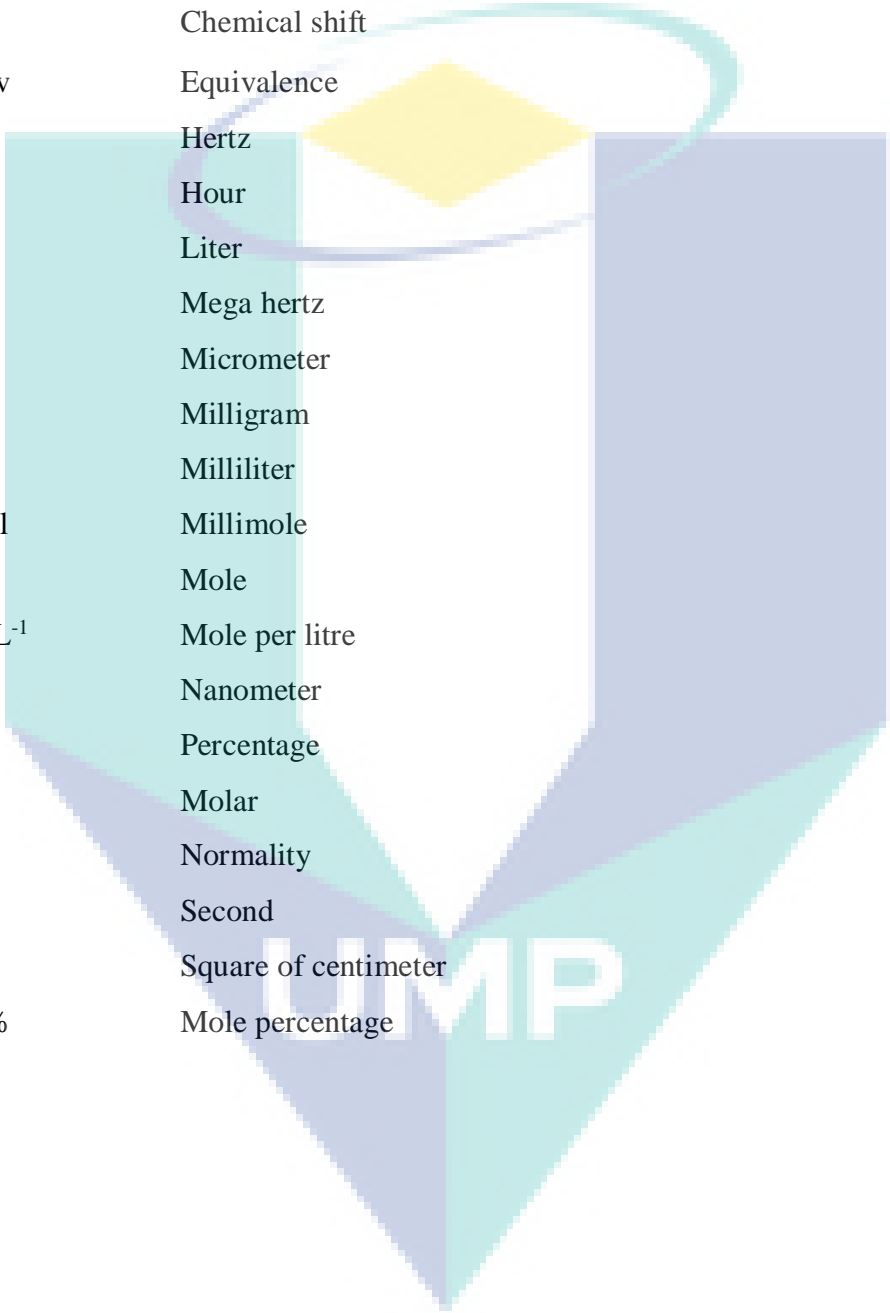


## LIST OF TABLES

Table 2.1	History of Cross-Coupling Reactions	12
Table 4.1	Catalyst screening of the Aza-Michael addition reaction	47
Table 4.2	Aza-Michael reaction by recycled catalyst <b>CuNs@PA</b>	50
Table 4.3	Suzuki-Miyaura reaction	62



## LIST OF SYMBOLS



$^{\circ}\text{C}$	Degree centigrade
g	Gram
$\text{cm}^{-1}$	Per centimeter
$\delta$	Chemical shift
Equiv	Equivalence
Hz	Hertz
h	Hour
L	Liter
MHz	Mega hertz
mm	Micrometer
mg	Milligram
mL	Milliliter
mmol	Millimole
mol	Mole
$\text{mol L}^{-1}$	Mole per litre
nm	Nanometer
%	Percentage
M	Molar
N	Normality
Sec	Second
$\text{cm}^2$	Square of centimeter
mol%	Mole percentage

## LIST OF ABBREVIATIONS

$\alpha$	Alpha
Ar	Aromatic
$\beta$	Beta
$^{13}\text{C}$ NMR	Carbon nuclear magnetic resonance
J	Coupling constant
d	Doublet
dd	Doublet of doublet
EDX	Energy dispersive X-ray spectroscopy
FTIR	Fourier transform infrared spectroscopy
HR-TEM	High resolution transmission electron microscopy
HR-SEM	High resolution scanning electron microscopy
H-bond	Hydrogen bond
IR	Infrared
ICP-AES	Inductively coupled plasma atomic emission spectroscopy
m	Multiplet
$^1\text{H}$ NMR	Proton nuclear magnetic resonance
pH	Potential of hydrogen
q	Quartet
s	Singlet
TLC	Thin layer chromatography
t	Triplet
XPS	X-ray photoelectron spectroscopy
XRD	X-ray diffraction

## CHAPTER 1

### INTRODUCTION

#### 1.1 Background

Heterogeneous catalytic process of synthesis of chemical compounds is particularly attractive as it allows high production and readily separation of large quantities of products with the use of slight amount of catalyst (Reddy, Kumar et al. 2006). In recent years scientists are searching for more environmentally friendly and sustainable resources and processes of synthesis. From this aspect, cellulose is the most commonly sighted biopolymer used vastly in industries. Though, the use of cellulose has been limited to textile, paper, plastic and lumber industries but massive amount of cellulose is left to decay (Dhepe and Fukuoka 2007). The macromolecular architectures of cellulose provide several advantages, such as low density, bio-renewable character, universal availability at low cost and interesting mechanical properties like glass fibers (Bolton 1994). The development of renewable and biodegradable resources has growing interest nowadays because the bio-based materials and composites could be a promising solution both in terms of environmental and performances aspects. Thus, for the exploration of the solid support of catalysts, natural celluloses can act as most attractive and highly appreciable candidates for heterogeneous catalysts (O'Connell, Birkinshaw et al. 2008). Recently, several biopolymers, for example chitosan (Quignard, Choplin et al. 2000), alginate (Wei, Zhu et al. 2004), gelatin (Zhang, Geng et al. 2001) and starch (Huang, Xue et al. 2002). derivatives have been utilized as supports for catalytic applications. But cellulose has some attractive character just as, high sorption capacity, high stability, insolubility in solvents, eco-friendly nature, physical and chemical versatility, all such qualities make it to act as a perfect support. Cellulose can be chemically modified to attain sufficient structural strength, so that chelating ligands can effectively introduce onto the cellulose

chain, which can make a easy coordination with metal ions (O'Connell, Birkinshaw et al. 2008). Cellulose supported nano-particles are introducing as an interesting protocol for the immobilization of transition metal complexes which are used for the synthesis of natural products, polymers, liquid crystals and many bioactive compounds. Because with the decrease of supporting materials size on nanoscale, the increase of surface area of such particles take place dramatically. Therefore, supports of nanoparticle can develop high metal loading capacity, high catalytic performance rather than general supported catalyst. The synthesis of a variety of organic molecules through heterogeneous catalytic process is particularly attractive as it allows high production and readily separation of large quantities of products with the use of slight amount of catalyst. Not only from an industrial point of view, but also in the field of fine chemicals, heterogeneous catalyst is arguably the most versatile and the most widely applied category of catalysts to carry out chemical reactions, mainly because of its impressive potentials just as separation, recycling, stability, handling, and commercially availability (Blaser, Indolese et al. 2001). During the past fifteen years, because of rapid progress of surface science, mainly the structural development and surface reactivity of metal catalysts (Boudart and Djéga-Mariadassou 2014).

In recent years, numerous heterogeneous supported palladium/copper catalysts were successfully employed for C-C and C-N bond formations. (Calo, Nacci et al. 2005, Huang, Weng et al. 2008, Dewan, Bora et al. 2014, Ghaderi, Gholinejad et al. 2016). Cross-coupling reactions have grown into an extensively powerful and general strategy for forming C-C bonds and C-hetero atom bonds. Several methods are available for the construction of C-C and C-hetero atom bonds such as Aza-Michael addition reaction, Sonogashira coupling reaction, Kharash coupling, Negishi coupling, Stille coupling, Himaya coupling, Liebeskind-Srogl coupling, Kumuda coupling and many more.

These types of bond formations constitute the backbone of organic synthesis and used widely for the synthesis of natural products and many other useful compounds. However, certain well-known reactions, used in organic chemistry are not economically preferable and create hazardous byproducts. With a recent focus on “green” methodologies, reactions that minimize such byproducts yet produce the desired bonds or high product are of great interest.

## 1.2 Pd-Nano Particles as Catalyst

In the field of advanced chemicals sector, palladium is considered as the most useful and widely applicable catalytic metal. Indeed, contamination caused by Pd residues is quite acute for large-scale synthesis. Moreover, Pd is significantly cheaper than other economically and environmentally considerable metals like rhodium, platinum, iridium, gold etc. Also supported Pd-metal catalysts are easily removed by filtration and leaving materials almost free from any Pd residues. Also different types of supports have been used for Pd-nanoparticles, such as organic polymers and carbon materials, inorganics as metal oxides, silica, zeolites and other hybrid supports as grafted silica etc. Various methods are available for the preparation of supported Pd-nanoparticles, such as co-precipitation, liquid or vapor phase impregnation, sol-gel techniques, supercritical fluid deposition, polymer supported and many more.

For example, supercritical fluid deposition is considered as a notable method for the preparation of Pd-nanocatalysts. This method simply includes the dissolution of a metal complex in a supercritical fluid, afterward the metal complex was adsorbed on the support, and finally, by chemical or thermal reduction the adsorbed complex converted into the metal species (Ulusal, Darendeli et al. 2017).

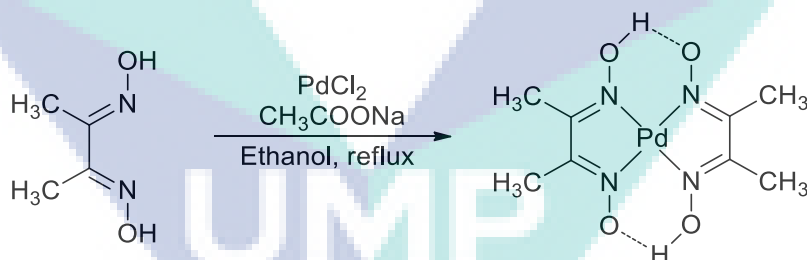


Figure 1.1 Preparation of Pd-nanocatalysts by supercritical fluid deposition.

Recently, the polystyrene anchored Pd(II) azo-complex heterogeneous catalysts showed large exposition degree of Pd and very good compatibility in various cross-coupling reactions such as Suzuki–Miyaura reaction (Islam, Mondal et al. 2010).

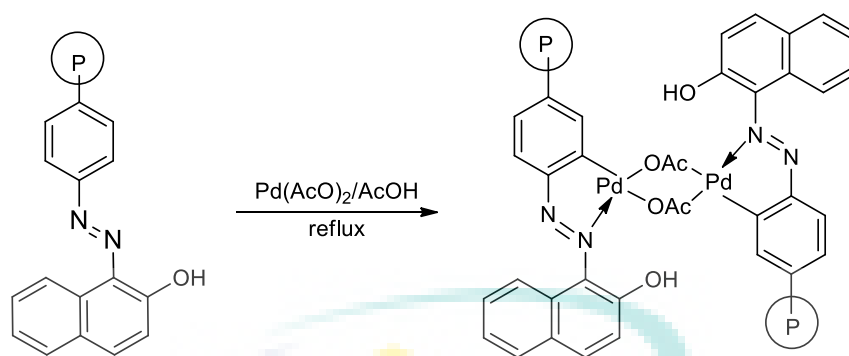


Figure 1.2 Preparation of polystyrene anchored Pd(II) azo-complex.

### 1.3 Cu-Nano Particle as Catalyst

Variety of metal catalysts such as Cu, Co Ni, Fe are using more frequently for synthesis of C- hetero bonding. But the high cost and air and moisture sensitive property hamper the synthesis in the large scale. Moreover, some catalysts (Co, Ni) are associated with toxicity (Bhadra, Sreedhar et al. 2009). So, Cu is considered as most appropriate and environment friendly metal catalyst.

The first C-S cross coupling reaction using CuO nanoparticle is mentioned in the Fig. 1.3 (Rout, Sen et al. 2007). The copper oxide nanoparticles was used for the purpose of high catalytic activity and environmental suitability. The reaction conditions were found to be simple and gives about 95% products.

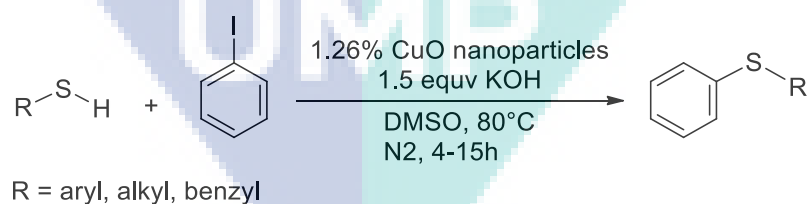


Figure 1.3 CuO-nanoparticle catalysed C-S cross-coupling of thiols with iodobenzene.

From this perspective R. B. Nasir Baig and Rajender S. Varma reported the synthesis of magnetically recoverable heterogeneous Cu catalyst, that was prepared by the sonication of nanoferrite with dopamine hydrochloride (Baig and Varma 2012) for the organic synthesis of carbon-sulphur cross coupling reactions. This catalyst is

magnetically separable, environmentally sustainable and suitable for the greener developments.

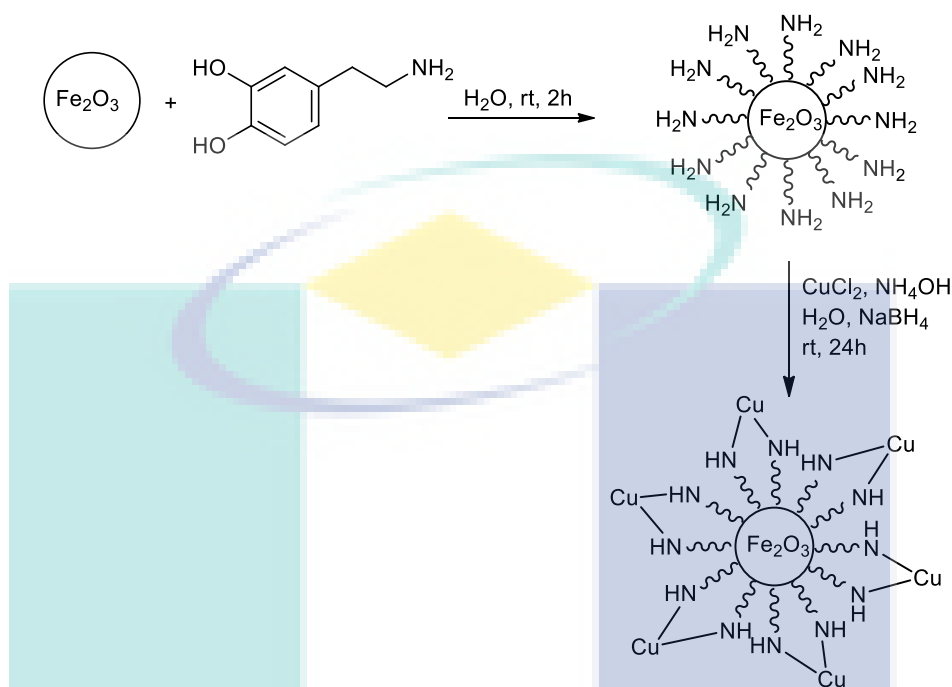


Figure 1.4 Synthesis of nano-Fe<sub>3</sub>O<sub>4</sub>-DOPA-Cu catalyst (nano-FeDOPACu).

Prior to 1979, the constructions of aryl-aryl C-C bonds were difficult to achieve. But in 1981, Suzuki and Miyaura were introduced palladium catalyzed Suzuki-Miyaura cross-coupling reaction of an aryl or vinyl halide with an aryl or vinyl boronic acid or ester. Later on a lot of applications of this reactions were found in the synthesis of a number of biologically active and functional molecules, (Horton, Bourne et al. 2003) natural products, (Schmidt, Leitenberger et al. 1992) pharmaceuticals, (Leek, Carr et al. 1997) valsartan, telmisartan, felbinac, losartan, Imatinib, agrochemical boscalid, (Matheron and Porchas 2005) liquid crystals for LCD screens (Geelhaar 1998) and so on.

The Suzuki-Miyaura reaction is considered as an important reaction due to its high yield of product, non-toxic boronic acid byproduct or free from any byproducts and high functional group tolerance. As a result of its great importance, Suzuki shared the Nobel Prize with other two workers Y. Kousuke and D. Thomas in 2010.



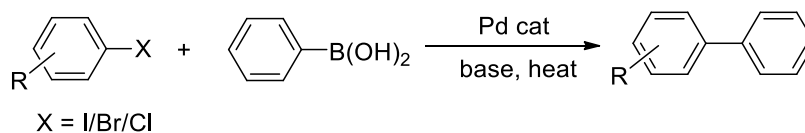


Figure 1.5 A general Suzuki-Miyaura reaction.

For example this route synthesizes the anti-hypertensive Losartan (Larsen, King et al. 1994). The Suzuki-Miyaura cross-coupling reaction has also been applied as key step reaction for the synthesis of anti-hypertensive Losartan.

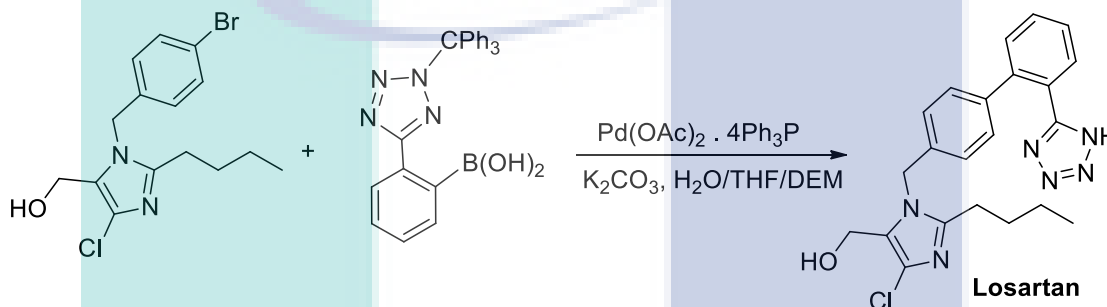


Figure 1.6 Synthesis of Losartan.

Also, different substituted chloroaryl compounds reacts with different substituted boronic acid and give relatively high yield and have high potential towards the synthesis. The Suzuki reaction provided some selective reactions, which were considered as intermediate to conduct different reactions. For example, coupling reaction of substituted boronic acid with 2,4-dichlorobenzaldehyde underwent through monocoupling reaction to give a related product, which was difficult to achieve. (Dey, Sreedhar et al. 2010)

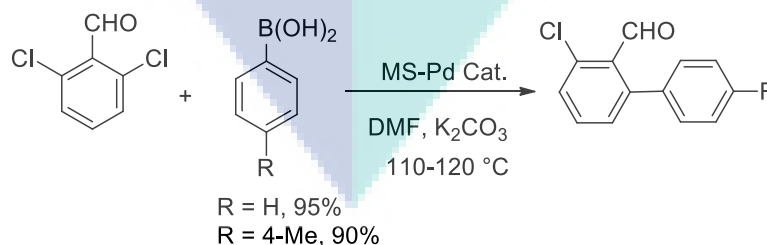


Figure 1.7 Selective mono coupling reaction.

On the other hand the Aza-Michael addition reaction of amines and  $\alpha,\beta$ -unsaturated carbonyl compounds has grasped enormous attraction as one of the most effective methods to prepare  $\beta$ -amino carbonyl compounds and their derivatives. (Ai, Wang et al. 2010) Which includes biologically important natural products, antibiotics, peptide analogues, chiral auxiliaries, and other nitrogen-containing compounds (Surendra, Krishnaveni et al. 2006).

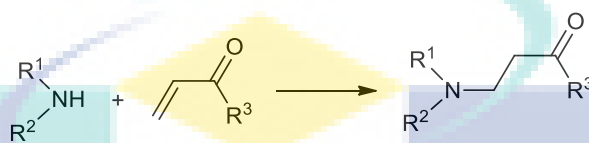


Figure 1.8 Aza-Michael reaction.

Aza-Michael reaction procedure was applied for the preparation of anticancer drug 5-fluorouracil (5-FU) (Wang, He et al. 2017). This process involved the efficiency of Aza-Michael addition reaction for the *in-situ* formation of polyamidoamine (PAMAM) dendrimer hydrogels (DHs) from EDA-core PAMAM dendrimer generation 5 (G5) and acetic anhydride (Ac) followed by PEG-DA and formed a cross-lined network.

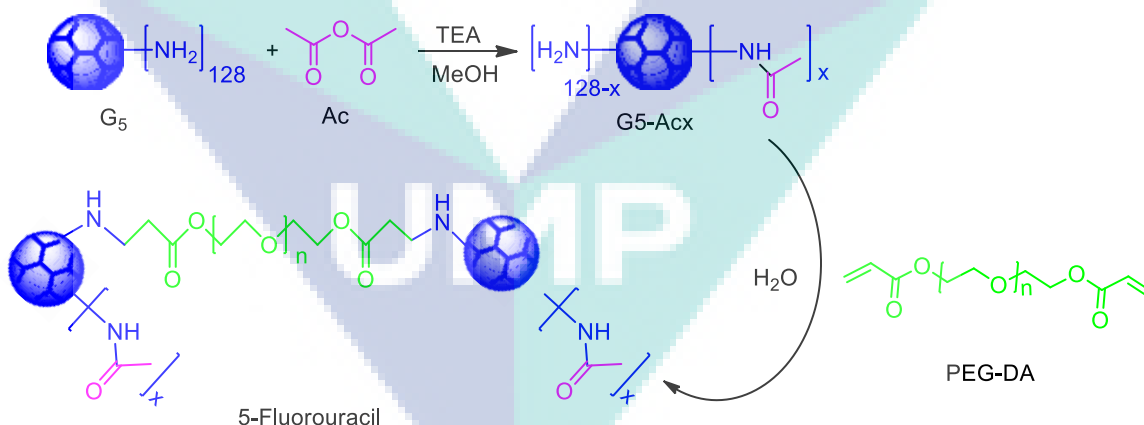


Figure 1.9 Synthesis of anti-cancer drug 5- Fluorouracil.

Another significance of Aza-Michael addition reaction was obtained in ring closure reaction initiated with 1-aminoadamantane and  $\alpha$ -halogenated Michael acceptors (Fedotova, Komarova et al. 2017). The reaction was conducted through Aza-

Michael intermediate with the target formation of *N*-containing heterocyclic compound to provide a new route of synthesis of biologically active polyfunctional compounds.

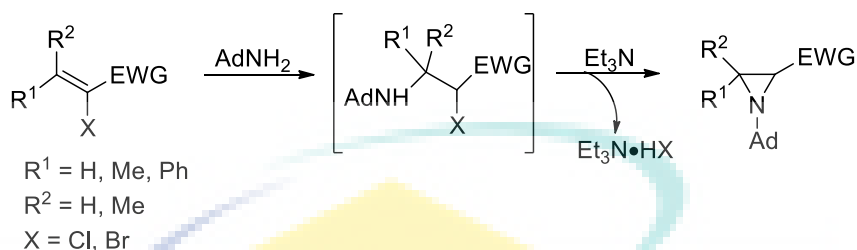


Figure 1.10 Ring formation reaction of 1-aminoadamantane with Michael acceptors.

#### 1.4 Problem Statement

Most of the chemical transformations have been extensively studied with the homogeneous metal complexes in solution media. However, homogeneous metal catalyzed reaction involved several serious limitations like purification of product, lack of reuse of precious metals as well as environmental pollution issues. Furthermore, homogeneous catalyst loses its activity during the reaction since it undergoes aggregation. Whereas, heterogeneous metal catalysts can overcome these aforementioned problems. They allow easy separation of large quantities of products; using a small amount of catalyst and the reuse of the catalysts. In recent years, numerous heterogeneous supported palladium catalysts were successfully investigated both in Aza-Michael and Suzuki-Miyaura cross-coupling reactions. The supporting materials include functionalized polymers, graphene oxide, carbon nanotubes, inorganic substrates such as silica, zeolites, and mesoporous materials. However, most of these methods undergo harsh conditions, long reaction times, require expensive reagents and give unsatisfactory yields. Considering the fact, attention of researchers is moving towards bio polymers, mainly cellulose and its derivatives (Klemm, Heublein et al. 2005) and studying on it widely during the past decades for their unique properties, availability in nature, biodegradability and renewability. The utility of cellulose as support has been come in to many research applications (Maddila, Momin et al. 2016), (Cirtiu, Dunlop-Briere et al. 2011), (Reddy, Kumar et al. 2006) but in most cases the commercially available cellulose was used. Therefore attention was shifted on collecting cellulose from waste source such as sugarcane baggase [(Kumar, Negi et al.

2014), mango seeds (Henrique, Silvério et al. 2013)], waste polyester/cotton blended fabrics (Sun, Lu et al. 2013), agricultural waste such as rice straw, wheat straw, corn stalks and dhaincha (Nuruddin, Chowdhury et al. 2011). But the application the extracted cellulose as support for heterogeneous catalyst has not much studied.

The activity and selectivity, easy separation of product from the reaction mixture and recyclability are considered as the main desirable attributes for metal catalysts according to the green and sustainability protocol. To attain the above features, chemists are exploring to find renewable metal nanoparticles but it is still challenging to obtain truly efficient and sustainable heterogeneous catalysts. Because of the large surface area of metal nanoparticles, they are very attractive for catalytic reactions providing effective utilization of expensive metals. Nanoparticles (<10 nm) exhibit high catalytic activities toward a variety of fields, such as electronics and optics, magnetism, chemistry and energy technology. Unfortunately, along with decreasing the catalytic efficiency, aggregations of unstable nanoparticles often increase the particle size. Nanoparticles are generally dispersed onto the supporting materials to overcome this issue. When the size of the supporting materials is decreased into the nanometer scale; the surface area of nanoparticles will increase dramatically. As a consequence, nanoparticle supports could have high catalyst loading capacity, leading to the high catalytic activity of the nanoparticle-supported catalysts compared to the conventional support materials. A limited number such of studies obtained in the case of cellulose.

Thus, the present work mainly focused to prepare and characterized a highly active sustainable cellulose supported heterogeneous metal nanoparticles (Pd and Cu) for the construction of C-C and C-N bonds formation with regeneration of the nanoparticles.

## **1.5 Research Objectives**

The main objective of this research is to develop highly active cellulose supporting metal nanoparticles for a variety of chemical transformation reactions.

The specific aims to achieve the goals as follows:

1. To synthesis and characterize of the corn-cob cellulose supported Cu and Pd catalyst.
2. To evaluate the activity and selectivity of these cellulose supported metal catalysts in Suzuki-Miyaura (C-C) and Aza-Michael addition reactions (C-N).
3. To investigate the reusability of the catalysts.

## 1.6 Research Scope

The following objectives are required to achieve the objectives:

- This research introduces a new type of bio-waste supported metal nanoparticles that will be characterized by using of several spectroscopic methods (NMR, FT-IR, ICP-AES, TEM, XPS, FE-SEM and EDX).
- The nanoparticles will be screened for C-C and C-N bonds formation reactions.
- All cross-coupling products will be characterized through FTIR and NMR analyses.
- The reusability of the metal nanoparticles will be determined by hot filtration method and ICP-MS analyses.

From the point of green technology, it is desirable to develop a simple and convenient reaction method to proceed a large number of reaction under milder and environment friendly conditions. Therefore, such a catalyst is needed that can have a quality of extreme activity, easily separability, selectivity and reusability. Cellulose supported metal catalysts (Cu and Pd) have exhibited such qualities successfully in Aza-Michael and Suzuki-Miyaura reaction. This research is concentrating not only to upgrade the catalytic characteristics but also to make it environmental friendly. Though various researches have targeted to extract cellulose from waste materials but in this research, cellulose was extracted from waste corn-cob through a very simple method under mild condition, use it as support for the preparation of heterogeneous metal catalyst containing all qualities of a perfect catalyst, converting to nanosize to increase the catalytic activity and successfully applied to two selective reactions, which is difficult to find in any research. The metal selection was done for Cu and Pd on the basis of being cheap and ecofriendly. One of the aim of research was focused on the

formation of C-C and C-N bonding with the target of applying it to natural product synthesis. Keeping on this mind, Aza-Michael and Suzuki-Miyaura reaction was conducted in this research and all reactions were performed under environmental friendly conditions and obtained the targeted bond products with high yields.

## 1.7 Thesis Outline

The study presented in this thesis aims to understand the catalytic activity of cellulose supported palladium and copper complexes and nanoparticles as catalyst in Suzuki-Miyaura and Aza-Michael reactions. It also intended to apply the complexes in the synthesis of biologically important molecules. The outline of this thesis is as follows: Chapter 1: Presented of the research background, problem statement, objectives of the study, scope of the research, and the thesis outline. Chapter 2: Included the theoretical aspects which are related to the research. Chapter 3: Presented the procedures and the synthetic pathways conducted in the research. Chapter 4: Presented the characterization of the synthesized compounds. Chapter 5: Concluded the study by relating the results with the theoretical and experimental findings.

## CHAPTER 2

### LITERATURE REVIEW

#### 2.1 Introduction

Metal catalyzed cross-coupling reactions are used to construct a variety of chemical bonds formation and widely used as an intermediate reaction to synthesis of natural products, polymers, advanced materials, liquid crystals, and pharmaceutical compounds. Many scientists applied different types of catalytic process for the cross-coupling reactions. Many of them exhibit a very good result with higher yield but every effort whether successful or unsuccessful provide a step forward to the chemical synthesis. Some of the incredible research related to this work mentioned below:

Table 2.1 History of metal catalyzed cross-coupling reactions.

Name	First Publication	Catalyst	Reactant A	Reactant B
Gomberg-Bachmann	1924	Cu/CuCl	Ar-X	Ar-N <sub>2</sub> X
Cadiot-Chodkiewicz	1957	Cu	R <sup>1</sup> -C≡C-H	R-C≡C-Br
Castro-Stephens	1963	Cu	R <sup>1</sup> -C≡C-H	Ar-X
Gilman Reagent	1967	Cu	R <sub>2</sub> CuLi	R-X
Kumada Coupling	1972	Pd/Ni	R <sup>1</sup> MgX	R-X
Heck Reaction	1972	Pd	Alkene	R-X
Sonogashira Reaction	1975	Pd and Cu	R <sup>1</sup> -C≡C-H	R-X

Table 2.1 Continued

Name	First Publication	Catalyst	Reactant A	Reactant B
Negishi Coupling	1977	Pd/Ni	$R^1ZnX$	R-X
Stille Coupling	1978	Pd	$R^1SnR^2_3$	R-X
<b>Suzuki-Miyaura</b>	1979	Pd/Ni	$R^1B(OR)_2$	R-X
Hiyama Coupling	1988	Pd	$R^1SnR^2_3$	R-X
Buckwald-Hartwig	1994	Pd	$RN_2R$	Ar-X
Fukuyama Coupling	1998	Pd	$R^1ZnI$	R-CO(SEt)
Liebeskind-Srogl	2000	Pd	$R^1B(OR^2)_2$	R-CO(SEt)

## 2.2 Cu catalyzed reactions

Cellulose supported Cu is now using widely to conduct cross coupling reaction for the formation of C-C and C-hetero atom bonding. (Chan, Monaco et al. 1998) From the last decade, nanostructured Cu systems are being explored in both homogeneous and heterogeneous form in varieties of cross coupling reactions. (Meldal and Tornøe 2008, Jin, Yan et al. 2012). Copper catalysis also possesses some indisputable advantages over the other catalytic systems because of having low cost and readily accessible and formation of stable ligands. A new type agarose-supported copper nanoparticles (**CuNPs@agarose**) was introduced which is air stable, and five times recyclable (Gholinejad and Jeddi 2014).

Catalytic systems based on different transition metals like nickel, cobalt and iron have also been studied. But these systems also faced some major disadvantages like metal toxicity, low turnover numbers which is not suitable for environment in the long run. So now researcher's interest in the development of copper based catalytic systems increased because of the low cost and use of readily accessible and form stable ligands.



### 2.3 Pd-Catalyzed Reaction

The formation of carbon-carbon bonds is considered as the most fundamental transformations of organic chemistry. From simple compounds to complex biological systems, the carbon-carbon bond is incorporated in a wide range. Organic chemists are also interested in focusing green methodology where the reactions contain lower byproduct and higher formation of the desired bonds (Li, 2008). However, some of the most well-known reactions used in organic chemistry have no economic value and also create hazardous byproducts. Whereas transition-metal-catalyzed coupling reactions including cross dehydrogenative coupling or oxidative coupling consider as a versatile tool for chemical bond formation (C. Liu, Zhang, Shi, & Lei, 2011). Specifically, nowadays cross-coupling reactions have grown as an extremely powerful and general strategy for forming C-C, and C-heteroatom bonds and fulfilling the green methodology.

### 2.4 Use of Supports for Catalyst

Most of the heterogeneous catalysts supports are based on silica. Silica displays many advantages properties such as excellent stability (both chemical and thermal), high surface area, good accessibility, and organic groups can be robustly anchored to the surface to provide catalytic centers. Numerous solid supports have been utilized as anchors such as N-heterocyclic carbene (NHC) ligands and their metal complexes for example, polystyrene (Kang, Feng et al. 2005), polysilylethers (Wang, Hu et al. 2014) and mesoporous silica (Pozo, 2011).

Furthermore, phosphine-based ligands also have endured to be the most popular selection for the palladium catalyzed cross-coupling reactions (Chow et al. 2011);(P. Das et al. 2010); (Demchuk, Yoruk et al. 2006); (Hatakeyama et al., 2009); (Mao et al., 2012); (Valente et al., 2012). But, their stability and shelf life are hampered because of their sensitivity to air and moisture and also toxic nature. The progress in the quality of catalysts on solid support found to be relatively slow as compared to soluble homogeneous complexes because of the deactivation that results from particle aggregation, metal leaching and matrix degradation (Molnár & Papp, 2014). Another

major problem is the environmental concern arising from the use of poisonous and often costly materials applied in catalyst synthesis (Gates, 1995).

To overcome these obstacles number of different supports have been invented and introduced including porous materials. Porous materials such as clays, rocks or biological tissues (e.g. bones), membranes and including metal oxides, ceramics, carbonaceous like synthetic materials act as a great support for nanoparticles. To remove some of the difficulties obtained by the solid supports, they play a great role for the heterogeneous catalytic process. Such as generating specific absorption site, create a partition between interior and exterior structures and prevent particle aggregation by inhibiting the growth of particles size (White, Luque, Budarin, Clark, & Macquarrie, 2009).

Still not many of them are biodegradable, economical, widely available, and easy to use. On the basis of environmental appreciably different researcher used/synthesized variety of biopolymer supported metal catalysts (Sarkar, Guibal, Quignard, & SenGupta, 2012; White et al., 2009).

## **2.5 Suzuki-Miyaura Cross-Coupling Reactions using Pd Catalyst**

The Suzuki-Miyaura cross-coupling reaction is the reaction between alkyl or aryl boronic acids with alkyl or aryl halides to give a coupled product using a Pd catalyst and base. This cross-coupling reaction is considered as an efficient and less toxic method to construct the carbon-carbon bonds. The reaction can be used with a large range of functional groups and can be carried out under aqueous media. In 1979 Suzuki and Miyaura were discovered the cross-coupling between 1-alkenylboranes with 1-alkenyl, 1-alkynyl halides and with aryl halides in presence of homogeneous palladium salt (Miyaura, Yamada, & Suzuki, 1979). In the palladium catalyzed Suzuki-Miyaura cross-coupling reaction base is required to facilitate the activation of boronic acid during transmetallation steps. Bases like NaOH, NaOMe, NaOEt, and NaOAc were found to give successful cross-coupling than Lewis bases such as triethyl amine. Additionally, a high degree of stereo- and regioselectivity noted in the article by Suzuki and Miyaura, which was not previously obtainable, by catalytic methods at that time.

Thus a new pathway was opened for the synthesis of  $sp^2$ - $sp^2$  and  $sp^2$ - $sp$  carbon-carbon bonds.

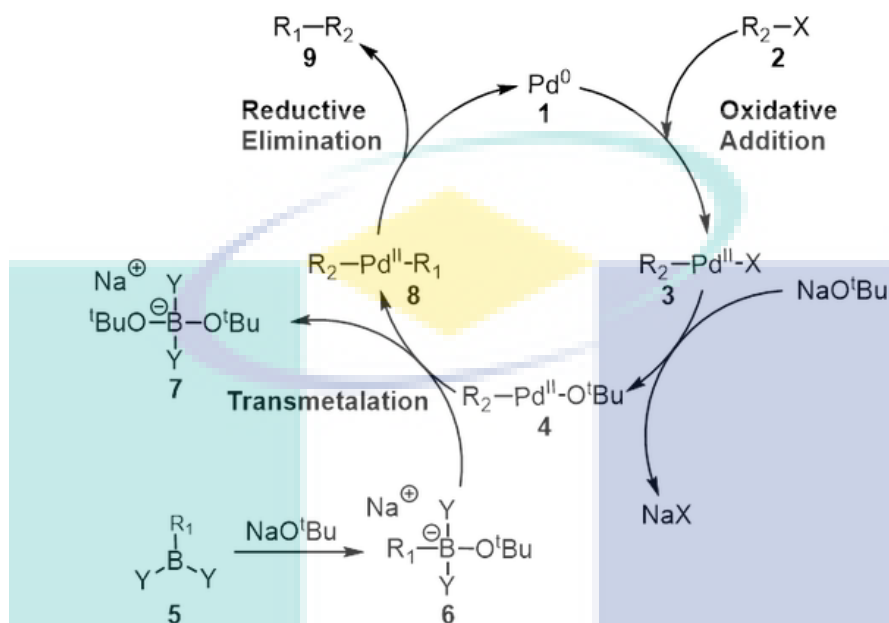


Figure 2.1 Mechanism of Suzuki-Miyaura Reaction.

The mechanism for the Suzuki-Miyaura cross-coupling reaction is shown in Figure 2.1. The mechanism begins with oxidative addition of aryl/alkyl halide with Pd(0) to form an aryl Pd(II) as an intermediate. In the following step, base (mainly hydroxide) replace the halide from the Pd(II) complex. Whereas another molecule of base activated the alkyl/aryl boronic acid by making alkyl/aryl group more nucleophilic. Transmetalation with the borate take place by replacing the alkyl/aryl group onto the Pd(II) complex. In the final step, by di-alkyl/aryl Pd(II) complex is produced through the reductive elimination process with regeneration of Pd(0) catalyst and the catalytic cycle can begin again.

### 2.5.1 Suzuki-Miyaura Cross-Coupling Reactions using Homogeneous Pd Catalyst

C. Zhang and researchers introduced palladium-imidazol-2-ylidene complex catalyzed Suzuki-Miyaura cross-coupling reaction. ((Zhang, Huang et al. 1999)) This palladium imidazol-2-ylidene complex act as a homogeneous catalyst with the target of forming C-C bond between aryl chloride and aryl boronic acid. One of the advantages of the catalyst is the stability and bonding with the bulk metal Pd. In this reaction the Pd

complex and imidazol-2-ylidene ligand was added separately in the reaction mixture to produce the palladium-imidazol-2-ylidene catalyst instantly and catalyze the reaction and provide excellent correspondent yield (99%). As the reaction was conducted in homogeneous condition, no reuse of catalyst was possible. Though the production amount was high but the reaction process was quite complicated, used catalytic percent was also higher (Fig. 2.2) and stability of this catalyst was not confirmed.

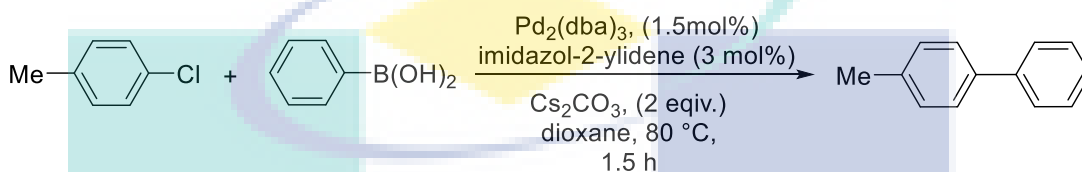


Figure 2.2 Suzuki-Miyaura reaction of Palladium-Imidazol-2-ylidene catalyst.

Jinyi Song and his group reported the Suzuki-Miyaura reaction over homogenous catalytic system, where a bidentate ligand 2,5-dihydroxyterephthalaldehyde dioxime (L<sub>8</sub>) coordinate with PdCl<sub>2</sub>. The activity of this homogeneous ligand was studied for Pd-catalyzed Suzuki-Miyaura cross-coupling reactions (Song et al., 2017). The reaction was conducted with aryl chloride in presence of under mild conditions for 5 hours. The coupling reactions were performed in the presence of base Na<sub>2</sub>CO<sub>3</sub> in the ethanol/water (1:1) solvent system at 85 °C and produce up to 80% yield.

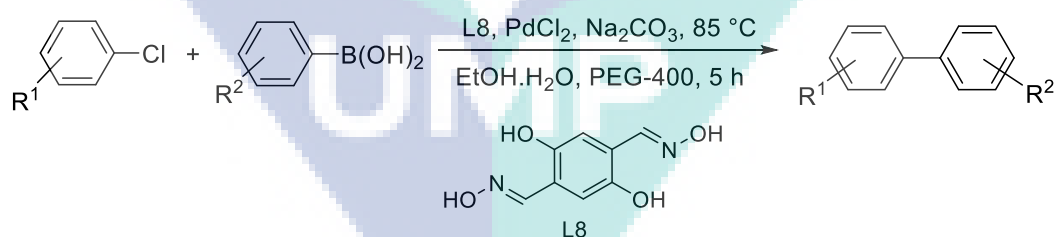


Figure 2.3 Suzuki-Miyaura reaction of bidentate ligand based Pd-catalyst.

### 2.5.2 Suzuki-Miyaura Cross-Coupling Reactions using Heterogeneous Pd Catalyst

Taoufik Ben Halima and co-researchers applied Suzuki-Miyaura reaction for aryl esters (Halima et al., 2017). In this reaction Pd(IPr)(cinnamyl)Cl-catalyst was used with the main focusing of the cleavage of C-O bond with the formation of product

containing keto-group. From the reaction Figure it was easy to observe that the 3-5 mol% catalyst was used in this reaction (Fig. 2.4). Potassium phosphate was used as base in the presence of THF (tetra hydro furan). The whole process was conducted for 16 hours, at 100 °C temperature. It was really challenging to use such bulky catalyst into application for Suzuki-Miyaura reaction and providing a satisfactory yield (95%). But, the amount of catalyst was found to be higher and the reaction time as well. Also the reusability of the catalyst was not obtained in this work which is one of the remarkable quality of heterogenous catalysts.

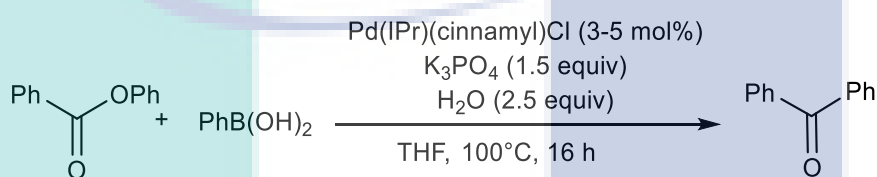


Figure 2.4 Suzuki-Miyaura Reaction of Pd(IPr)(cinnamyl)Cl catalyst.

M. T. Reetz and E. Westermann analyzed on Pd-catalysed C-C bond formation Suzuki-Miyaura reactions. (Reetz & Westermann, 2000) In this reaction phenylboronic acid was treated with *p*-bromoacetophenone in presence of Pd(OAc)<sub>2</sub> nanoparticles gave the corresponding product with 93% yield. This reaction introduced a new ligand for metal catalyst apart from the use of traditional phosphine ligand for cross-coupling reactions. Though, in this research the used catalyst amount was 1 mol % but reaction took a very long time (10 h) and conducted at high temperature 130 °C (Fig. 2.5). In the sense of green technology such conditions are not approached as environmentally friendly.

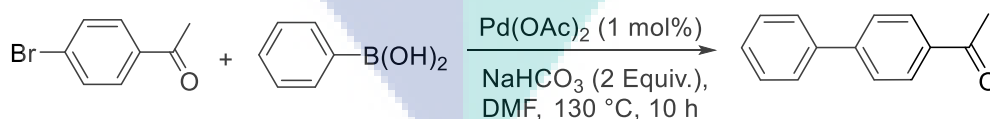


Figure 2.5 Suzuki-Miyaura reaction of Pd (OAc)<sub>2</sub> catalyst.

### 2.5.3 Suzuki-Miyaura Cross-Coupling Reactions using Supported Pd Catalyst

S. M. Islam and coworkers conducted Suzuki-Miyaura reaction using a new polystyrene anchored Pd(II) azo complex heterogeneous catalyst. (SM Islam et al., 2010) This reaction was conducted very smoothly with 0.5 mol % of catalyst, in water media and gave 83-100% of corresponding yields. According to this research (Figure 2.6), the catalyst showed its stability during reaction and easily recycled by simple filtration. Also, it was able to show the catalytic activity more than six times without any significance change of catalytic activity. But reaction progress time was found to be quite long 6-12 hours.

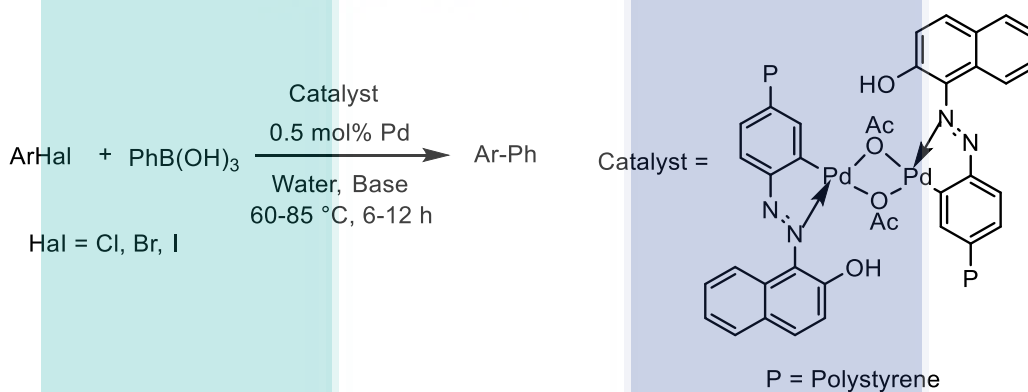


Figure 2.6 Poly styrene anchored-Pd(II) catalyzed Suzuki-Miyaura coupling.

Nano porous ionic liquid supported Palladium acetate (PDVB-[C<sub>3</sub>vim][SO<sub>3</sub>CF<sub>3</sub>]-Pd-xs) was introduced by Fujian Liu and co-researchers (F. Liu et al., 2014). Its efficiency on Suzuki-Miyaura reaction was observed and found to improve reactants enrichment property. This catalyst was synthesized by copolymerization of divinylbenzene and vinylimidazole followed by treatment with Pd(OAc)<sub>2</sub>. This catalyst contained large surface area, high stability excellent recyclable property (six times) and high desired yield (85-99%).

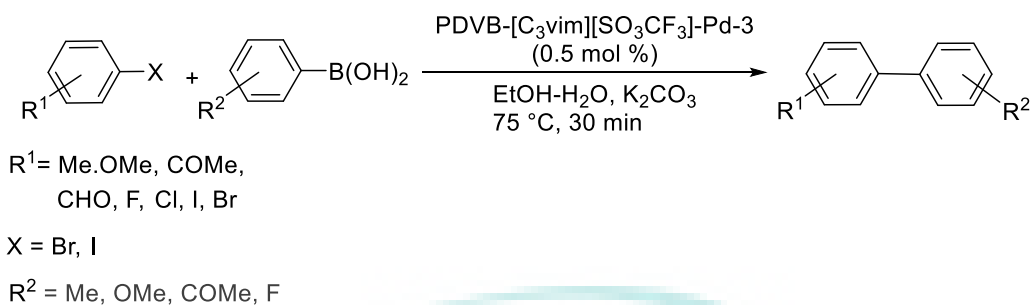


Figure 2.7 Ionic liquid Pd catalyzed Suzuki-Miyaura coupling.

#### 2.5.4 Suzuki-Miyaura Cross-Coupling Reactions using Cellulose Supported Pd Catalyst

Cellulose supported palladium nanoparticles were used by N. Jamwal and his researchers as both heterogeneous and recyclable catalyst for the synthesis of biaryls and polyaryls via Suzuki coupling between aryl bromides and phenyl boronic acid in water at 100 °C to give the corresponding biaryl products 80-96% yields. (Fig. 2.8) Commercially available cellulose was used for this purpose. Though the reaction time is long (12 h) but lower amount of catalyst conducted the reaction with good yields and five times reusability. (Jamwal, Sodhi et al. 2011)

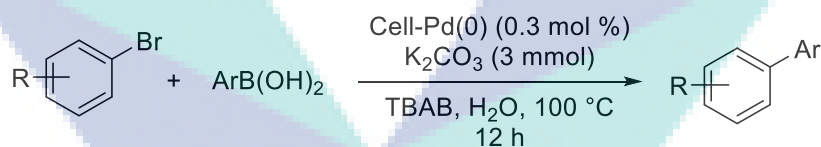


Figure 2.8 Cell-Pd(0) catalyzed Suzuki-Miyaura coupling.

Sanjay Jadhav and his research group applied a different approach for modified catalyst. They synthesized a well-dispersed TiO<sub>2</sub>-Cellulose based palladium nanoparticles (PdNPs@TiO<sub>2</sub>-Cell) through a simple route and observed the catalytic activity in Suzuki-Miyaura reaction at different temperature and in different solvent system. (Fig. 2.9) But the best result was obtained in presence of 95% EtOH solution, K<sub>3</sub>PO<sub>4</sub> as base, 2 mol % catalyst at 80°C, where the yield was 90 %. This catalyst showed reusability four times without disturbing the yield (Jadhav, Jagdale, Kamble, Kumbhar, & Salunkhe, 2016).

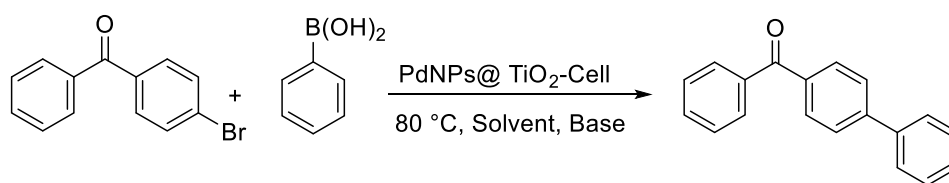


Figure 2.9 TiO<sub>2</sub>-Cellulose supported Pd catalyzed Suzuki-Miyaura coupling.

## 2.6 Aza-Michael Reaction

Due to the formation of carbon nitrogen bond the Aza-Michael reaction appears to be the most versatile one. The Aza-Michael addition reaction of amines and  $\alpha,\beta$ -unsaturated carbonyl compounds has attracted significant attention because of being the most effective methods for the preparation of  $\beta$ -amino carbonyl compounds and their derivatives (Bartoli, Cimarelli, & Palmieri, 1994). These structures serve as essential intermediates in the synthesis of a variety of biologically important natural products, antibiotics, peptide analogues, chiral auxiliaries, and other nitrogen-containing compounds (Surendra et al., 2006).

In Aza-Michael reaction primary amines addition to electron poor alkenes undergo to nucleophilic attack to give secondary and tertiary derivatives. The first product can be the mono-adduct, which may react further to form the tertiary derivative, or bis-adduct. So to maintain the reaction's selectivity and to obtain the desired product primary amines is not always suitable. Most of the literature focused to secondary amines, so that there should have no possibility of second addition. (Camara et al., 2014)

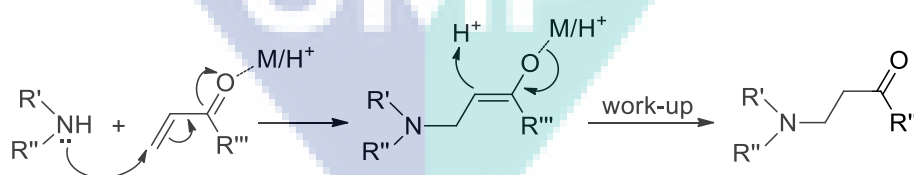


Figure 2.10 Mechanism of Aza-Michael addition reaction.

Usually, Lewis acids, such as AlCl<sub>3</sub> (Ying et al. 2009), PtCl<sub>4</sub>.5H<sub>2</sub>O (Hahn, Szalecki et al. 1978), InCl<sub>3</sub>/TMSCl (Kobayashi, Kakumoto et al. 2002), Bi(NO<sub>3</sub>)<sub>3</sub> (Yang, Xu et al. 2007), samarium iodobinaphtholate, (Didier, Meddour et al. 2011), boric acid (Didier et al. 2011), [Ni(PPP)(THF)](ClO<sub>4</sub>)<sub>2</sub> (Fadini and Togni 2003), Pd(N,N'-ppo)Cl<sub>2</sub>



(Ardizzoia, Brenna et al. 2012), N-heterocyclic carbenes (Kang and Zhang 2011), bases (Yang, Xu et al. 2006) and ionic liquid (Roy and Chakraborti 2010) such homogeneous catalysts were reported for Aza-Michael reactions.

### 2.6.1 Aza-Michael using Homogeneous Catalyst

Neeta Srivastava and her research group underwent to bismuth catalyzed aza-Michael addition reaction to overcome the difficulties of Michael addition reaction product characterization. (Srivastava & Banik, 2003) They introduce a very simple, environment friendly method that also gave significantly high yield.

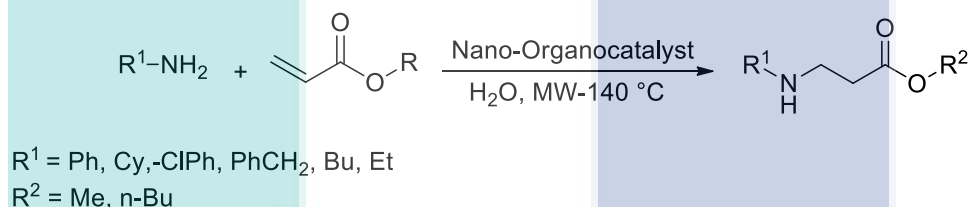


Figure 2.11 Aza-Michael reaction of homogenous  $\text{Bi}(\text{NO}_3)_3$  catalyst.

Conduction of Aza-Michael reaction with a boric acid was considered as safe catalyst by M. K. Chaudhuri and coresearchers (Chaudhuri, Hussain, Kantam, & Neelima, 2005). It was a simple reaction of aromatic amines with  $\alpha,\beta$ -unsaturated halide to give the relative  $\beta$ -amino product 70-92% in water as solvent. The catalyst was recycled and reused for 3-times with relatively high product.

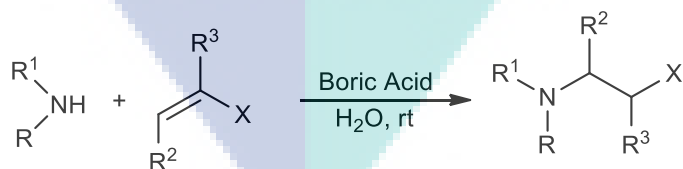


Figure 2.12 Aza-Michael reaction of homogenous boric acid catalyst.

## 2.6.2 Aza-Michael Reactions using Heterogeneous Cu Catalyst

Copper(II) acetylacetonate [Cu (acac)<sub>2</sub>] in ionic liquids, catalyzed the aza-Michael reaction of amines with  $\alpha,\beta$ -unsaturated carbonyl compounds introduced by M. L. Kantam and researchers to produce the corresponding  $\beta$ -amino carbonyl compounds with great yields (98%). (Kantam, Neeraja et al. 2005) The applied amount of [Cu (acac)<sub>2</sub>] was 2 mol % in the ionic liquid and was able to be reused for the several times with constant activity. This methodology worked with great advantages of having a low catalyst loading with easy recycling of catalyst and solvent.

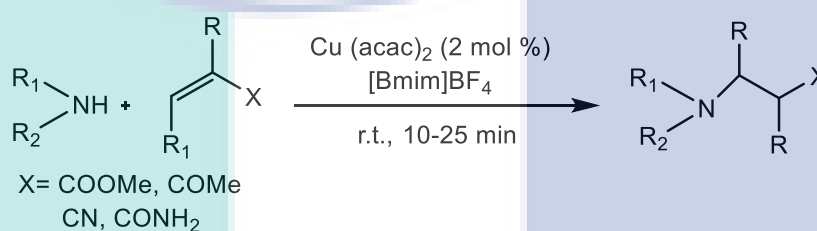


Figure 2.13 Aza-Michael Reactions of amines with  $\alpha,\beta$ -unsaturated compound using Copper(II) acetylacetonate [Cu (acac)<sub>2</sub>].

Copper-catalysis also possesses some indisputable advantages over the other catalytic systems because of having low cost and readily accessible and formation of stable ligands. Copper is used for the synthesis of highly porous metal organic framework (MOF-199) by reaction of copper nitrate trihydrate and 1,3,5-benzenetricarboxylic acid, which has employed as both solid catalyst and catalyst support for multiple organic reactions by Nguyen and his group (Nguyen, Nguyen et al. 2012) It was observed that the aza-Michael reaction of benzylamine with ethyl acrylate proceeded readily in the presence of a catalytic amount of the MOF-199 by employing 5 mol% MOF-199, a conversion of 89% was achieved after 60 minutes and the catalyst was reused several times without any degradation and provide excellent performance in aza-Michael reaction product (Phan, Nguyen et al. 2013).

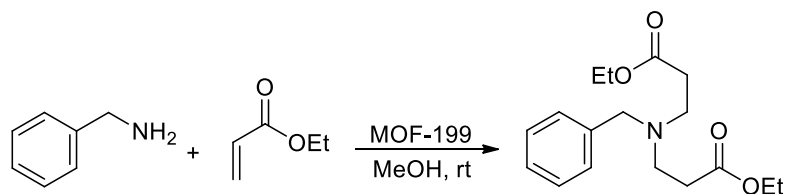


Figure 2.14 Aza-Michael reaction using the MOF-199 catalyst.

### 2.6.3 Aza-Michael Reactions using Supported Cu Catalyst

M. Lakshmi Kantam and co researchers conducted Aza-Michael addition reaction by using Polyaniline (PANI) supported Cu(0) catalyst (Kantam, Roy et al. 2008). Polyaniline is a famous conducting polymer and used for optical applications. (Reynolds, Skotheim et al. 1998) In this work PANI Cu(0) catalyze (2.5 mol%) the reaction between substituted aliphatic amines with electron withdrawing group (EWG) substituted  $\alpha,\beta$ -unsaturated compounds at 60 °C and providing the corresponding yield about 95% (Fig. 2.15). The catalyst was easily separated from the reaction media and reused for seven times.

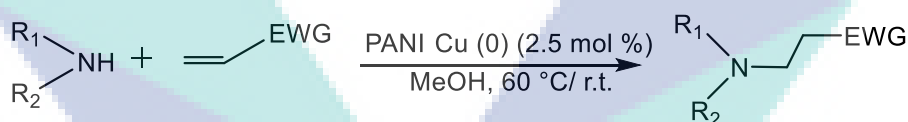


Figure 2.15 PANI-Cu catalyzed aza-Michael reaction.

The polystyrene-supported CuI-imidazole (PS-imCuI) complex catalyst was prepared by Li and co-researchers. (Li, Liu et al. 2012) This catalyst performed in aza-Michael reaction of imidazoles to  $\alpha,\beta$ -unsaturated compounds in 4-8 hours with good yields (95%). PS-imCuI catalyst was used 8.5 mol % and showed excellent reusability property over five cycles without distinct leaching of metal from the support.

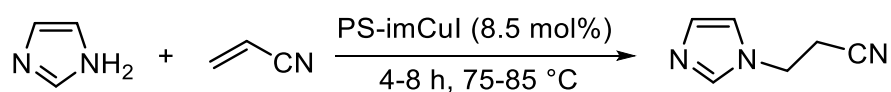


Figure 2.16 Aza-Michael reaction of N-substituted imidazoles using PS-imCuI catalyst.

#### 2.6.4 Aza-Michael Reactions using Cellulose Supported Cu Catalyst

Cellulose supported Cu(0) catalyst was prepared by Rajender Reddy and his group for catalyzing aza-Michael reaction of amines with  $\alpha,\beta$ -unsaturated compounds as Michael acceptor to produce the corresponding  $\beta$  amino compound. (Fig. 2.17) This reaction was conducted by using CELL-Cu(0) catalyst of 1.2 mol % for 0.4 hours on average to give an excellent yield up to 98%. This cellulose supported catalyst also recovered very easily and reused for four times without any significant change (Reddy and Kumar 2006).

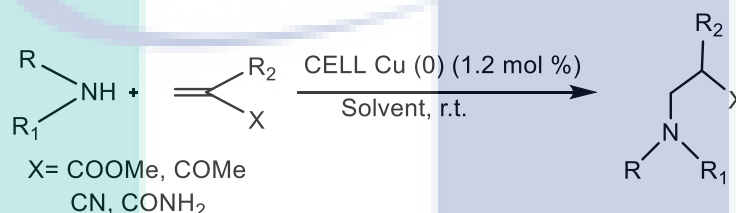


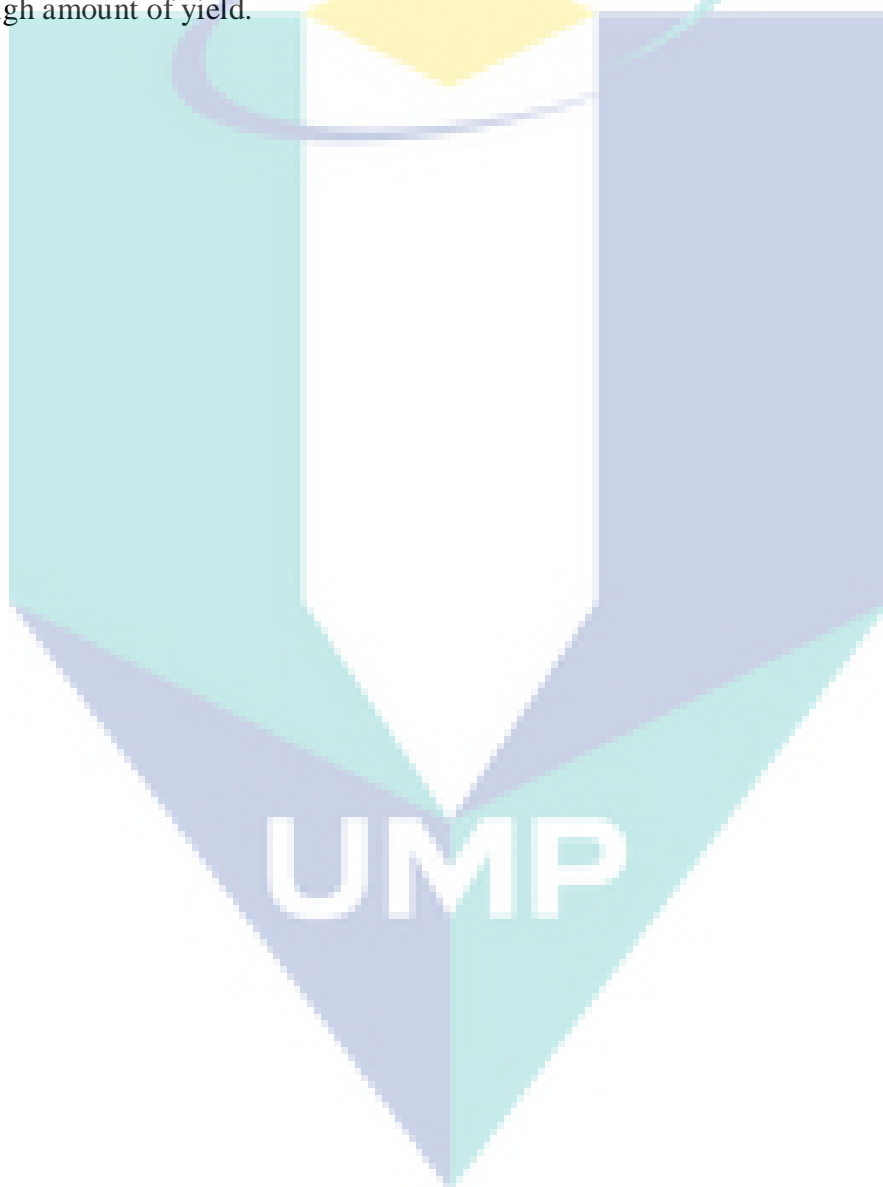
Figure 2.17 Cell-Cu(0) catalyzed aza-Michael reaction.

#### 2.7 Conclusion

The purpose of this literature review was to evaluate how previous researchers have been carried out this C-C and C-N bond formation reactions for Suzuki-Miyaura and aza-Michael reactions using different types of catalysts. In a comparative study of such catalysts it is confirmed that each catalyst might provide its best to give a high yield in each of reaction and some of heterogeneous catalysts showed an excellent activity and reusability. From the literature review, it was clear that the heterogeneous catalyst would be more reliable than the homogeneous catalyst. However, it was found that, heterogeneous catalysts are expensive, toxic, sometimes not sustainable under harsh reaction conditions and not easy to prepare. Therefore, from the green technology aspects, there is still a high demand to pursue more admissible catalysts for chemical transformation reactions.

Keeping this in view, in this report, cellulose supported poly(amidoxime) palladium and copper nanoparticles were synthesized and characterized. With the target of beating the catalytic activity of any previous catalyst. The focus was on the utilization of waste source of cellulose into application as support for green aspects, the

minimum use of catalyst to give maximum yield under mild condition and shorter reaction time. This study creates a great millstone by applying the waste in a very useful way that was beyond of thought. An excellent support of catalyst was prepared and in the application to various reactions, it provides not only a good amount of yield but also reduce the cost for catalyst preparation. The cellulose supported metal (Cu/Pd) nanoparticles were successfully prepared and applied for C-C (Suzuki-Miyaura) and C-N (Aza-Michael) bond formation reactions with regeneration of their catalytic activity and high amount of yield.



## CHAPTER 3

### MATERIALS AND METHODS

#### 3.1 Introduction

The development of non-hazardous chemical processes or methodologies for synthesis of chemical compounds is a challenge to organic chemists. In this context, organic molecules were synthesized under mild reaction condition which rapidly gaining importance because it prohibits the use of many toxic organic chemicals. In the industrial aspects the minimum use of catalyst to obtain the maximum amount of product is considered to be the profitable one. Because of the simplified recovery, recyclability and potential for incorporation in continuous reactors and micro reactors, the development of heterogeneous catalysts is leading over homogeneous counterparts.

#### 3.2 General Information

All reagents and solvents were purchases from commercial suppliers (Aldrich/Merck) and used without any further purification. Water was deionized with a Millipore system as a Milli-Q grade.  $(\text{NH}_4)_2\text{PdCl}_4$  was purchased from Aldrich Chemical Industries, Ltd. The  $^1\text{H}$  NMR (500 MHz) and  $^{13}\text{C}$  NMR (125 MHz) spectra were measured by BRUKER-500 spectrometer, central laboratory, University Malaysia Pahang. The  $^1\text{H}$  NMR chemical shifts were reported relative to *tetra*-methylsilane (TMS, 0.00 ppm). The  $^{13}\text{C}$  NMR chemical shifts were reported relative to  $\text{CDCl}_3$  (77.0 ppm). Inductively coupled plasma atomic emission spectrometry (ICPAES) was performed on a Shimadzu ICPS-8100 equipment by the central laboratory, University Malaysia Pahang. FTIR spectra were measured with a Perkin Elmer (670) spectrometer equipped with an ATR device (ZnSe crystal), FIST, University Malaysia Pahang. The powder X-ray diffraction was carried out by using Bruker D8 Advanced, Central Lab, UMP. The XPS spectra were measured with a Scanning X-ray Microprobe PHI Quantera II, MIMOS, Kuala

Lumpur, Malaysia. FE-SEM was measured with JSM-7800F, central laboratory, University Malaysia Pahang. TEM was measured with HT-7700, Hi-Tech Instruments SDN BHD, Puchong, Malaysia. TLC analysis was performed on Merck silica gel 60 F<sub>254</sub>. Column chromatography was carried out on silica gel (Wakogel C-200).

### 3.3 Research Methodology

The work flow process in this study is shown in a flowchart diagram in Figure 3.1

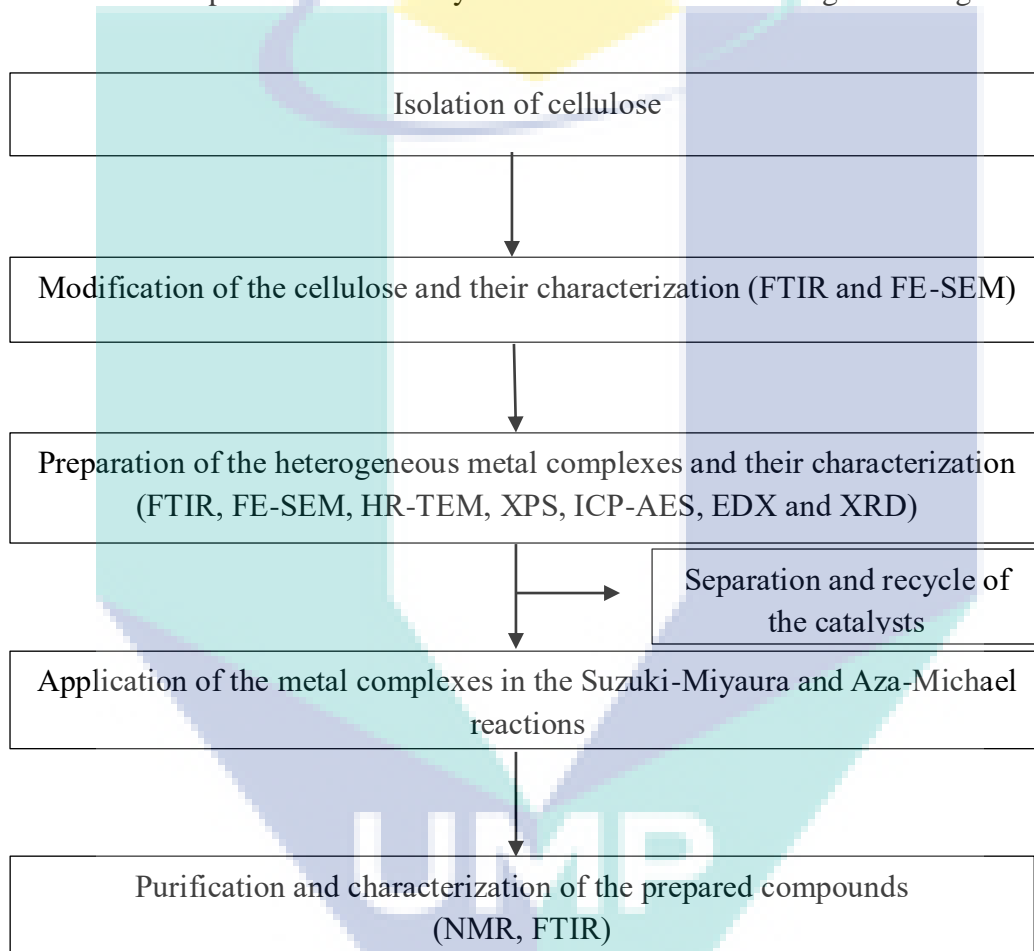


Figure 3.1 Research methodology flow chart.

### 3.4 Characterization of Catalyst Nanoparticles

#### 3.4.1 Fourier Transform Infrared Spectroscopy (FTIR)

In this study, FTIR used for identification of elements and phase of the elements. For example, when water is in liquid phase, the fundamental vibrational modes are at 3219 ( $\nu_1$ ), 1645 ( $\nu_2$ ) and 3405 ( $\nu_3$ )  $\text{cm}^{-1}$ , where in vapor phase the infrared modes appear

at 3652 ( $\nu_1$ ), 1595 ( $\nu_2$ ) and 7765 ( $\nu_3$ )  $\text{cm}^{-1}$ . Another use of FTIR spectroscopy is to detect the functional groups in pure compounds and mixtures, and also for compound comparison. These compounds absorb energy of electromagnetic in the infrared region of the spectrum.

### **3.4.2 Field Emission Scanning Electron Microscope and Energy Dispersive X-Ray (FESEM-EDX)**

The silica nanoparticles morphology was observed using FESEM-EDX. FESEM supplies information of elemental and topographical at magnifications of  $10_x$  to  $300,000_x$  with virtually unlimited depth of field. By comparing with scanning electron microscopy, FESEM-EDX produces clearer image, less electrostatically distorted images with spatial resolution down to  $1 \frac{1}{2}$  nanometers – three to six times better. Other benefits are resolution is great and ease of sample observation and preparation. Energy Dispersive X-Ray (EDX) is an x-ray technique used to identify the elemental composition of materials. EDX systems are attaching to the FESEM instruments where the imaging capability of the microscope identifies the specimen of interest. The data generated by EDX analysis consist of spectra showing peaks corresponding to the elements making up the true composition of the sample being analyzed. In a multi-technique EDX becomes very powerful, particularly in contamination analysis and industrial forensic science investigates.

### **3.4.3 X-Ray Diffraction (XRD) Analysis**

X-ray Diffraction (XRD) Analysis was carried out to determine the crystalline structure and surface elemental compositions cellulose supported poly(amidoxime) Pd and Cu catalyst nanoparticles and reused nanoparticles. XRD is the primary, non-destructive tool for identifying and quantifying the mineralogy of crystalline compounds in rocks, soils and particulates. Every mineral or compound has a characteristic X-ray diffraction pattern whose 'fingerprint' can be matched against a database of over 250000 recorded phases. Modern computer-controlled diffraction systems can interpret the diffraction traces produced by individual constituents and highly complex mixtures. XRD is an essential technique for identifying and



characterizing the nature of clay minerals, providing information which cannot be determined by any other method.

### **3.5 Preparation of Catalyst**

The waste corn-cobs materials (Figure 3.4a) were collected from Gambang, Pahang, Malaysia. The collected waste corn-cob materials were cleaned to remove dust and other contaminants.

#### **3.5.1 Extraction of Cellulose from waste corn-cob**

To extract pure corn-cob cellulose, the corn-cobs were cut into ~2-3 cm sizes and boiled in a 1L beaker with 10% NaOH (450 mL) for 2.5 h and washed with distilled water. To extract the cellulose, 100 g of corn-cob was treated with glacial acetic acid followed by boiling in a 2L beaker with 17% NaOH (800 mL) for 4 hours and then washed with distilled water. The obtained fiber was bleached with H<sub>2</sub>O<sub>2</sub> (500 mL), 7% NaOH (300 mL) and washed several times with distilled water respectively, to remove all access reagents and then dried at 50 °C.

#### **3.5.2 Synthesis of Poly(acrylonitrile) 1**

The graft copolymerization reaction was performed using ceric ammonium nitrate (CAN) as an initiator. Ceric ions initiate free radical sites on the polysaccharide backbone and therefore, minimized the formation of homopolymers (Dahou et al., 2010). The mechanism by which the ceric ion reacts with cellulose materials in the presence of vinyl monomers to produce grafted copolymers has been widely studied.

The graft copolymerization reaction was carried out in one-liter three-neck round bottom flask equipped with a stirrer and condenser in a thermostat water bath. The cellulose slurry was prepared by stirring 6 g of corn-cob cellulose in 150 mL of distilled water overnight. The slurry was heated to 55 °C before the addition of 2.17 mL of diluted sulphuric acid (H<sub>2</sub>SO<sub>4</sub>:H<sub>2</sub>O, 1:1). After 5 min, 2 g of ceric ammonium nitrate (in 10 mL aqueous solution) was added and the reaction mixture was stirred

continuously (Siew et al., 2011). After 20 min, 14 mL of acrylonitrile monomer was added to the cellulose suspension and stirred for 4 h under nitrogen atmosphere. The reaction mixture was cooled and the resulting poly(acrylonitrile) **1** was washed (Figure 3.2) several times with aqueous methanol (methanol:water, 4:1). The poly(acrylonitrile) **1** was oven dried (Fig. 3.2) at 50 °C to a constant weight with a yield of 214 wt.%

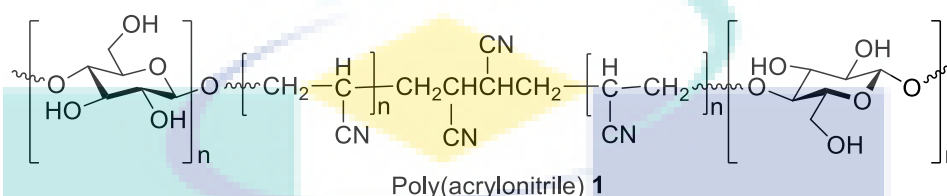


Figure 3.2 Synthesis of poly(acrylonitrile) **1**.

Soxhlet extraction method was used to purify cellulose grafted [poly(acrylonitrile)] by treatment of with dimethylformamide for 12 h. Then, the purified grafted copolymer (cellulose-graft-PAN) was dried at 50 °C to a constant weight. The percentage of grafting (Gp) was determined with the formula  $Gp = W2/W1 \times 100$ , where W1 is the weight of the parent polymer (cellulose) and W2 is the weight of the grafted polymer [poly(acrylonitrile)].

### 3.5.3 Synthesis of Poly(amidoxime) ligand **2**

Hydroxylamine hydrochloride (NH<sub>2</sub>OH·HCl) (20 g) was dissolved in 500 mL of aqueous MeOH (MeOH/H<sub>2</sub>O 4:1) in a 2L beaker with lead and the mixture was neutralized using NaOH solution and the resulting NaCl precipitate was removed by filtration. The pH of the reaction was maintained at pH 11 through adding the NaOH solution and the ratio of methanol and water was maintained at 4:1 (v/v). Then the prepared poly(acrylonitrile) grafted corn-cob cellulose **1** (10 g) was taken into a two-neck round bottom flask furnished with a magnetic stirrer, condenser and thermostatic water bath. After that hydroxylamine solution was then pour into the flask and the reaction was allowed to stir for 4 h at 70 °C. The chelating ligands were filtered and washed by the aqueous methanol. This cellulose based amidoxime ligand was then neutralized with 100 mL of methanolic 0.1 M HCl solution. Finally, the ligand was filtered carefully and washed five times with an aqueous methanol solution and dried in

oven at 50 °C for 6 h to obtain poly(amidoxime) ligand **2** with a yield of 220 wt.% (Lutfor et al., 2001; Siew et al., 2011; Rahman et al., 2014).

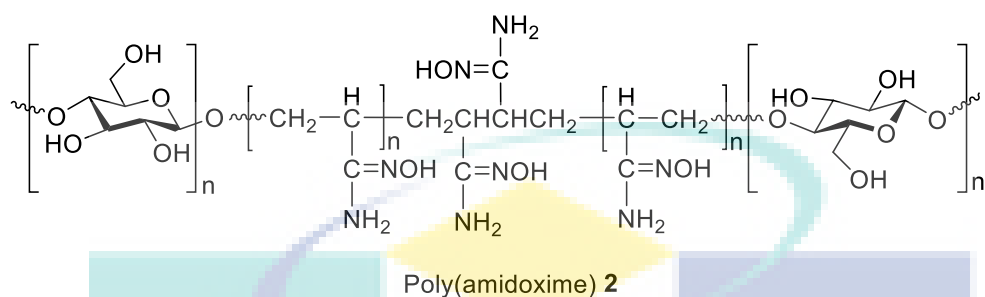


Figure 3.3 Synthesis of poly(amidoxime) **2**.

### 3.5.4 Preparation of the poly(amidoxime) Cu(II) Complex **3**

An aqueous solution of  $\text{CuSO}_4 \cdot 5\text{H}_2\text{O}$  (0.6 g, in 10 mL  $\text{H}_2\text{O}$ ) was added into a stirred mixture of 1 g poly(amidoxime) ligand **2** in 50 mL of water at room temperature. The blue colour  $\text{CuSO}_4$  was turned into green colour and the mixture was stirred for 1.5 h at room temperature. The reaction mixture was then filtrate and washed with excess amount of  $\text{H}_2\text{O}$ , MeOH and dried at 60 °C for 2 h. The ICP-AES analysis revealed that 0.5 mmol  $\text{g}^{-1}$  of Cu was coordinate with the poly(amidoxime) Cu(II) complex **3**.

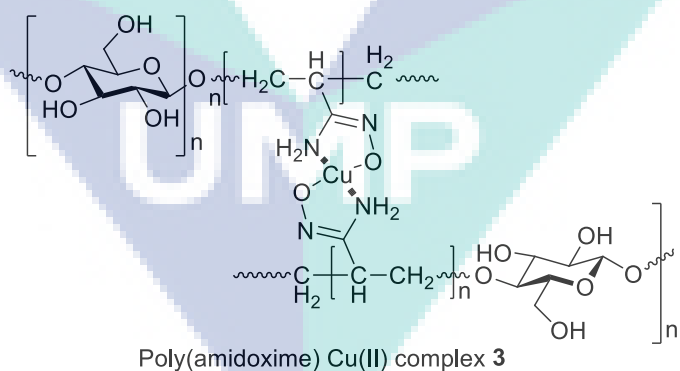


Figure 3.4 Synthesis of poly(amidoxime) Cu(II) complex **3**.

### 3.5.5 Preparation of the Poly(amidoxime) Cu-nanoparticles (CuNs@PA)

Poly(amidoxime) Cu(II) complex **3** (500 mg) was dispersed into 50 mL of water and hydrazine hydrate (0.8 mL) was added. The resulting dark brown colored **CuNs@PA** material was collected by filtration, washed with MeOH, dried under vacuum at 80 °C and stored under nitrogen atmosphere.

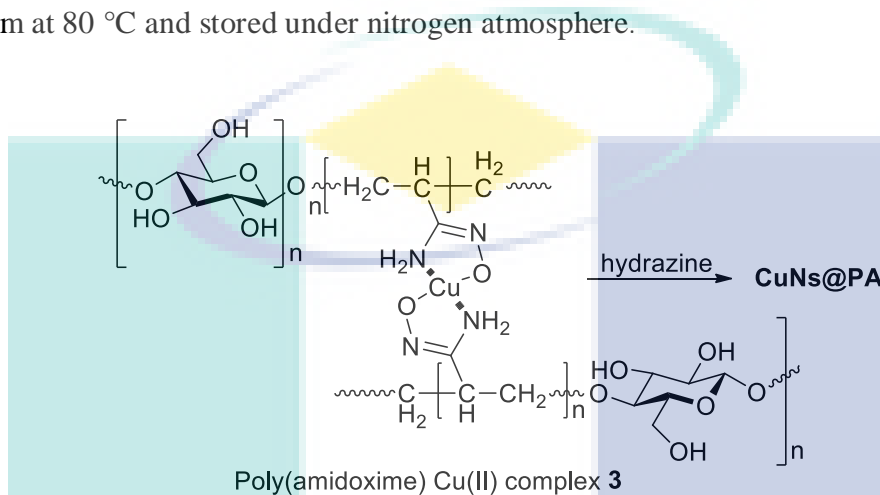


Figure 3.5 Synthesis of poly(amidoxime) **CuNs@PA**.

### 3.5.6 Preparation of the Poly(amidoxime) Pd(II) Complex **4**

To a stirred suspension of **2** (1 g) in 30 mL water, an aqueous solution of  $(\text{NH}_4)_2\text{PdCl}_4$  (250 mg, in 30 mL water) was added. The resulting mixture was stirred for 2 h at room temperature to give light brown color poly(amidoxime) Pd(II) complex **4**. The Pd(II) complex **4** was filtered, washed with water, MeOH and dried at 70 °C for 2.5 h. The ICP-AES analysis revealed that 0.56 mmol  $\text{g}^{-1}$  of palladium was adsorbed onto the poly(amidoxime) Pd(II) complex **4**.

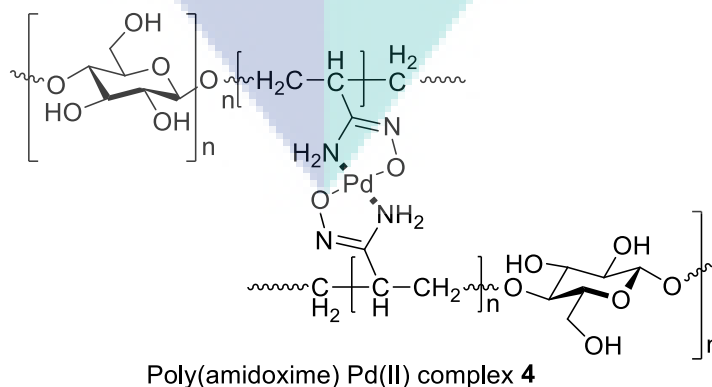


Figure 3.6 Synthesis of poly(amidoxime) Pd(II) complex **4**.

### 3.5.7 Preparation of the Poly(amidoxime) Pd-nanoparticles (PdNs@PA)

The poly(amidoxime) Pd(II) complex **4** (500 mg) was dispersed in 50 mL deionized water and then hydrazine hydrate (1 mL) was added and stirred for 3 h. The resulting black color **PdNs@PA** materials were collected by filtration, washed with excess amount of water, methanol and dried under vacuum at 100 °C. The **PdNs@PA** was stored under nitrogen atmosphere.

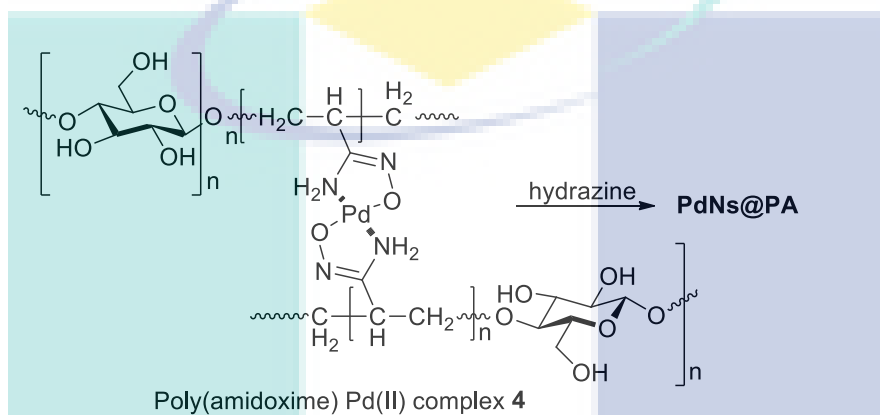
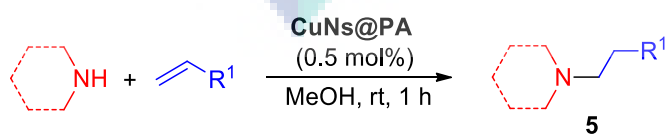


Figure 3.7 Synthesis of poly(amidoxime) PdNs@PA.

### 3.6 General procedure for Aza-Michael Addition Reaction

In a typical experiment, a mixture of amine (1 mmol),  $\alpha,\beta$ -unsaturated Michael acceptor (1.1 mmol), corn-cob cellulose supported **CuN@PA** (0.5 mol%, 10 mg) in 5 mL MeOH was stirred at room temperature for 1 h. The reaction progress was monitored by TLC analysis. After completion of the reaction, **CuNs@PA** was removed by filtration and the filtrate was concentrated to give crude product of Aza-Michael reaction. The crude product was purified by column chromatography (hexane/ethyl acetate) to give the corresponding pure Michael addition product **5**.

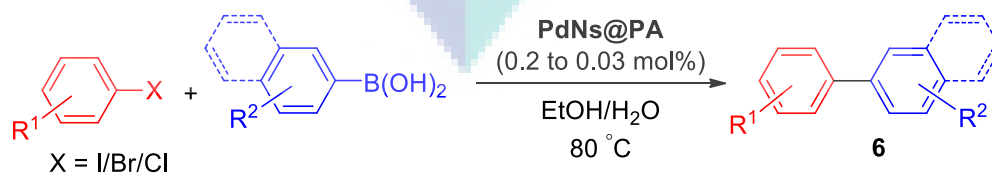


### 3.7 Recycling of the CuNs@PA

A mixture of piperidine (10 mmol), butyl acrylate (1.1 mol equiv), and **CuNs@PA** (1 mol%, 20 mg) in 5 mL MeOH was stirred at room temperature for 1 h. After completion of the reactions, it was centrifuged and the organic layer was separated by decantation. The **CuNs@PA** remained inside the flask which was washed with methanol, dried at 80 °C under vacuum. Then the flask having **CuNs@PA** was charged again with piperidine, butyl acrylate, methanol (5 mL) and the reaction was carried out under the identical reaction conditions. This recycle process was continued up to seven times.

### 3.8 General Procedure for Suzuki-Miyaura Reaction

To conduct the Suzuki-Miyaura reaction, cellulose supported poly(amidoxime) Pd complex catalyst, **PdNs@PA** (0.2 to 0.03 mol%) was added to a mixture of aryl halide (1.0 mmol), arylboronic acid (1.2 mmol), K<sub>2</sub>CO<sub>3</sub> (2 mmol) in aqueous ethanol (1:1, 2 mL), in a 5 mL glass vial and the reaction mixture was stirred at 80 °C. The reaction progress was monitored by TLC analysis after each 30 mins. After completion of the reaction, obtained from TLC analysis, the catalyst, **PdNs@PA** was removed by filtration using syringe filter and the filtrate was washed with ethyl acetate 3 times by 3 mL of ethyl acetate (3 × 3 mL). It should be noted that from the TLC analysis no trace of any byproduct found. Whenever ethyl acetate was added in the filtrate, two layers was formed. The upper layer was organic layer and the down one was water layer. Thus after adding ethyl acetate, the organic layer was dissolved in the ethyl acetate and he ethyl acetate layer was separated and concentrated under reduced pressure. The crude product was purified by silica gel column chromatography to give the corresponding biaryl coupling product mentioned as **6**.



$$\text{Yield} = \frac{\text{wt. of product after column chromatography}}{\text{theoretical yield of the product}} \times 100\%$$

### 3.9 Recycling of the PdNs@PA

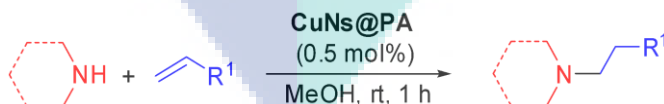
A mixture of 4-bromoanisole (1 mmol), phenylboronic acid (1.2 mol equiv), and PdNs@PA (10 mg) in 2 mL aqueous ethanol was stirred at 80 °C for 3 h. After completion of the reactions, the insoluble PdNs@PA was separated by simple filtration, washed with methanol and dried. The recycle PdNs@PA was used in the next reaction without changing the reaction conditions. This recycle process was continued up to six times.

### 3.10 Calculation of Yield and Mole Percent

To calculate the yield of the product, the following equation was used. The raw product was purified by column chromatography using silica gel as stationary phase. The obtained product was then dried and weight was measured. The theoretical yield mainly obtained from the theoretical reaction product. Thus the ratio of pure obtained product and theoretical product from the same reaction multiplied by 100 to detect the yield percentage of any reaction.

$$\text{Yield} = \frac{\text{wt. of product after column chromatography}}{\text{theoretical yield of the product}} \times 100\%$$

Mole percent of any catalyst depend on the reactant and the amount of catalyst used. For example, in the following reaction 10 mg of CuN@PA was used in a reaction of 1 mmol piperidine a substituted diene. From the ICP analysis it was found that 0.5 mmol g<sup>-1</sup> of Cu was coordinated with the poly(amidoxime) Cu(II) complex.



So the mol% of Cu can be calculated as

$$\begin{aligned} 10 \text{ mg Cu} &= \frac{0.5 \times 10}{1000} \times 100 \\ &= 0.5 \text{ mol\%} \end{aligned}$$

## CHAPTER 4

### RESULT AND DISSCUSSION

#### 4.1 Introduction

This chapter discusses the synthesis, characterization of **CuNs@PA/PdNs@PA** catalysts and application of the catalysts towards Suzuki-Miyaura (**PdNs@PA**) and Aza-Michael (**CuNs@PA**) reactions. The catalysts were well characterized using various analysis techniques such as FTIR, XRD, FE-SEM, EDX, ICP-AES, TEM and XPS. The reusability of the catalysts were also performed and found that no metals were leached out from the cellulose support. It was further confirmed by hot filtration and ICP-MS analyses. For the development of greener processes, reactions using heterogeneous catalysts would be favored in terms of the ease of handling, simple workup, recyclability and reusability. The waste corn-cob cellulose supported metal catalysts were found not only very promising but also an active heterogeneous catalyst towards Suzuki-Miyaura and Aza-Michael in terms of environmental and performance aspects.

#### 4.2 Synthesis and Characterization of CuNs@PA

The waste corn-cobs were collected from Gambang, Pahang, Malaysia. The waste corn-cobs were made into small pieces and boiled with 10% NaOH and glacial acetic acid for 4 h and 2 h respectively. The resulting cellulose fiber was washed with H<sub>2</sub>O and bleached with H<sub>2</sub>O<sub>2</sub> and 5% NaOH respectively. The obtained white color cellulose was graft co-polymerized with acrylonitrile using ceric ammonium nitrate (CAN) as an initiator to afford cellulose supported poly(acrylonitrile) **1** (Figure 4.1).



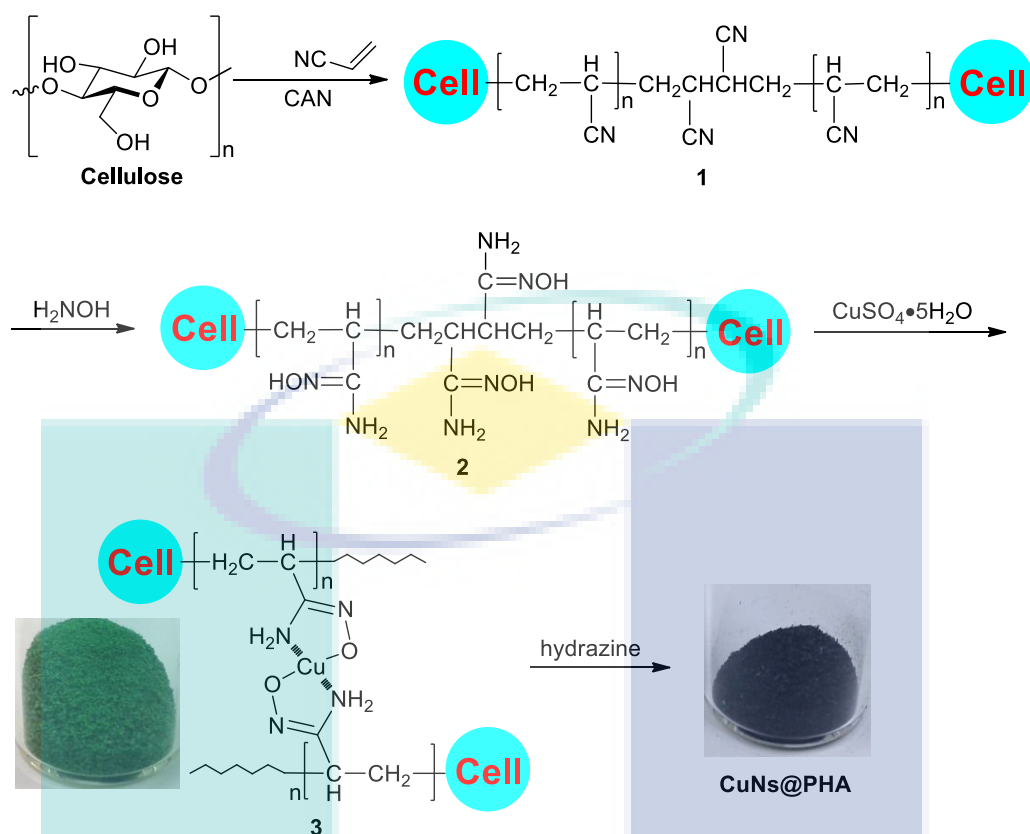


Figure 4.1 Synthesis of waste corn-cob cellulose-supported CuNs@PA.

#### 4.2.1 Fourier Transform Infrared Spectroscopy (FTIR) Analysis of poly(amidoxime) Cu complex 3

FTIR analysis of poly(amidoxime)Cu complex was indicated in Fig. 4.2. The IR absorption bands of cellulose showed at 3438 cm<sup>-1</sup> and 2921 cm<sup>-1</sup> for O-H and C-H stretching, respectively (Fig. 4.2a). A small peak at 1426 cm<sup>-1</sup> belongs to the CH<sub>2</sub> symmetric stretching. A small peak at 1376 and a broad band at 1160 cm<sup>-1</sup> showed for C-O stretching. The C-O-C pyranose ring skeletal vibration gives a strong band at 1065 cm<sup>-1</sup>. The IR spectrum of acrylonitrile-grafted cellulose **1** exhibited a new absorption band at 2244 cm<sup>-1</sup> attributed to the CN stretching of nitrile (Fig. 4.2b).

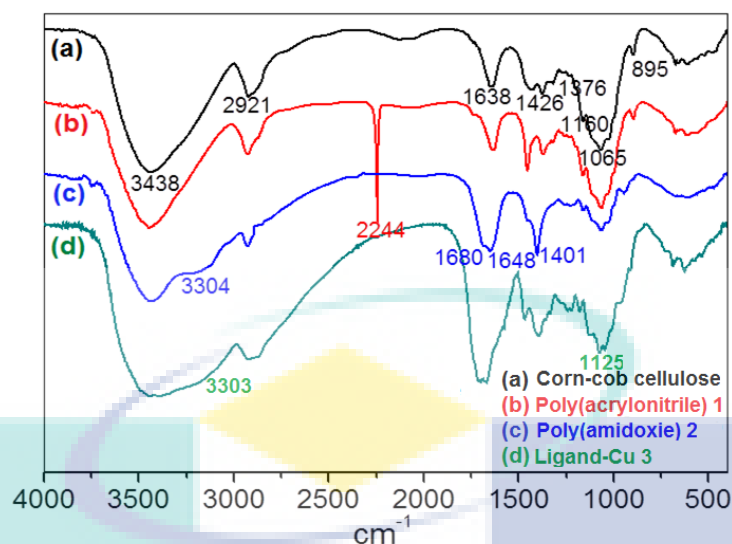


Figure 4.2 FTIR spectra of cellulose and modified cellulose.

The poly(acrylonitrile) **1** was further reacted with hydroxylamine provided poly(amidoxime) chelating ligand **2**. The poly(amidoxime) chelating ligand showed new absorption bands at 1680 and 1648  $\text{cm}^{-1}$  correspond to the C=N stretching and N-H bending modes, respectively. In addition, a shoulder created at 3304  $\text{cm}^{-1}$  for N-H and OH stretching bands and 1401  $\text{cm}^{-1}$  for bending. A clear evidence for the CN band for 2244  $\text{cm}^{-1}$  (Fig. 4.1c) was disappeared and a new absorption bands for amidoxime group was appeared, which confirmed the successful production of poly(amidoxime) function onto the corn-cob cellulose grafted copolymers (Sarkar & Rahman, 2017). The poly(amidoxime) **2** amino functional group was then treated with aqueous copper sulfate at room temperature (25 °C) to give green color poly(amidoxime) copper complex **3** (Fig. 4.2d).

The copper complex **3** was treated with hydrazine hydrate (Huang, Li et al. 2011) to give dark brown color copper **CuNs@PA** nanoparticles which were stabilized by the poly(amidoxime) chelating ligand. Figure 4.2 showed the photographic images of waste corn-cob, corn-cob cellulose, poly(amidoxime) copper complex **3**, and **CuNs@PA** respectively.

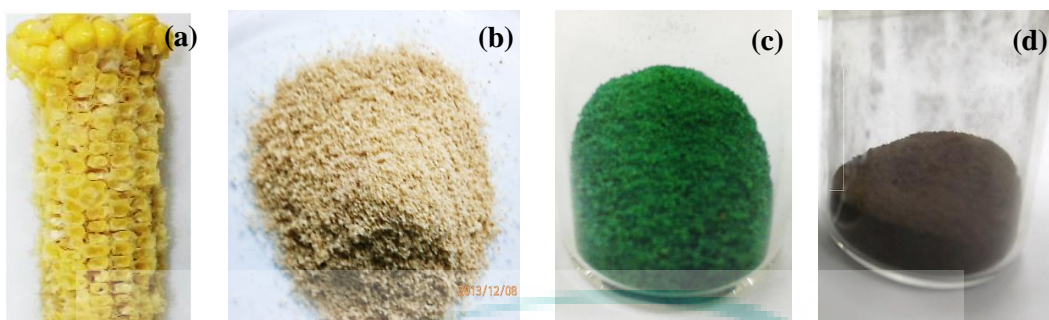


Figure 4.3 (a) Photo image of waste corn-cob, (b) Photo image of **2**, (c) Photo image of **3**, (d) Photo image of CuNs@PA.

#### 4.2.2 Field Emission Scanning Electron Microscopy (FE-SEM) Images of Ligand **2**, Cu(II) Complex **3**

The FE-SEM micrograph of the corn-cob cellulose showed unsmooth morphologies including fine crystalline surface (Fig. 4.17a). The FE-SEM micrograph of the poly(acrylonitrile) grafted corn-cob cellulose **1** showed spherical shape beads structure which is distinguishable surface of corn-cob cellulosic fine crystalline structure and it is clear evidence for grafting occurred on the cellulosic materials (Fig. 4.4b). The poly(amidoxime) chelating ligand **3** showed distinct morphologies with finest beads structure looks small gain like structure (Fig. 4.4c). The SEM micrograph of poly(amidoxime) ligand after adsorption of CuSO<sub>4</sub> is compact surface (Fig. 4.4d), which is different with finest beads structure of **2** (Fig. 4.17c). The EDX analysis of **3** indicated the presence of copper on to the poly(amidoxime) ligand (Fig. 4.5).

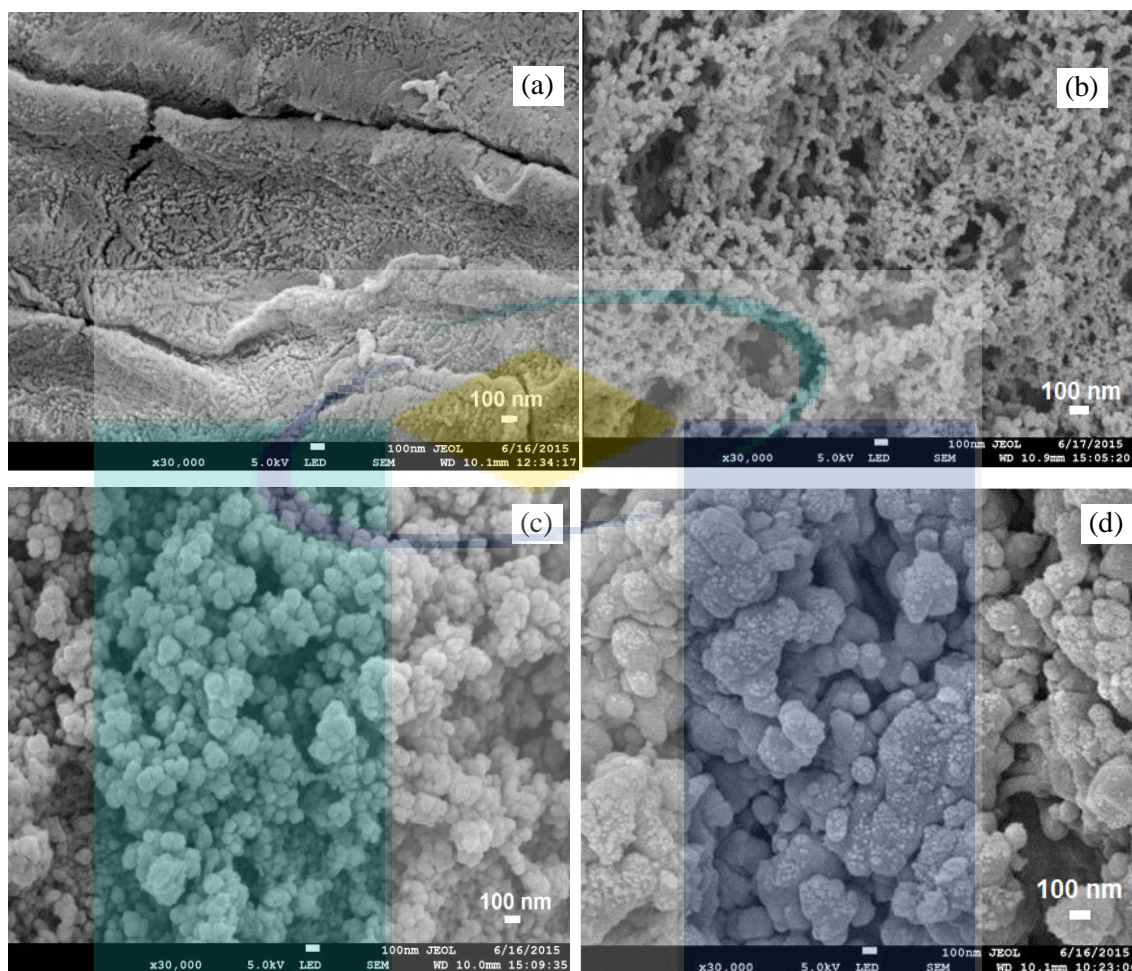


Figure 4.4 SEM images of (a) cellulose, (b) cellulose supported poly(acrylonitrile) **1**, (c) poly(amidoxime) ligand **2**, and (d) poly(amidoxime) copper complex **3**.

#### 4.2.3 Energy-Dispersive X-Ray Spectroscopy (EDX) of Cu(II) Complex **3**

Additionally, the EDX analysis of poly(amidoxime) Cu(II) complex **3** further confirmed the presence of copper species in the cellulose-supported poly(amidoxime) Cu(II) complex **3** (Fig. 4.5).

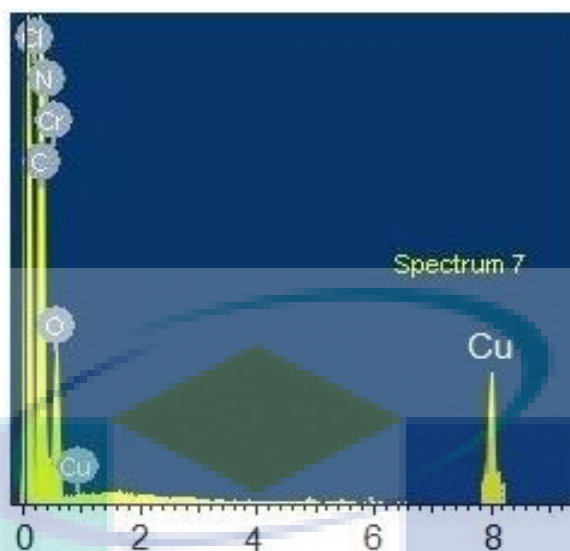


Figure 4.5 EDX image of poly(amidoxime) Cu(II) complex **3**.

#### 4.2.4 High-Resolution Transmission Electron Microscopy (HR-TEM) Images of Cu(II) complex **3** and CuNP@PA

To determine the size of copper complex **3**, TEM analysis was carried out and found that the average copper complex size was  $15 \pm 3$  nm. TEM was measured with HT-7700, Hi-Tech Instruments SDN BHD, Puchong, Malaysia. This spectroscopic analysis proved that the presence of copper ion onto the cellulose surface (Fig. 4.6a). XPS spectra were measured with a Scanning X-ray Microprobe PHI Quantera II, MIMOS, Kuala Lumpur. The full scan XPS analysis of **3** was further confirmed the presence of copper, oxygen, carbon and nitrogen atoms onto the cellulose surface (Fig. 4.6b). The narrow scan XPS analysis of **3** shown a peak at 934.6 eV for Cu 2p<sub>3/2</sub> (Fig. 4.6c) which is assigned as Cu(II) (Yamada, Sarkar et al. 2012). These results suggest that the poly(amidoxime) ligand **2** was coordinated with Cu(II) to give the polymeric cellulose supported Cu(II) complex **3**.

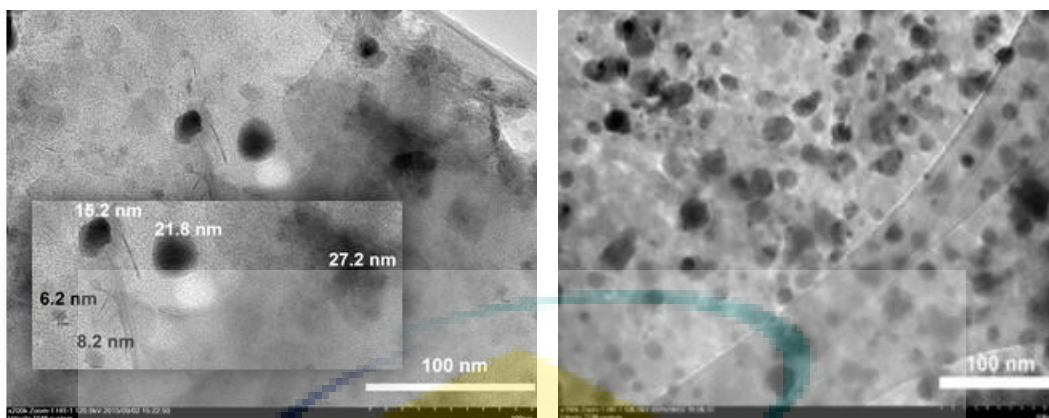


Figure 4.6 (a) TEM image of Cu(II) complex **3** and (b) **CuNs@PA**.

The TEM analysis of **CuNs@PA** showed well dispersion of copper nanoparticles onto the polymeric cellulose (Fig. 4.6b). The copper nanoparticles sized were calculated and found that the average particles size was  $\text{Ø} = 6.8 \pm 2 \text{ nm}$  (Fig. 4.7).

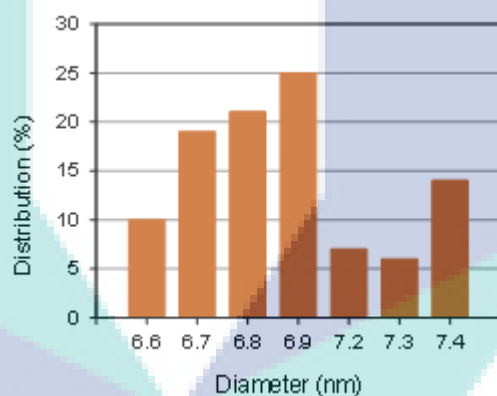


Figure 4.7 Size distribution of the **CuNP@PA** (the sizes were determined for 100 nanoparticles selected randomly).

The HR-TEM image of the **CuNP@PA** demonstrated that it was well dispersed on the cellulose backbone (Figure 4.6) and the nanoparticles were stabilized by the amidoxime functional group as well as the cellulose backbone itself and size distribution were shown in Fig. 4.7.

#### 4.2.5 X-Ray Powder Diffraction (XRD) of Cu(II) Complex 3, Fresh and Reused CuNP@PA

The powder X-ray diffraction study of cellulose-supported poly(amidoxime) fresh CuN@PA nanoparticles showed Bragg's reflections at  $2\theta = 43.6, 50.5,$  and  $74.5$  which were attributable to Cu(0) Cu(111), Cu(200), and Cu(220) phases (Gholinejad & Jeedi, 2014). After Aza-Michael reaction, the X-ray diffraction study of the reused CuN@PA was also carried out and from the XRD pattern of reused CuN@PA, similar Bragg's reflections planes with fresh CuN@PA were obtained (Fig. 4.8).

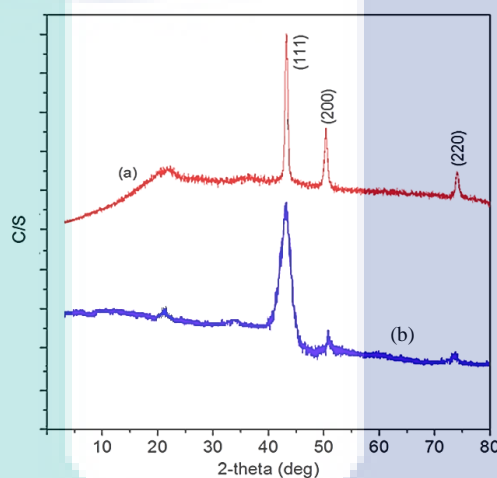


Figure 4.8 XRD pattern of (a) fresh CuN@PA and (b) reused CuN@PA.

#### 4.2.6 X-Ray Photoelectron Spectroscopy (XPS) of Poly(amidoxime) Cu(II) Complex 3 and CuNP@PA

To determine the size of copper complex **3**, TEM analysis was carried out and found that the average copper complex size was  $15 \pm 3$  nm. TEM was measured with HT-7700, Hi-Tech Instruments SDN BHD, Puchong, Malaysia. This spectroscopic analysis proved that the presence of copper ion onto the cellulose surface (Fig. 4.9a). XPS spectra were measured with a Scanning X-ray Microprobe PHI Quantera II, MIMOS, Kuala Lumpur. The full scan XPS analysis of **3** was further confirmed the presence of copper, oxygen, carbon and nitrogen atoms onto the cellulose surface (Fig. 4.9b). The narrow scan XPS analysis of poly(amidoxime) Cu(II) complex **3** shown a peak at 934.6 eV for Cu  $2p_{3/2}$  (Fig. 4.9c) which is assigned as Cu(II) (Yamada, Sarkar,

& Uozumi, 2012). These results suggest that the poly(amidoxime) ligand **2** was coordinated with Cu(II) to give the polymeric cellulose supported Cu(II) complex **3**. The XPS spectrum of **CuNs@PA** showed two peaks at Cu2p<sub>3/2</sub> 951.4 eV and Cu2p<sub>3/2</sub> 932.1 eV (Fig. 4.6a) which were obtained for the binding energy of Cu(0). The obtained values were match with the reported literature (Prenesti and Berto 2002).

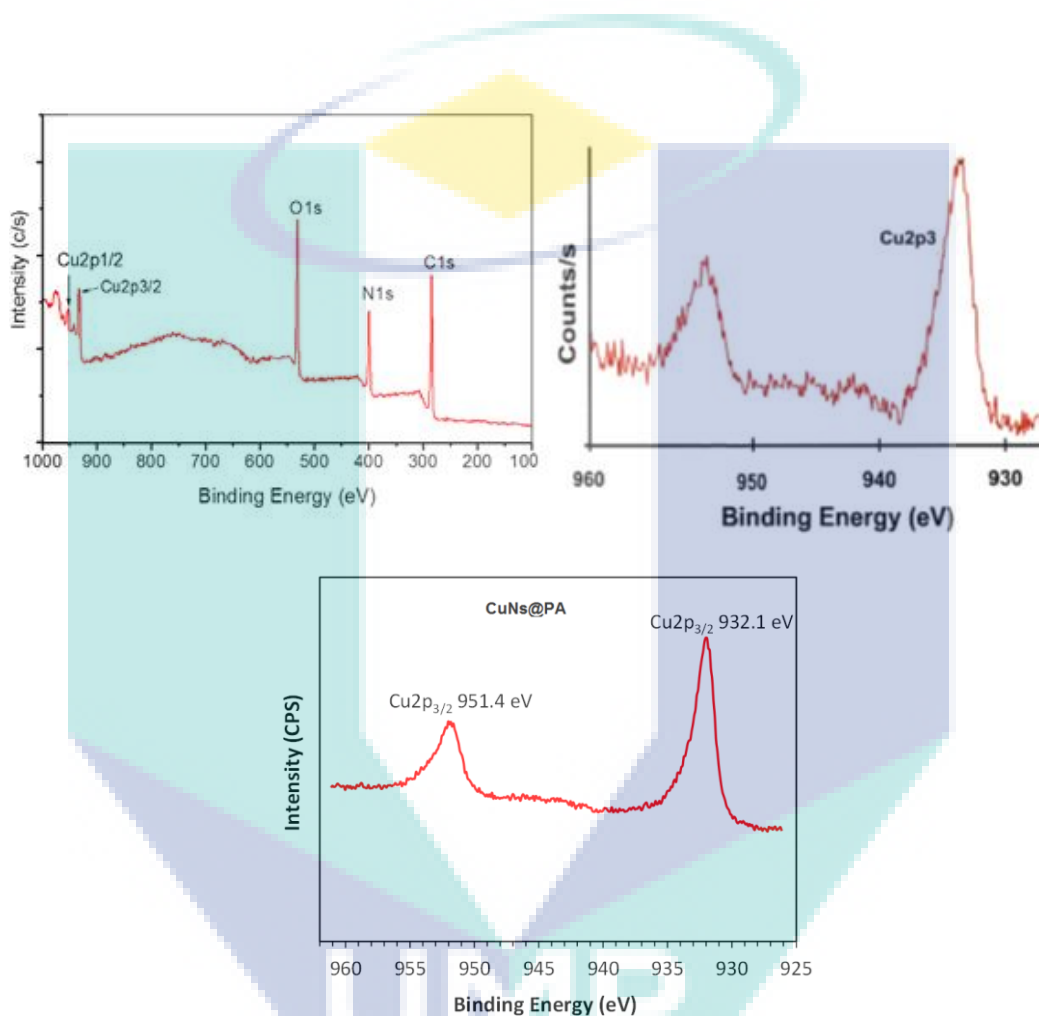


Figure 4.9 (a) full XPS of fresh poly(amidoxime) Cu(II) complex **3**, (b) narrow scan XPS of fresh poly(amidoxime) Cu(II) complex **3** and (c) **CuNs@PA**.

An UV-Vis absorption spectrum showed a peak at 694 nm (Yamada, Sarkar et al. 2012) which indicated the formation of poly(amidoxime) Cu(II) complex **3** (Fig. 4.10).



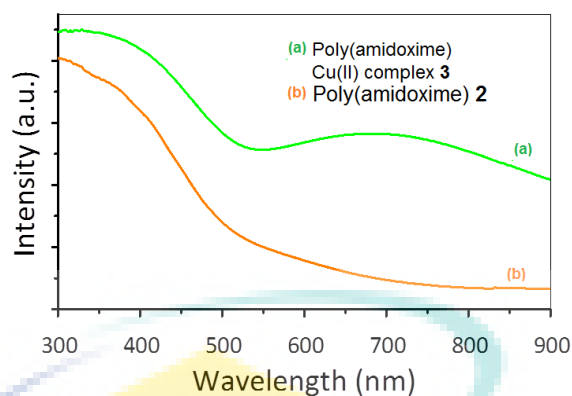
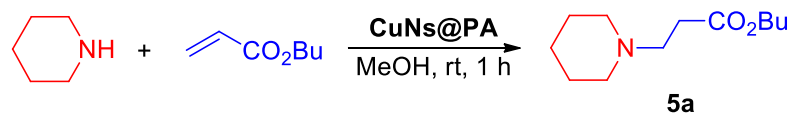


Figure 4.10 UV-Vis of poly(amidoxime) **2** and poly(amidoxime) Cu(II) complex **3**.

### 4.3 Aza-Michael Addition Reaction

Aza-Michael addition reaction of amine and  $\alpha,\beta$ -unsaturated Michael acceptor was considered to find the catalytic activity of the prepared kenaf cellulose supported **CuNs@PA** and the addition reaction between piperidine and butyl acrylate was taken as a model reaction at room temperature to screen the optimum catalyst loading of **CuNs@PA**. Table 4.1 presents the results of the effect of catalyst amounts. Initially, 5 mol% of **CuNs@PA** was used as a catalytic dose. The **CuNs@PA** efficiently conducted the reaction to give the corresponding addition product **5a** in 96% yield at room temperature in MeOH. (Run 1). When the loading of **CuNs@PA** was reduced to 2.5 mol% the corresponding product 93% was achieved (Run 2). When the loading of **CuNs@PA** is further decreased 1 to 0.5 mol%, the yield of the product was not significantly changed (Run 3 & 4). The catalyst loading was again decreased to 0.05 mol% (1 mg) which also effectively forwarded the addition reaction with lower yield of the product (Run 5). The further decrease of the catalyst loading was not carried out due to the sensitivity of the electric balance. The Aza-Michael reaction was also carried out using copper complex **3** to ensure that the **CuNs@PA** is necessary to promote the Aza-Michael reaction. It is interesting to notice that Aza-Michael addition reaction carried out using **3** which generated only 8% yield of **5a** (Run 6). Thus the activity of nano-sized cellulose supported Cu catalyst (**CuNs@PA**) was easily obtained.

Table 4.1 Catalyst screening of the Aza-Michael addition reaction<sup>[a]</sup>



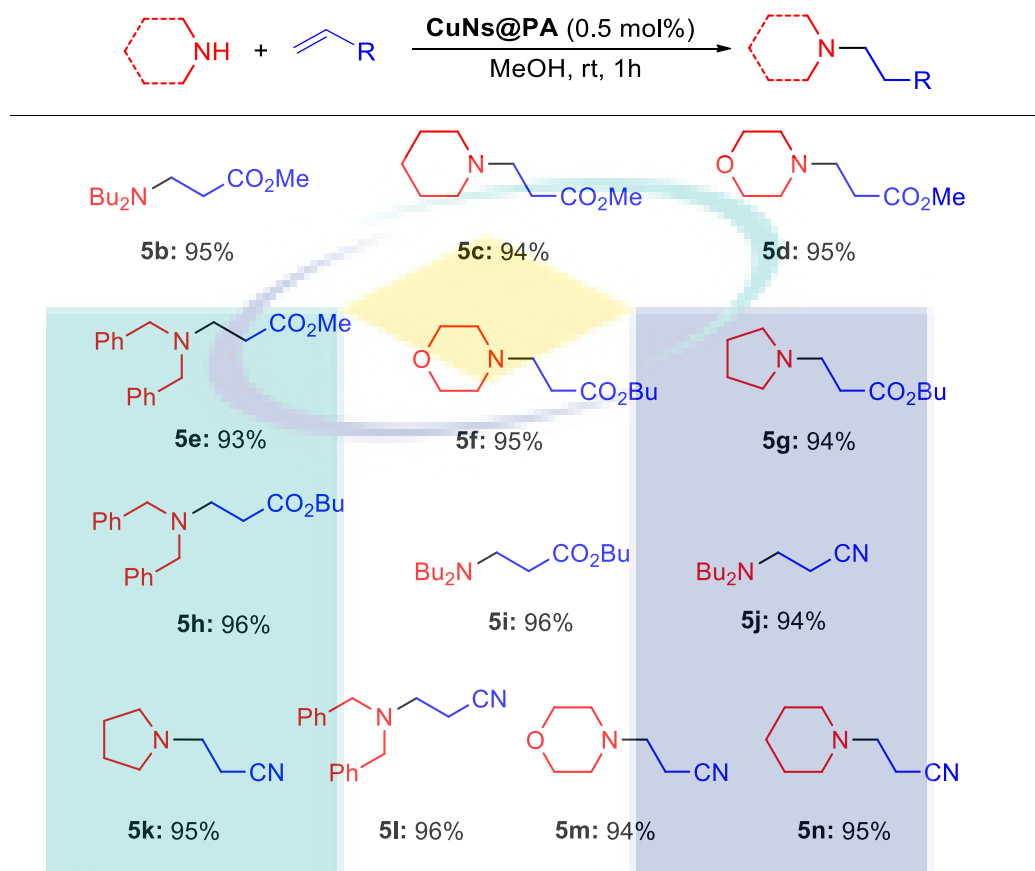
Run	Catalyst (mol%)		Yield (%) <sup>[b]</sup>
	CuNs@PA	<b>3</b>	
1	5		96
2	2.5		93
3	1		92
4	0.5		93
5	0.05 (1 mg)		84
6 <sup>[c]</sup>	-	<b>3</b> (1 mg)	8

<sup>[a]</sup>Reactions were carried using 1 mmol of piperidine, 1.1 mmol of butyl acrylate in 5 mL MeOH at room temperature. <sup>[b]</sup>Yields were determined after column chromatography. <sup>[c]</sup>Reaction was carried out using **3** (1 mg).

When the minimum doses of **CuNs@PA** were established, it was concentrated to find the wide applicability of **CuNs@PA** according to Table 1, Run 4. The Aza-Michael acceptor methyl acrylate was efficiently forward the addition reaction with secondary alicyclic and cyclic aliphatic amine such as dibutylamine, piperidine, morpholine and even sterically hindered secondary dibenzylamine to give the corresponding products in up to 93-95% yields (Figure 4.22, **5b-e**). In the same fashion, relatively bulky butyl acrylate was also efficiently combined with different alicyclic and cyclic amines under the same reaction condition to produce the corresponding Aza-Michael addition products in up to 96% yields (**4e-i**). The  $\alpha,\beta$ -unsaturated Michael acceptor acrylonitrile was also promoted the addition reaction to give the mono alkylated products (**5j-n**) in 94-96% yields.

For example, R. K. Reddy et al. (Reddy and Kumar 2006) reported that, microcrystalline cellulose supported Cu-nanoparticles catalyzed Aza-Michael reaction of primary and secondary amines. In their report, they used 3.6 mol% of the copper nanoparticles and obtained similar results. Wherein, in this research, only 0.5 mol% of **CuNs@PA** was used which was seven times lower than this report. Thus it should be noted that our catalyst has better catalytic activity compared to their report.

Figure 4.11 Aza-Michael addition reaction of amines<sup>a</sup>



<sup>a</sup>Reactions were carried out using 1 mmol of amine, 1.1 mol equiv of Michael acceptor, 0.5 mol% of **CuN@PA** in 2 mL MeOH at room temperature for 1 h.

In addition, it was attempted to synthesis multi alkylated products using **CuNs@PA**. Thus, the Aza-Michael addition reactions of cyclohexylamine and ethylenediamines with  $\alpha,\beta$ -unsaturated compounds (2.2 to 4.4 mol equiv) were carried out under the similar reaction conditions using 1 to 2 mol% of **CuNs@PA**. The multi alkylated Aza-Michael reactions were efficiently promoted to afford the corresponding multi alkylated products **5o-q** with 93-94% yields (Fig. 4.12).

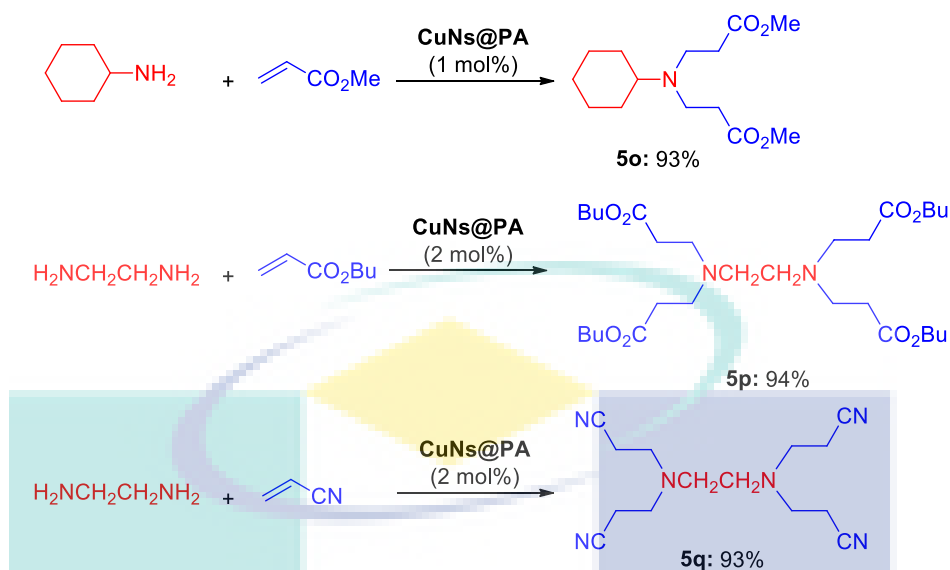
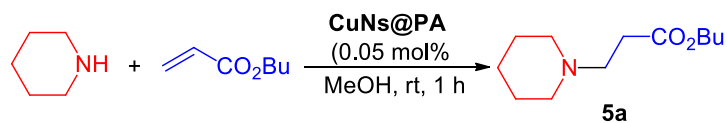


Figure 4.12 Preparation of multi-alkylated products.

#### 4.4 The recyclability of the CuNs@PA catalyst

The recyclability of the catalyst is an important issue in the heterogeneous catalysis system. The CuNs@PA was recovered from the reaction mixture and reused eight times without significant loss of its catalytic performance and the results are summarized in Table 4.2. After completion of the first cycle Aza-Michael reaction of piperidine and butyl acrylate under the identical conditions, the reaction mixture was filtrated and CuNs@PA was washed with methanol. The CuNs@PA was dried at 80 °C under vacuum and used it for the next cycle. The CuNs@PA could be used eight conjugative cycles without significance loss of catalytic activity. Only slight loss of catalytic activity was observed under the same reaction conditions as for initial run. After five cycle, the ICP-AES analysis of the reaction mixture was carried to determine the leaching amount of the copper species. A trace amount of copper species (<0.11 mol ppm of Cu) was found in the reaction mixture (MeOH). Thus, it is reasonable to believe that the cellulose supported copper catalyst can be repeatedly used for large-scale production without significant loss of its catalytic performance.

Table 4.2 Aza-Michael reaction by recycled catalyst **CuNs@PA**<sup>a</sup>



Cycle	Yield (%) <sup>a</sup>	Cycle	Yield (%) <sup>a</sup>
1	94	6	90
2	93	7	88
3	93	8	85
4	91		
5	90 (<0.11 mol ppm Cu was leached out)		

<sup>a</sup>Reaction was carried out using 1 mmol of piperidine, 1.1 mmol of butyl acrylate, 0.5% of **CuNs@PA** in 5 mL of MeOH at room temperature.

Furthermore, the characterization of spent **CuNs@PA** was also carried out. The XPS analysis of **CuNs@PA** showed almost similar peaks at Cu2p<sub>3/2</sub> 950.9 eV and Cu2p<sub>3/2</sub> 931.9 eV (Fig. 4.13) which indicated that, after reaction the oxidation state of Cu(0) was not changed. The TEM analysis of **CuNs@PA** was also confirm that, after reaction the **CuNs@PA** nanoparticles were not aggregated (Fig. 4.14) and found the similar nanoparticles size ( $\varnothing = 7.3 \pm 5$  nm) with fresh **CuNs@PA** ( $\varnothing = 6.8 \pm 2$  nm).

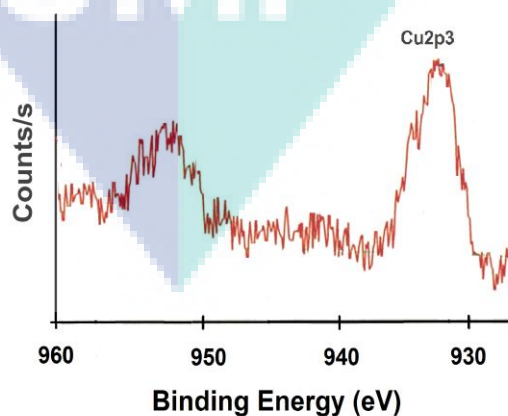


Figure 4.13 XPS image of 4<sup>th</sup> reused of **CuNs@PA**.

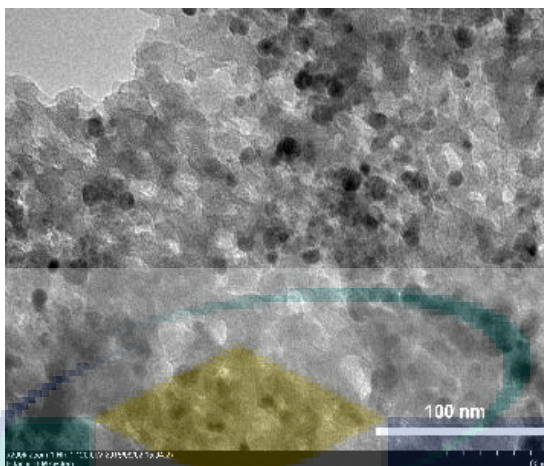
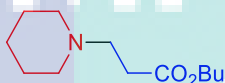


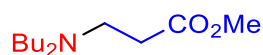
Figure 4.14 TEM image of 4<sup>th</sup> reused of CuNs@PA.

#### 4.5 NMR Analysis of Aza-Michael Products

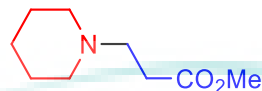
The Aza-Michael Products were characterized using proton nuclear magnetic resonance (<sup>1</sup>H NMR), carbon nuclear magnetic resonance (<sup>13</sup>C NMR). BRUKER-500 spectrometer was used to perform the analysis. To prepare the sample for NMR, 10 mg product was dissolved in a deuterated chloroform (CDCl<sub>3</sub>) and make a clear solution by dissolving the sample completely. Then the solution was taken out with the help of a clean pipette and transferred in a clean NMR tube. The solution depth was kept 4.5-5 cm in the NMR tube. For <sup>13</sup>C and <sup>1</sup>H analysis the same prepared sample was used. The characteristic NMR of every aza-Michael are given as follows.



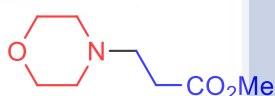
**5a:** <sup>1</sup>H NMR (CDCl<sub>3</sub>, 500 MHz) δ 4.08 (t, *J* = 7.0 Hz, 2 H), 2.65 (t, *J* = 7.0 Hz, 2 H), 2.50 (t, *J* = 7.0 Hz, 2 H), 2.45-2.33 (m, 4 H), 1.62-1.55 (m, 6 H), 1.42-1.36 (m, 4 H), 0.91 (t, *J* = 7.0 Hz, 3 H). <sup>13</sup>C NMR (CDCl<sub>3</sub>, 125 MHz) δ 172.18, 63.31, 53.44, 31.44, 29.82, 25.03, 23.42, 18.25, 12.80.



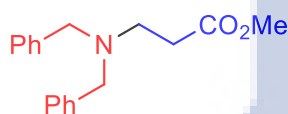
**5b:**  $^1\text{H}$  NMR ( $\text{CDCl}_3$ , 500 MHz)  $\delta$  3.66 (s, 3 H), 2.77 (t,  $J = 7.0$  Hz, 2 H), 2.42 (t,  $J = 7.0$  Hz, 2 H), 2.39 (t,  $J = 7.0$  Hz, 4 H), 1.44-1.38 (m, 4 H), 1.32-1.28 (m, 4 H), 0.90 (t,  $J = 7.0$  Hz, 6 H).  $^{13}\text{C}$  NMR ( $\text{CDCl}_3$ , 125 MHz)  $\delta$  173.16, 53.60, 51.29, 49.36, 32.24, 29.26, 20.53, 13.98.



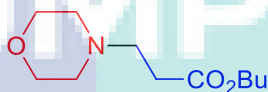
**5c:**  $^1\text{H}$  NMR ( $\text{CDCl}_3$ , 500 MHz)  $\delta$  3.67 (s, 3 H), 2.66 (t,  $J = 7.0$  Hz, 2 H), 2.54-2.50 (m, 2 H), 2.43-2.36 (m, 4 H), 1.61-1.54 (m, 4 H), 1.41-1.40 (m, 2 H).  $^{13}\text{C}$  NMR ( $\text{CDCl}_3$ , 125 MHz)  $\delta$  173.28, 54.35, 53.30, 51.71, 32.08, 25.97, 24.35.



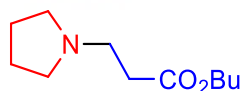
**5d:**  $^1\text{H}$  NMR ( $\text{CDCl}_3$ , 500 MHz)  $\delta$  3.66 (s, 7 H), 2.68 (t,  $J = 7.0$  Hz, 2 H), 2.51 (t,  $J = 7.0$  Hz, 2 H), 2.47-2.44 (m, 4 H).  $^{13}\text{C}$  NMR ( $\text{CDCl}_3$ , 125 MHz)  $\delta$  172.50, 66.62, 53.73, 53.20, 51.36, 31.64.



**5e:**  $^1\text{H}$  NMR ( $\text{CDCl}_3$ , 500 MHz)  $\delta$  7.33-7.27 (m, 8 H), 7.21 (dd,  $J = 7.5$  Hz, 2 H), 3.59 (s, 3 H), 3.55 (s, 4 H), 2.78 (t,  $J = 7.0$  Hz, 2 H), 2.48 (t,  $J = 7.0$  Hz, 2 H).  $^{13}\text{C}$  NMR ( $\text{CDCl}_3$ , 125 MHz)  $\delta$  172.48, 139.14, 128.62, 128.05, 126.81, 57.91, 51.10, 48.99, 32.47.

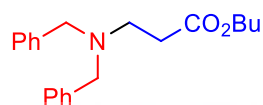


**5f:**  $^1\text{H}$  NMR ( $\text{CDCl}_3$ , 500 MHz)  $\delta$  4.09 (t,  $J = 7.0$  Hz, 2 H), 3.69 (t,  $J = 7.0$  Hz, 4 H), 2.68 (t,  $J = 7.0$  Hz, 2 H), 2.52-2.44 (m, 6 H), 1.63-1.57 (m, 2 H), 1.42-1.36 (m, 2 H), 0.93 (t,  $J = 7.0$  Hz, 3 H).  $^{13}\text{C}$  NMR ( $\text{CDCl}_3$ , 125 MHz)  $\delta$  171.96, 66.52, 63.86, 53.73, 53.12, 31.85, 30.40, 18.81, 13.38.

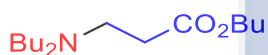


**5g:**  $^1\text{H}$  NMR ( $\text{CDCl}_3$ , 500 MHz)  $\delta$  4.08 (t,  $J = 5.0$  Hz, 2 H), 2.77 (t,  $J = 5.0$  Hz, 2 H), 2.55-2.48 (m, 6 H), 1.80-1.62 (m, 4 H), 1.64-1.57 (m, 2 H), 1.42-1.35 (m, 2 H), 0.94 (t,

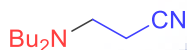
$J = 5.0$  Hz, 3 H).  $^{13}\text{C}$  NMR ( $\text{CDCl}_3$ , 125 MHz)  $\delta$  172.38, 64.08, 53.84, 51.28, 34.05, 30.53, 23.32, 18.98, 13.55.



**5h:**  $^1\text{H}$  NMR ( $\text{CDCl}_3$ , 500 MHz)  $\delta$  7.32 (dd,  $J = 7.5$  Hz, 4 H), 7.28 (dd,  $J = 7.5$  Hz, 4 H), 7.20 (dd,  $J = 7.5$  Hz, 2 H), 4.00 (t,  $J = 7.0$  Hz, 2 H), 3.54 (s, 4 H), 2.79 (t,  $J = 7.0$  Hz, 2 H), 2.47 (t,  $J = 7.0$  Hz, 2 H), 1.54-1.47 (m, 2 H), 1.34-1.28 (m, 2 H), 0.89 (t,  $J = 7.0$  Hz, 3 H).  $^{13}\text{C}$  NMR ( $\text{CDCl}_3$ , 125 MHz)  $\delta$  172.30, 139.19, 128.68, 128.09, 126.84, 64.02, 57.95, 49.17, 32.71, 30.53, 19.04, 13.64.



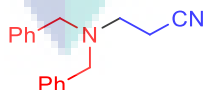
**5i:**  $^1\text{H}$  NMR ( $\text{CDCl}_3$ , 500 MHz)  $\delta$  4.07 (t,  $J = 7.0$  Hz, 2 H), 2.78 (t,  $J = 7.0$  Hz, 2 H), 2.45-2.37 (m, 6 H), 1.63-1.57 (m, 2 H), 1.45-1.41 (m, 6 H), 1.35-1.26 (m, 4 H), 0.93 (t,  $J = 7.0$  Hz, 9 H).  $^{13}\text{C}$  NMR ( $\text{CDCl}_3$ , 125 MHz)  $\delta$  172.89, 53.65, 49.49, 32.48, 30.71, 29.34, 20.60, 19.15, 13.99, 13.65.



**5j:**  $^1\text{H}$  NMR ( $\text{CDCl}_3$ , 500 MHz)  $\delta$  2.77 (t,  $J = 7.0$  Hz, 2 H), 2.44-2.40 (m, 6 H), 1.44-1.39 (m, 4 H), 1.38-1.29 (m, 4 H), 0.91 (t,  $J = 7.0$  Hz, 6 H).  $^{13}\text{C}$  NMR ( $\text{CDCl}_3$ , 125 MHz)  $\delta$  119.05, 53.45, 49.57, 29.44, 20.38, 16.12, 13.90.

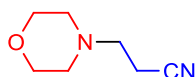


**5k:**  $^1\text{H}$  NMR ( $\text{CDCl}_3$ , 500 MHz)  $\delta$  2.78 (t,  $J = 7.0$  Hz, 2 H), 2.58-2.52 (m, 6 H), 1.80-1.77 (m, 4 H).  $^{13}\text{C}$  NMR ( $\text{CDCl}_3$ , 125 MHz)  $\delta$  119.02, 53.97, 51.45, 23.69, 17.74.

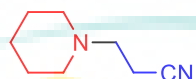


**5l:**  $^1\text{H}$  NMR ( $\text{CDCl}_3$ , 500 MHz)  $\delta$  7.38 (dd,  $J = 7.5$  Hz, 4 H), 7.32 (dd,  $J = 7.5$  Hz, 4 H), 7.24 (dd,  $J = 7.5$  Hz, 2 H), 2.77 (t,  $J = 7.0$  Hz, 2 H), 2.37 (t,  $J = 7.0$  Hz, 2 H).  $^{13}\text{C}$  NMR ( $\text{CDCl}_3$ , 125 MHz)  $\delta$  138.48, 128.60, 128.48, 128.30, 127.16, 118.75, 57.99, 48.56, 16.12.

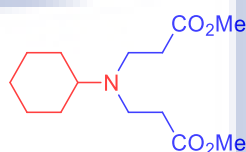




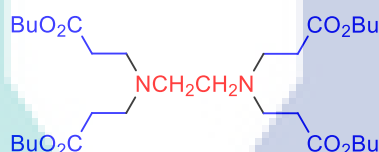
**5m:**  $^1\text{H}$  NMR ( $\text{CDCl}_3$ , 500 MHz)  $\delta$  3.71 (t,  $J = 7.0$  Hz, 4 H), 2.67 (t,  $J = 7.0$  Hz, 2 H), 2.55-2.47 (m, 6 H).  $^{13}\text{C}$  NMR ( $\text{CDCl}_3$ , 125 MHz)  $\delta$  118.61, 66.52, 53.42, 52.86, 15.48.



**5n:**  $^1\text{H}$  NMR ( $\text{CDCl}_3$ , 500 MHz)  $\delta$  2.68 (t,  $J = 7.0$  Hz, 2 H), 2.50 (t,  $J = 7.0$  Hz, 2 H), 2.45-2.39 (m, 4 H), 1.62-1.56 (m, 4 H), 1.44-1.41 (m, 2 H).  $^{13}\text{C}$  NMR ( $\text{CDCl}_3$ , 125 MHz)  $\delta$  119.13, 54.19, 25.86, 24.13, 15.69.



**5o:**  $^1\text{H}$  NMR (500 MHz,  $\text{CDCl}_3$ )<sup>5</sup>:  $\delta$  3.51 (s, 6H), 2.64 (t,  $J = 7.15$  Hz, 3H), 2.28 (t,  $J = 7.13$  Hz, 4H), 1.62-1.44 (m, 6H), 1.07-0.91 (m, 6H).  $^{13}\text{C}$  NMR (125 MHz,  $\text{CDCl}_3$ ):  $\delta$  173.05, 172.95, 68.77, 53.40, 53.39, 52.25, 51.08, 51.07, 49.15, 49.15, 32.03, 29.04, 20.32, 13.73.



**5p:**  $^1\text{H}$  NMR ( $\text{CDCl}_3$ , 500 MHz)  $\delta$  4.06 (t,  $J = 7.0$  Hz, 8 H), 2.77 (t,  $J = 7.0$  Hz, 8 H), 2.52 (m, 4 H), 2.27-2.40 (m, 8 H), 1.67-1.57 (m, 8 H), 1.43-1.34 (m, 8 H), 0.93 (t,  $J = 7.0$  Hz, 12 H).  $^{13}\text{C}$  NMR ( $\text{CDCl}_3$ , 125 MHz)  $\delta$  172.03, 63.72, 51.97, 49.52, 32.43, 30.37, 18.80, 13.32.



**5q:**  $^1\text{H}$  NMR ( $\text{CDCl}_3$ , 500 MHz)  $\delta$  2.92 (t,  $J = 7.0$  Hz, 4 H), 2.85 (t,  $J = 7.0$  Hz, 4 H), 2.70 (s, 4 H), 2.53 (t,  $J = 7.0$  Hz, 8 H).  $^{13}\text{C}$  NMR ( $\text{CDCl}_3$ , 125 MHz)  $\delta$  118.93, 52.92, 52.31, 49.27, 48.00, 46.38, 44.85, 44.62, 18.46, 16.82.

#### 4.6 Preparation and Characterization of PdNs@PA

The waste corn-cob cellulose supported poly(amidoxime) chelating ligand **2** was prepared according to the Figure 4.4. The poly(amidoxime) ligand **2** was mixed with an aqueous solution of  $(\text{NH}_4)_2\text{PdCl}_4$  at room temperature to give light brown colour poly(amidoxime) Pd(II) complex **4**. The Pd(II) complex **4** washed with water and methanol to remove any unreacted palladium species. To determine the loading amount of the palladium species onto Pd(II) complex **4** ICP-AES analysis was carried out and it was showed that  $0.56 \text{ mmol g}^{-1}$  of palladium was anchored onto the poly(amidoxime) ligand **4**. The cellulose supported palladium complex **4** was then treated with hydrazine hydrate (Sreedhar, Yada et al. 2011) to give dark black color PdNs@PA (Fig. 4.15). The PdNs@PA was washed several times with methanol and dried at  $80^\circ\text{C}$  and storage under nitrogen atmosphere.

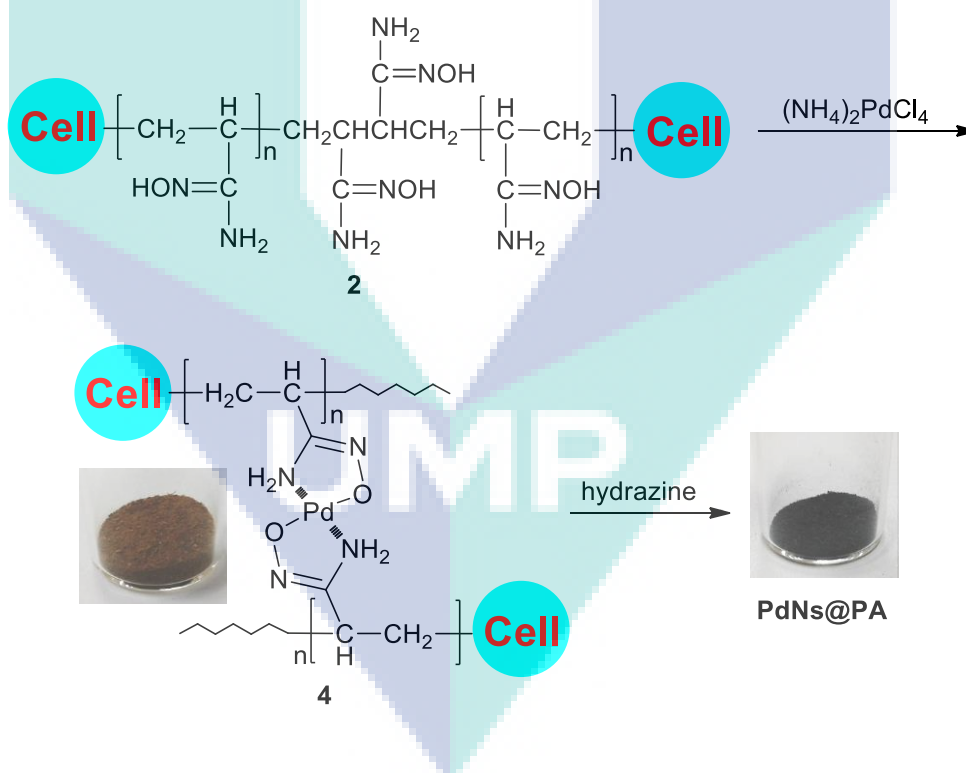


Figure 4.15 Synthesis of PdNs@PA.

#### 4.6.1 Fourier Transform Infrared Spectroscopy (FTIR) Analysis of Cellulose and Modified Celluloses

The isolated cellulose, modified celluloses **1** and **2**, and poly(amidoxime) Pd(II) complex **3** were characterized by PerkinElmer 670 FTIR spectrometer shown in Figure 4.2. and compared with the reported literature (Wen, Siew et al. 2012, Rahman, Rohani et al. 2014). The IR absorption bands of cellulose showed at  $3438\text{ cm}^{-1}$  and  $2921\text{ cm}^{-1}$  for O-H and C-H stretching, respectively (Fig. 4.16a). A small peak at  $1426\text{ cm}^{-1}$  belongs to the  $\text{CH}_2$  symmetric stretching. A small peak at  $1376$  and a broad band at  $1160\text{ cm}^{-1}$  showed for C-O stretching. The C-O-C pyranose ring skeletal vibration gives a strong band at  $1065\text{ cm}^{-1}$ . A small sharp peak at  $895\text{ cm}^{-1}$  corresponds to the glycosidic  $\text{C}_1\text{-H}$  deformation with ring vibration contribution and OH bending, which is characteristic of  $\beta$ -glycosidic linkages between glucose in cellulose. The FTIR spectrum of acrylonitrile-grafted cellulose **1** exhibited a new absorption band at  $2244\text{ cm}^{-1}$  attributed to the CN stretching of nitrile (Fig. 4.16b).

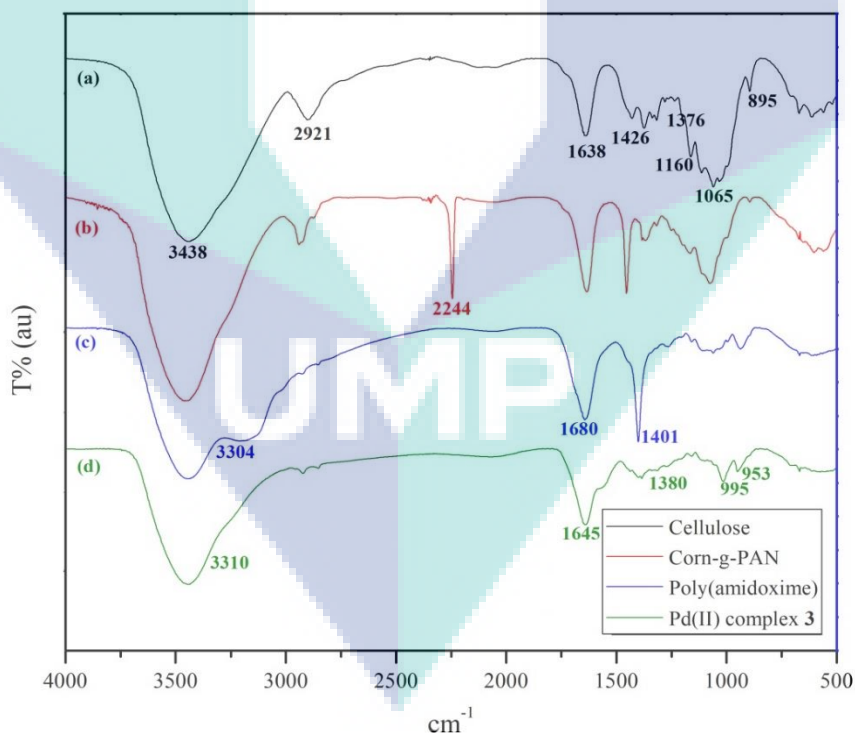


Figure 4.16 FTIR spectra of the (a) corn-cob cellulose, (b) Poly(acrylonitrile) **1** (corn-g-PAN), (c) poly(amidoxime) chelating ligand **2** and (d) poly(amidoxime) Pd(II) complex **4**.

The poly(acrylonitrile) **1** was further reacted with hydroxylamine provided poly(amidoxime) chelating ligand **2**. The poly(amidoxime) chelating ligand showed new absorption bands at 1680 and 1648  $\text{cm}^{-1}$  correspond to the C=N stretching and N-H bending modes, respectively. In addition, a shoulder created at 3304  $\text{cm}^{-1}$  for N-H and OH stretching bands and 1401  $\text{cm}^{-1}$  for OH bending. A clear evidence for the CN band for 2244  $\text{cm}^{-1}$  (Fig. 4.16c) was disappeared and a new absorption bands for amidoxime group was appeared, which confirmed the successful production of poly(amidoxime) function onto the corn-cob cellulose grafted copolymers (Sarkar & Rahman, 2017). This new band confirmed the successful synthesis of the amidoxime ligand onto the corn-cob cellulose backbone. The FTIR spectrum of corn-cob cellulose-supported poly(amidoxime) Pd(II) complex **4** showed a broad peak at 3310  $\text{cm}^{-1}$  and other peaks at 1645, 1380, 995, and 953  $\text{cm}^{-1}$  (Fig. 4.16d) which indicate a successful complexation of palladium with the poly(amidoxime) ligand **2**.

#### **4.6.2 Field Emission Scanning Electron Microscopy (FE-SEM) Images Analysis of Corn-Cob Cellulose, Modified Celluloses**

Field emission scanning electron microscopy (FE-SEM) was used to investigate the morphology of the cellulose synthesized celluloses, and Pd(II) complex **3**. The FE-SEM image of fresh corn-cob cellulose showed a smooth fine crystalline surface (Fig. 4.4a) whereas, the poly(acrylonitrile) **1** grafted cellulose showed distinguish surface compared to the fresh cellulose, which was less smooth surface with a small spherical like structure. (Fig. 4.4b) This change of surface morphology assumed (Fig. 4.17a) the successful graft polymerization occurred on the cellulose surface. The poly(amidoxime) chelating ligand **2** showed (Fig. 4.17a) a grain- shaped morphology in the FE-SEM image with a fine bead structure which is bigger than poly(acrylonitrile) **1**. Finally, the FE-SEM images of poly(amidoxime) Pd(II) complex **4** was found to have bigger sized spherical shapes (Figure 4.17b) compared to the size of the poly(amidoxime) ligand **2** and comparatively different from pure cellulose or poly(amidoxime) ligand **2**. Thus, it clearly confirmed that poly(amidoxime) ligand **2** has coordinated with the palladium species.

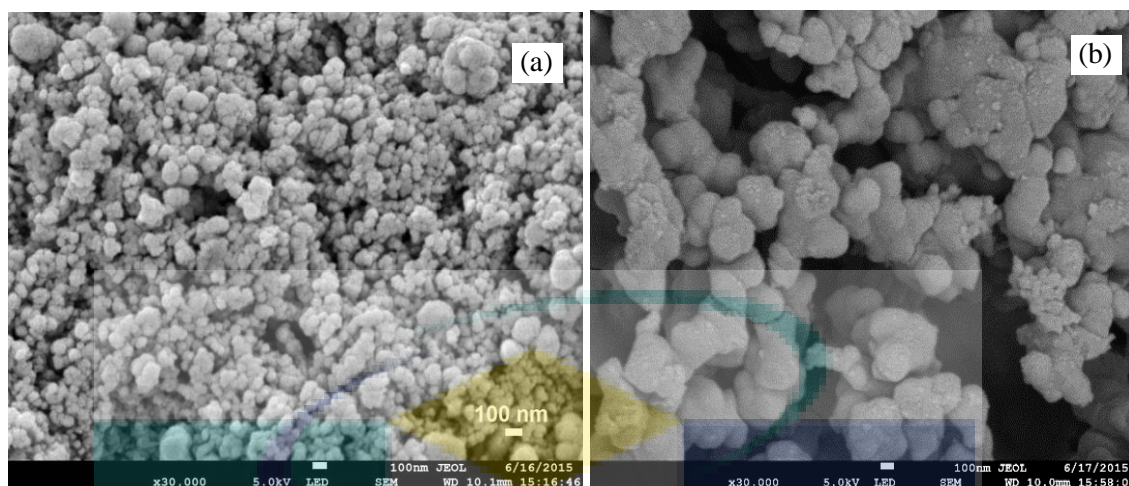


Figure 4.17 SEM images of (a) poly(amidoxime) ligand **2**, and (b) poly(amidoxime) Pd(II) complex **4** respectively.

#### 4.6.3 Energy-Dispersive X-Ray Spectroscopy (EDX) of Pd(II) Complex **4**

The energy dispersive X-ray spectroscopy analysis (EDX) of poly(amidoxime) Pd(II) complex **4** showed a peak around 3 eV which confirmed the presence of palladium metal in the poly(amidoxime) Pd(II) complex **4** (Fig. 4.18).

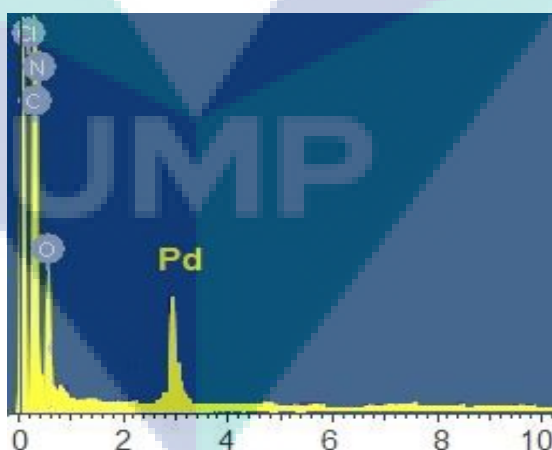


Figure 4.18 EDX spectrum of poly(amidoxime) Pd(II) complex **4**.

#### 4.6.4 Transmission Electron Microscopy (TEM) Images of Fresh and 4th Reused of Poly(amidoxime) Pd(II) Complex 4

The Pd(II) complex **4** was treated with hydrazine hydrate to afford **PdNs@PA** nanoparticles. To determine the nanoparticles size of **PdNs@PA**, TEM analysis was carried out. The TEM image showed a good distribution of Pd(II) complex **4** onto the modified cellulose surface with an average complex size  $\phi = 2.8 \pm 6$  nm (Fig. 4.19a). Thus, the HR-TEM micrograph confirmed the formation of cellulose supported Palladium nano particle. The HR-TEM micrograph of the 4<sup>th</sup> recycled (Suzuki-Miyaura reaction) poly(amidoxime) Pd(II) complex **4** (Fig. 4.19b) also showed a similar size ( $\phi = 2.9 \pm 3$  nm) of **PdNs@PA**. The similar complex size of fresh and reused Palladium catalyst revealed that, during the Suzuki-Miyaura reaction progress., **PdNs@PA** were not aggregated or dissociated.

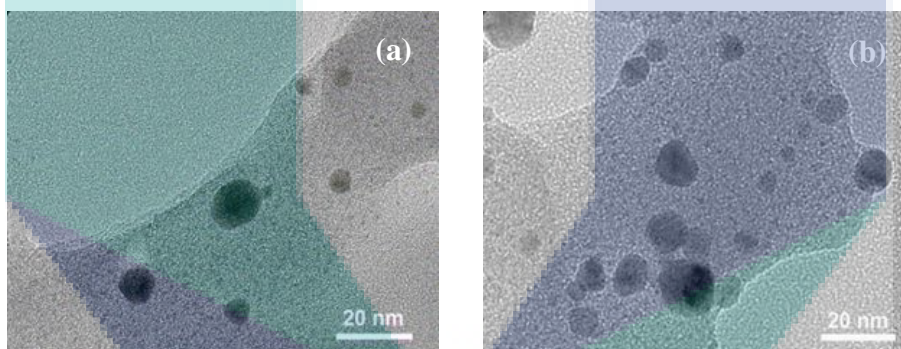


Figure 4.19 (a) TEM image of **PdNs@PA** and (b) 4<sup>th</sup> reused of **PdNs@PA**

#### 4.6.5 X-Ray Powder Diffraction (XRD) of poly(amidoxime) 2 and PdNs@PA catalyst

The powder X-ray diffraction study was conducted to determine the crystallinity of **PdNs@PA**. The powder X-ray diffraction was carried out by using Bruker D8 Advanced, Central Lab, UMP. The XRD (Fig. 4.20) showed combination of three cellulose peaks at  $2\theta$  values of  $14.8^\circ$ ,  $16.4^\circ$ , and  $22.9^\circ$  corresponding to the Bragg planes (101), (101') and (002), there were four peaks at  $2\theta$  values of  $40.2^\circ$ ,  $46.5^\circ$ ,  $67.9^\circ$

and  $81.7^\circ$  corresponding to (111), (200), (220) and (311) planes representing Pd(0) in PdNs@PA on cellulose. (Baruah, Das et al. 2015)

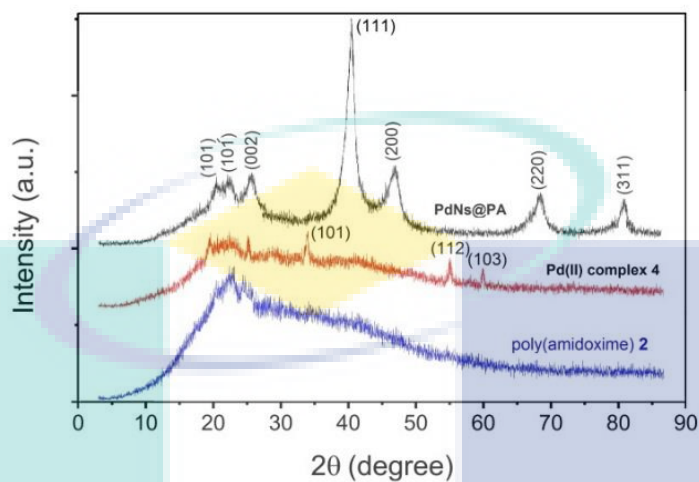


Figure 4.20 XRD of Pd(II) complex 4 and PdNs@PA.

#### 4.6.6 X-Ray Photoelectron Spectroscopy (XPS) of Fresh and Reused Poly(amidoxime) Pd(II) Complex 4

To check the oxidation state of PdNs@PA XPS analysis was also carried out. In the high resolution XPS spectrum, (Fig. 4.21) the doublet peaks of  $3d_{5/2}$  and  $3d_{3/2}$  was obtained at 335.32 eV and 340.62 eV which were assumed to be the binding energies of Pd(0) in the PdNs@PA. However, a doublet peaks of  $3d_{5/2}$  and  $3d_{3/2}$  was 337.62 eV and 342.82 eV which were obtained corresponds to the binding energies of Pd(II) complex 4 (Fu, Wu et al. 2015). It is reasonable that the upon reduction of Pd(II) by hydrazine the oxidation state of palladium is decreased thus the  $3d_{5/2}$  and  $3d_{3/2}$  values were also decreased.

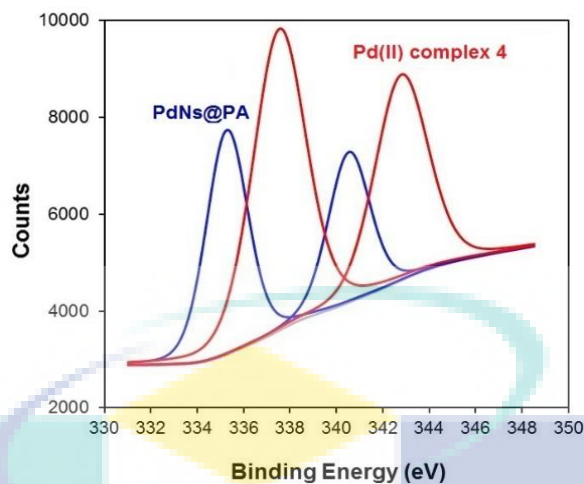
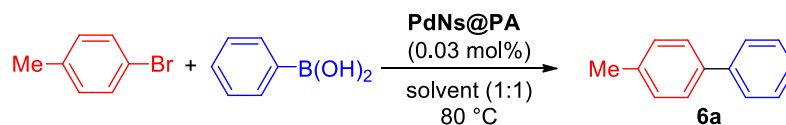


Figure 4.21 XPS of poly(amidoxime) Pd(II) complex **4** and **PdNs@PA**.

#### 4.7 PdNs@PA Catalyzed Suzuki-Miyaura Cross-Coupling Reaction

The Pd-catalyzed Suzuki-Miyaura cross-coupling reaction provides a powerful and general methodology for C-C bond formation. The waste corn-cob cellulose supported **PdNs@PA** was used to conduct the Suzuki-Miyaura reaction which provided higher yields of the corresponding products. In order to evaluate the catalytic performance of **PdNs@PA**, the coupling reaction between 4-bromotoluene and phenylboronic acid was chosen as a model reaction. The results of the effect of bases, solvent and reaction time are presented in Table 4.3. The reaction was carried out using 0.03 mol% (0.53 mg) of **PdNs@PA** in aqueous solution of DMF at 80 °C in presence of two mol equivalent of  $K_2CO_3$ . The **PdNs@PA** efficiently promoted Suzuki-Miyaura reaction within 3 h to give the corresponding biphenyl **6a** in 92% yield (Run 1). The production percentage was almost similar when aqueous ethanol was used instead of aqueous DMF solvent (Run 2). No significant improvement in the yield of product (entries 3-6) was as found with the change of bases. However 84% yield was obtained when aqueous TBAB was used (Run 7). Interestingly, the cross-coupling reaction was also proceeded when the reaction was carried out in pure water (Run 8). It should be noted that when Pd(II) complex **4** (0.53 mg) was used as catalyst, only 64% yield was obtained after 6 h prolonging reaction time (Run 9). Thus the reactivity of the nano particle **PdNs@PA** was proved to be higher than the Pd(II) complex **4**.



**Table 4.3** Suzuki-Miyaura reaction<sup>a</sup>

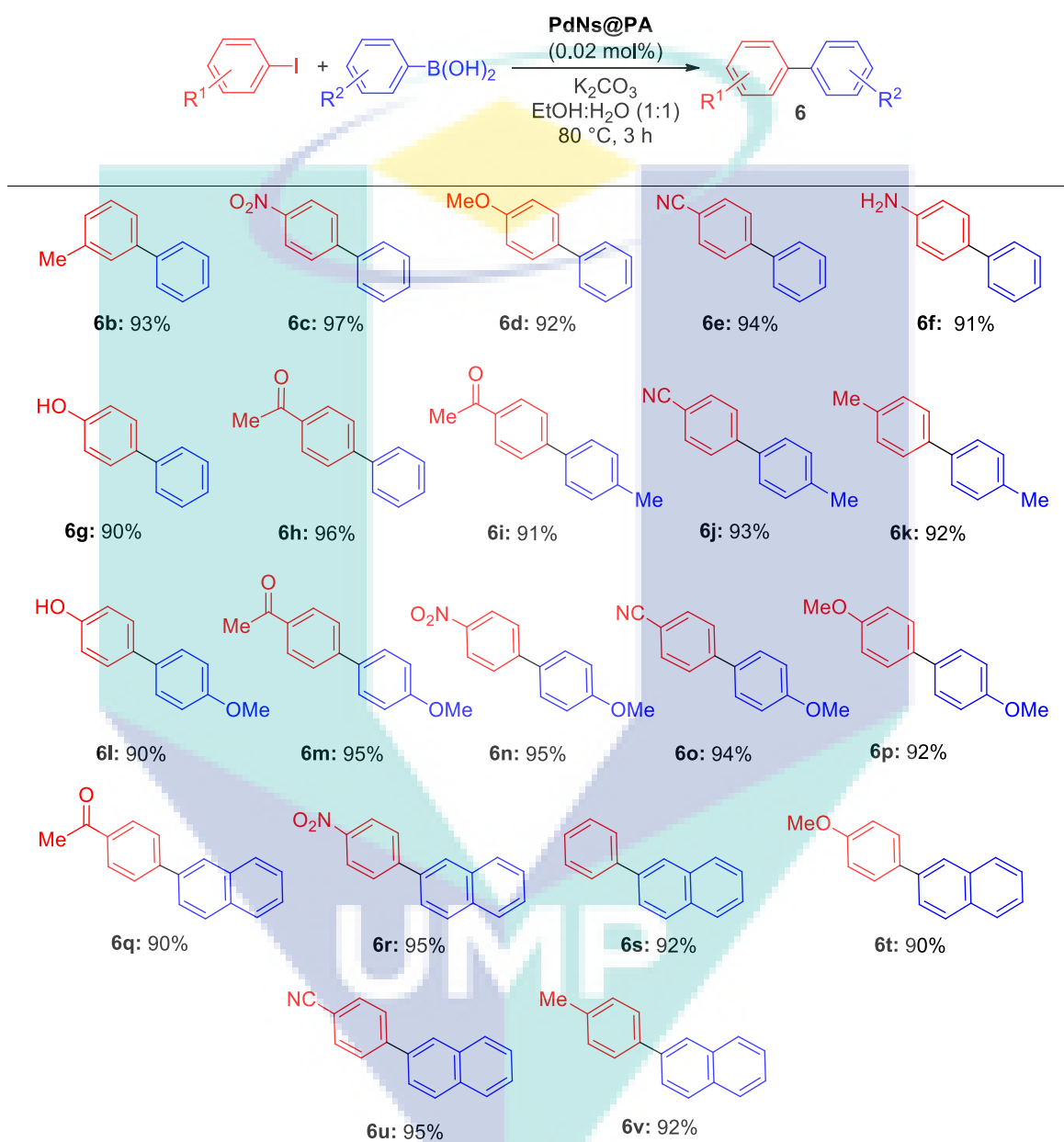
Run	Catalyst (0.03 mol%)	Time (h)	Base	Solvent (1:1)	Yield (%) <sup>b</sup>
1	<b>PdNs@PA</b>	3	K <sub>2</sub> CO <sub>3</sub>	DMF:H <sub>2</sub> O	92
2		2.5	K <sub>2</sub> CO <sub>3</sub>	EtOH:H <sub>2</sub> O	93
3		3	K <sub>3</sub> PO <sub>4</sub>	EtOH:H <sub>2</sub> O	92
4		3	NaOAc	EtOH:H <sub>2</sub> O	91
5		3	NaOH	EtOH:H <sub>2</sub> O	92
6		3	KOH	EtOH:H <sub>2</sub> O	88
7		5	K <sub>2</sub> CO <sub>3</sub>	H <sub>2</sub> O:TBAB	84
8		8	K <sub>2</sub> CO <sub>3</sub>	H <sub>2</sub> O	82
9	Pd(II) complex <b>4</b>	6	K <sub>2</sub> CO <sub>3</sub>	EtOH:H <sub>2</sub> O	64

<sup>[a]</sup>Reactions were carried out using 1 mmol of 4-bromotoluene, 1.2 mmol of phenylboronic acid, 2 mmol of base, and 0.03 mol% of **PdNs@PA** at 80 °C. <sup>[b]</sup>Yields were determined after column chromatography.

Upon receiving satisfactory catalytic performance of **PdNs@PA**, the extending applicability in wide range of substrates was then investigated. The efficiency of **PdNs@PA** was examined by employing 0.02 mol% of **PdNs@PA** at 80 °C. The **PdNs@PA** forwarded Suzuki-Miyaura reaction to a variety of aryl iodides and the results are depicted in Fig. 4.22. The reaction of electron efficient and electron deficient aryl iodides smoothly underwent the Suzuki cross-coupling reaction with phenylboronic acid to afford the corresponding biaryl products **6b-h** with 90-97% yields. The substituted with 4-methyl/methoxy-phenylboronic acid also efficiently promoted Suzuki-Miyaura reaction with aryl iodides to give the corresponding coupling products **6i-p** in 90-95% yields. The sterically hindrance 2-naphthylboronic acid was also

confirmed the promotion of cross-coupling reaction with electron withdrawing and electron poor aryl iodides to give the corresponding products **6q-v** in 90-95% yields.

Figure 4.22 Suzuki-Miyaura reaction of aryl iodide<sup>a</sup>

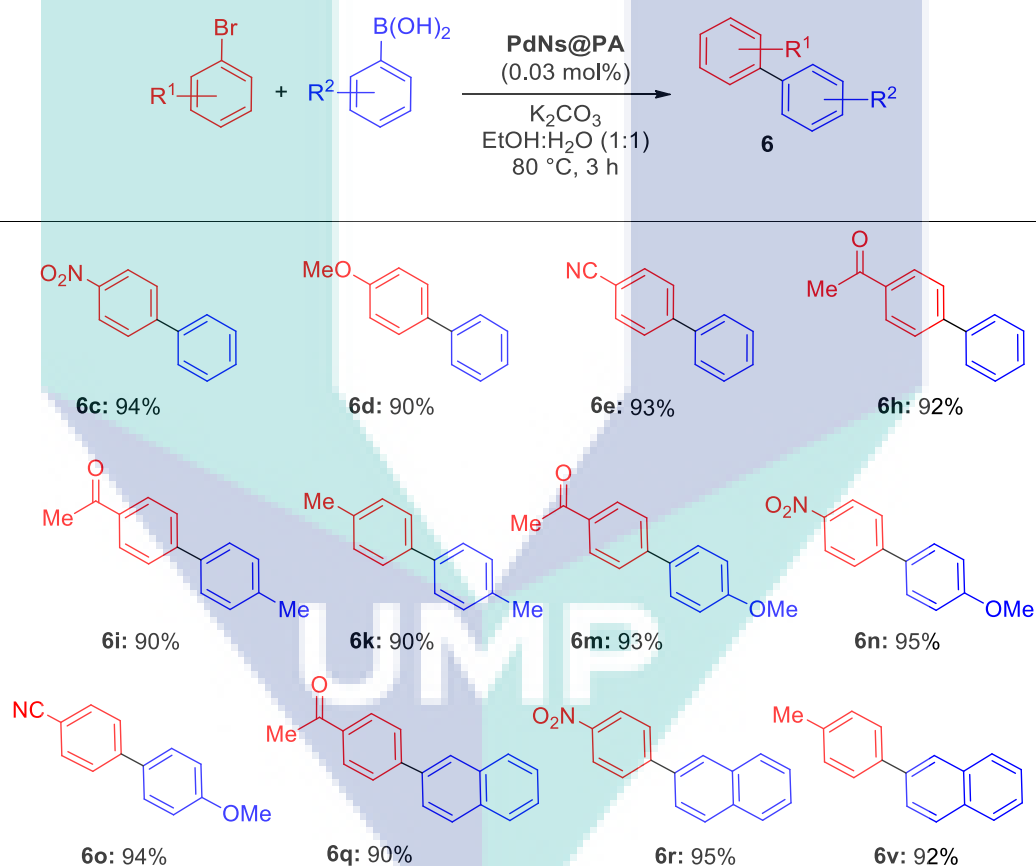


<sup>a</sup>Reactions were carried out using 1 mmol of aryl iodides, 1.2 mmol of arylboronic acid, 2 mmol of K<sub>2</sub>CO<sub>3</sub> and 0.02 mol % of PdNs@PA in 2 mL aqueous ethanol (EtOH:H<sub>2</sub>O, 1/1 mL) at 80 °C for 3 h.

Figure 4.23 illustrates the results were received applying PdNs@PA in the Suzuki-Miyaura reaction to a variety of less reactive aryl bromides. The reaction of electron rich and electron poor aryl bromides smoothly underwent the cross-coupling

reaction with phenylboronic acid to afford desired biaryl products **4c-e** and **4h** in up to 94% yield. The substituted 4-methyl/methoxyphenylboronic acids were also efficiently promoted Suzuki-Miyaura cross-coupling reaction with electron rich aryl bromide such as 4-bromoacetophenone and 4-bromonitrobenzene and electron poor aryl halide 4-bromotoluene to give the corresponding coupling products **4i, 4k**, and **4m-o** in 90-95% yields. It is interesting to note that the bulky 2-naphthylboronic acid also afforded the corresponding coupling products **4q, 4r** and **4v** in 90-95% yields when it was reacted with electron withdrawing or donating aryl bromides.

Figure 4.23 Suzuki-Miyaura reaction of aryl bromide<sup>a</sup>

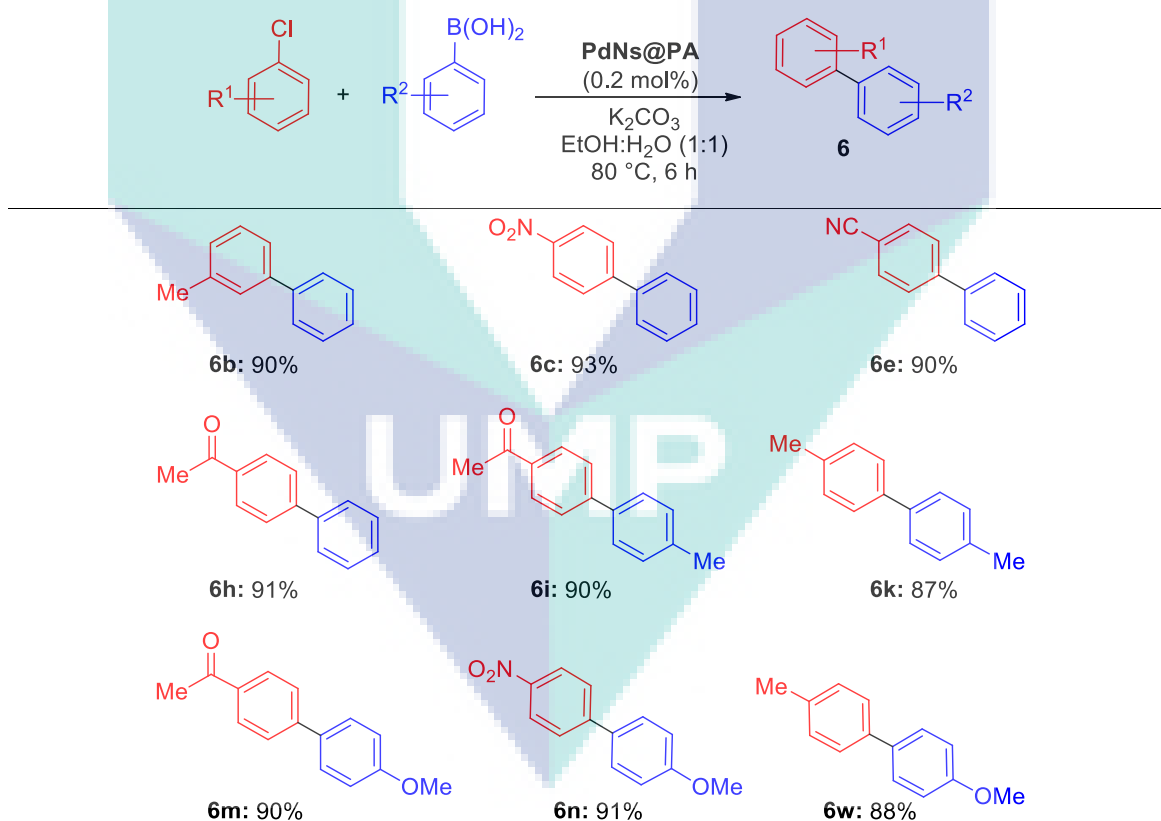


<sup>a</sup>Reactions were carried out using 1 mmol of aryl bromides, 1.2 mmol of arylboronic acid, 2 mmol of K<sub>2</sub>CO<sub>3</sub> and 0.03 mol% of PdNs@PA in 2 mL aqueous ethanol (EtOH:H<sub>2</sub>O, 1/1 mL) at 80 °C for 3 h.

Recently, researchers are interested to use commercially available low-cost aryl chlorides, although these chemicals are known to be less active aryl sources in the

Suzuki-Miyaura reaction at comparatively high temperature. To address the high temperature (>100 °C), long reaction time and high catalyst loading along with commercial metal/ligand were generally employed. Considering this issue, the Suzuki-Miyaura reaction of aryl chlorides with arylboronic acids were also performed. The **PdNs@PA** effectively forwarded the Suzuki-Miyaura reaction with 0.2 mol% of **PdNs@PA** at 80 °C (Fig. 4.24). Similar to arylbromides, the coupling between phenylboronic acids and aryl chlorides having electron withdrawing as well as electron donating groups were found to be afforded smoothly to their corresponding coupling products **6b**, **6c**, **4e** and **6h** in up to 93% yield within 6 h prolonging time. Moreover, 4-methyl and 4-methoxyphenylboronic acids were also promoted the Suzuki-Miyaura reaction with substituted aryl chlorides to give the corresponding arylated products **6i**, **6k**, **6m** and **6w** with high yields (87-91%).

Figure 4.24 Suzuki-Miyaura reaction of aryl chloride<sup>a</sup>



<sup>a</sup>Reactions were carried out using 1 mmol of aryl chloride, 1.2 mmol of arylboronic acid, 2 mmol of K<sub>2</sub>CO<sub>3</sub> and 0.2 mol% of **PdNs@PA** at 80 °C in 2 mL aqueous ethanol (EtOH:H<sub>2</sub>O, 1:1 mL) for 6 h.

## 4.8 Recycling of PdNs@PA

The recycling of the catalyst is considered to be a vital concern of heterogeneous catalysis system. The reusability of **PdNs@PA** was carried out in the reaction of 4-nitroiodobenzene and phenylboronic acid (Fig. 4.25, **6c**). After completion of the first cycle, the catalyst was separated by filtrated and the catalyst was washed with ethanol, dried at 80 °C and used it for next run under the same reaction conditions. The **PdNs@PA** was consecutively used six times without significant loss of catalytic activity (Fig. 4.18). The probable loss of activity after five cycles was only because of loss of **PdNs@PA** during the filtration process. So, it is reasonable that the waste corn-cob cellulose supported **PdNs@PA** are suitable for industrial application.

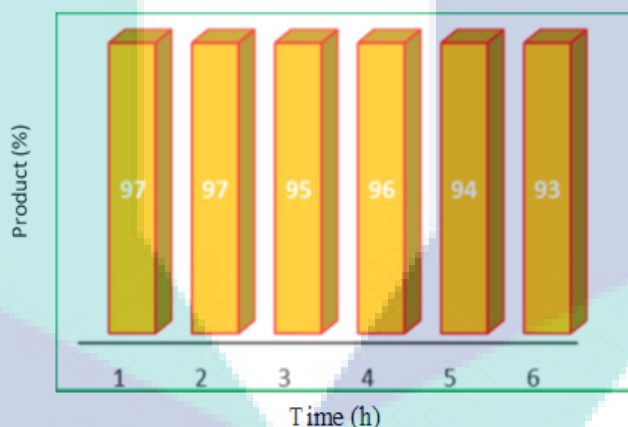


Figure 4.25 Recycling of **PdNs@PA** for Suzuki-Miyaura Reaction.

To check the reaction pathway whether it was proceeded through heterogeneous or homogeneous reaction condition, hot filtration test was carried out. The Suzuki-Miyaura reaction of 4-bromotoluene and phenylboronic acid was chosen for the hot filtration test. Firstly, the reaction was allowed to continue for one hour. After one-hour of reaction progress the catalyst was filtrated out at hot condition. Then filtrate reaction mixture was then heated for another 1.5 h under the same reaction condition to obtain any trace of further reaction progress. The reaction progress after each 30 min some of reaction mixture was taken out and was monitored by GC analysis (Fig. 4.26).

However, no reaction was observed to proceed further at all. Additionally, no leaching of palladium species was found by the ICP-AES analysis of the filtrate. So, it would be assumed that the Suzuki-Miyaura reaction was proceeded through heterogenic reaction condition.

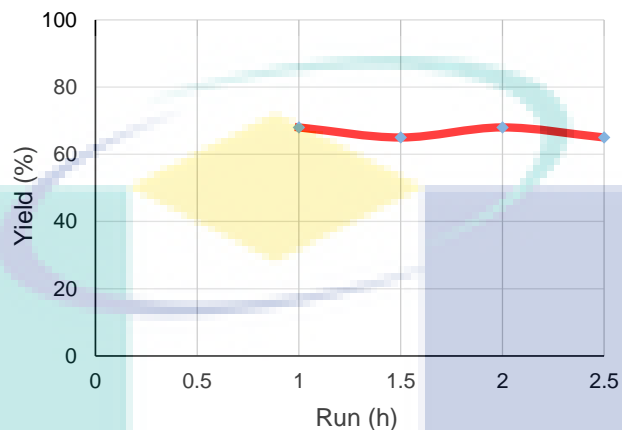


Figure 4.26 Hot filtration of Suzuki-Miyaura reaction.

To obtain the highest catalytic activity, the Suzuki-Miyaura cross-coupling reactions of 4-iodobenzene (10 mmol) and phenylboronic acid (11 mmol) with 0.0056 mol% (0.1 mg of PdNs@PA, 0.000056 mmol) of PdNs@PA was performed (Figure 4.13) under the identical conditions. Interestingly, the Suzuki-Miyaura reaction was smoothly proceeded to give the desired product **6a** with 91% yield, wherein high TON (16250) and TOF ( $5416 \text{ h}^{-1}$ ) were obtained. This is one of the highest TON and TOF for cellulose-supported heterogeneous catalyst promoted Suzuki- Miyaura reaction.

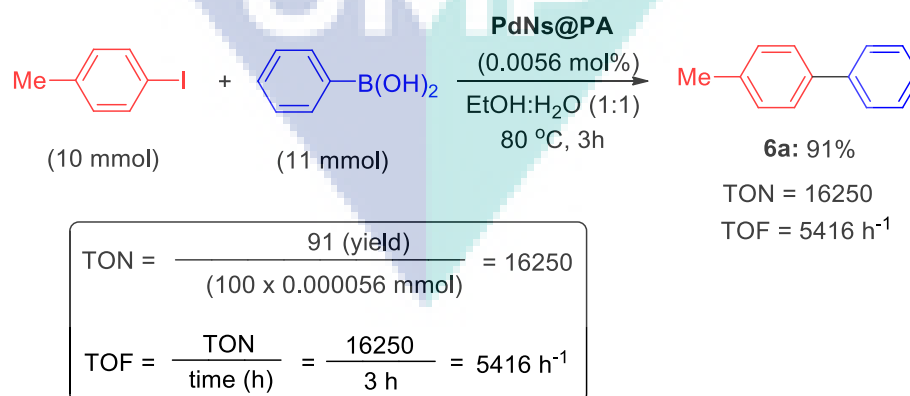
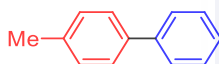


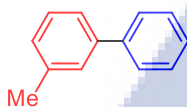
Figure 4.27 High TON and TOF in the Suzuki-Miyaura reaction.

## 4.9 NMR Analysis of Suzuki-Miyaura Reaction Products

The Suzuki-Miyaura reaction products were characterized using proton nuclear magnetic resonance ( $^1\text{H}$  NMR), carbon nuclear magnetic resonance ( $^{13}\text{C}$  NMR). BRUKER-500 spectrometer was used to perform the analysis. To prepare the sample for NMR, 10 mg product was dissolved in a deuterated chloroform ( $\text{CDCl}_3$ ) and make a clear solution by dissolving the sample completely. Then the solution was taken out with the help of a clean pipette and transferred in a clean NMR tube. The solution depth was kept 4.5-5 cm in the NMR tube. For  $^{13}\text{C}$  and  $^1\text{H}$  analysis the same prepared sample was used. The characteristic NMR of every Suzuki-Miyaura products are given as follows.



**6a:**  $^1\text{H}$  NMR (500 MHz,  $\text{CDCl}_3$ )  $\delta$  = 2.41 (s, 3 H), 7.26 (d,  $J$  = 8.0 Hz, 2 H), 7.32 (t,  $J$  = 7.4 Hz, 1 H), 7.44 (t,  $J$  = 7.4 Hz, 2 H), 7.51 (d,  $J$  = 8.0 Hz, 2 H), 7.60 (d,  $J$  = 8.0 Hz, 2 H);  $^{13}\text{C}$  NMR (125 MHz,  $\text{CDCl}_3$ )  $\delta$  = 21.09, 126.97, 127.04, 128.70, 129.47, 137.01, 138.36, 141.16.



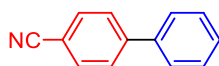
**6b:**  $^1\text{H}$  NMR (500 MHz,  $\text{CDCl}_3$ )  $\delta$  = 3.85 (s, 3 H), 6.99 (d,  $J$  = 8.8 Hz, 2 H), 7.32 (t,  $J$  = 7.35 Hz, 1 H), 7.42-7.52 (m, 2 H), 7.54-7.56 (m, 4 H).  $^{13}\text{C}$  NMR (125 MHz,  $\text{CDCl}_3$ )  $\delta$  = 55.35, 114.18, 126.72, 128.14, 128.70, 133.77, 140.8, 159.12.



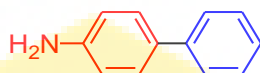
**6c:**  $^1\text{H}$  NMR (500 MHz,  $\text{CDCl}_3$ )  $\delta$  = 7.47-7.54 (m, 3 H), 7.64 (d,  $J$  = 7.0 Hz, 2 H), 7.77 (d,  $J$  = 8.5 Hz, 2 H), 8.34 (d,  $J$  = m, 8.5 Hz, 2 H).  $^{13}\text{C}$  NMR (125 MHz,  $\text{CDCl}_3$ )  $\delta$  = 124.09, 127.37, 127.79, 128.90, 129.14, 138.77, 147.63.



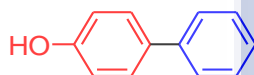
**6d:**  $^1\text{H}$  NMR (500 MHz,  $\text{CDCl}_3$ )  $\delta$  = 3.87 (s, 3 H), 7.01 (d,  $J$  = 8.5 Hz, 2 H), 7.31 (t,  $J$  = 8.0 Hz, 1 H), 7.44 (t,  $J$  = 8.0 Hz, 2 H), 7.54-7.58 (m, 4 H).  $^{13}\text{C}$  NMR (125 MHz,  $\text{CDCl}_3$ )  $\delta$  = 55.26, 114.19, 126.70, 128.14, 128.22, 128.75, 133.73, 140.79, 159.10.



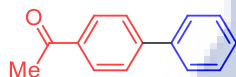
**6e:**  $^1\text{H}$  NMR (500 MHz,  $\text{CDCl}_3$ )  $\delta$  = 7.41 (d,  $J$  = 7.5 Hz, 1 H), 7.44 (t,  $J$  = 8.5 Hz, 2 H), 7.58 (d,  $J$  = 7.4 Hz, 2 H), 7.67 (d,  $J$  = 8.6 Hz, 2 H), 7.72 (d,  $J$  = 8.5 Hz, 2 H);  $^{13}\text{C}$  NMR (125 MHz,  $\text{CDCl}_3$ )  $\delta$  = 110.96, 118.98, 127.27, 127.78, 128.64, 129.15, 132.63, 139.22, 145.72.



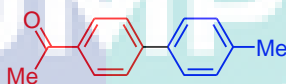
**6f:**  $^1\text{H}$  NMR (500 MHz,  $\text{CDCl}_3$ )  $\delta$  = 3.66 (brs, 2 H), 6.44 (d,  $J$  = 8.5 Hz, 2 H), 6.74 (d,  $J$  = 8.5 Hz, 1 H), 7.27 (t,  $J$  = 7.5 Hz, 1 H), 7.35-7.41 (m, 4 H), 7.57 (d,  $J$  = 7.5 Hz, 1 H);  $^{13}\text{C}$  NMR (125 MHz,  $\text{CDCl}_3$ )  $\delta$  = 115.4, 117.2, 126.4, 127.8, 128.6, 131.5, 135.5, 137.8, 141.1, 146.0.



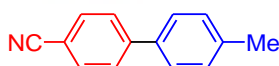
**6g:**  $^1\text{H}$  NMR (500 MHz,  $\text{CDCl}_3$ )  $\delta$  = 4.97 (brs, 1 H), 6.62 (d,  $J$  = 8.6 Hz, 2 H), 6.89 (d,  $J$  = 8.6 Hz, 1 H), 7.31 (t,  $J$  = 7.5 Hz, 1 H), 7.42 (t,  $J$  = 7.5 Hz, 1 H), 7.47-7.54 (m, 4 H);  $^{13}\text{C}$  NMR (125 MHz,  $\text{CDCl}_3$ )  $\delta$  = 116.0, 117.77, 126.7, 128.3, 138.4, 140.7, 155.4.



**6h:**  $^1\text{H}$  NMR (500 MHz,  $\text{CDCl}_3$ )  $\delta$  = 2.64 (s, 3 H), 7.46 (t,  $J$  = 7.5, Hz, 2 H), 7.57-7.68 (m, 5 H), 8.04 (d,  $J$  = 8.5 Hz, 2 H).  $^{13}\text{C}$  NMR (125 MHz,  $\text{CDCl}_3$ )  $\delta$  = 26.63, 127.21, 128.21, 128.90, 129.72, 135.82, 137.89, 139.85, 145.77, 197.77

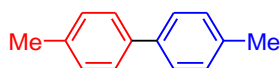


**6i:**  $^1\text{H}$  NMR (500 MHz,  $\text{CDCl}_3$ )  $\delta$  = 2.40 (s, 3 H), 2.62 (s, 3 H), 7.28 (d,  $J$  = 8.0 Hz, 2 H), 7.53 (d,  $J$  = 8.0 Hz, 2 H), 7.68 (d,  $J$  = 8.0 Hz, 2 H), 8.02 (d,  $J$  = 8.0 Hz, 2 H);  $^{13}\text{C}$  NMR (125 MHz,  $\text{CDCl}_3$ )  $\delta$  = 21.05, 26.50, 126.8, 127.0, 128.8, 129.4, 135.5, 136.8, 138.1, 145.6, 197.6.

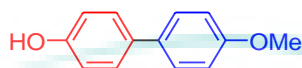


**6j:**  $^1\text{H}$  NMR (500 MHz,  $\text{CDCl}_3$ )  $\delta$  = 2.42 (s, 3 H), 7.30 (d,  $J$  = 8 Hz, 2 H), 7.50 (d,  $J$  = 8 Hz, 2 H), 7.67-7.73 (m, 4 H);  $^{13}\text{C}$  NMR (125 MHz,  $\text{CDCl}_3$ )  $\delta$  = 21.2, 110.5, 127.0, 127.4, 130.0, 132.5, 136.2, 138.8, 145.6.

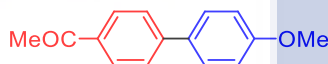




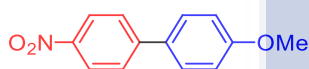
**6k:**  $^1\text{H}$  NMR (500 MHz,  $\text{CDCl}_3$ )  $\delta$  = 2.38 (s, 6 H), 7.22 (dd,  $J$  = 8.05, 1.7 Hz, 4 H), 7.48 (dd,  $J$  = 8.05, 1.8 Hz, 4 H);  $^{13}\text{C}$  NMR (125 MHz,  $\text{CDCl}_3$ )  $\delta$  = 21.1, 126.8, 129.4, 136.7, 138.3.



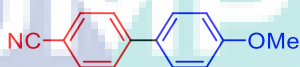
**6l:**  $^1\text{H}$  NMR (500 MHz,  $\text{CDCl}_3$ )  $\delta$  = 3.84 (s, 3 H), 4.75 (s, 1 H), 6.90 (dd,  $J$  = 6.5, 2.4 Hz, 2 H), 6.96 (dd,  $J$  = 6.5, 2.4 Hz, 2 H), 7.42 (dd,  $J$  = 6.5, 2.4 Hz, 2 H), 7.46 (dd,  $J$  = 6.5, 2.4 Hz, 2 H);  $^{13}\text{C}$  NMR (125 MHz,  $\text{CDCl}_3$ )  $\delta$  = 55.4, 114.2, 115.6, 127.7, 128.0, 133.4, 154.6, 158.7.



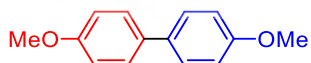
**6m:**  $^1\text{H}$  NMR (500 MHz,  $\text{CDCl}_3$ )  $\delta$  = 2.63 (s, 3 H), 3.86 (s, 3 H), 7.01 (d,  $J$  = 8.5 Hz, 2 H), 7.58 (d,  $J$  = 8.5 Hz, 2 H), 7.65 (d,  $J$  = 8.0 Hz, 2 H), 8.01 (d,  $J$  = 8.5 Hz, 2 H);  $^{13}\text{C}$  NMR (125 MHz,  $\text{CDCl}_3$ )  $\delta$  = 26.89, 69.59, 127.46, 127.50, 129.15, 136.07, 138.14, 140.32, 146.02, 198.02.



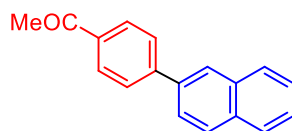
**6n:**  $^1\text{H}$  NMR (500 MHz,  $\text{CDCl}_3$ )  $\delta$  = 3.87 (s, 3 H), 7.02 (d,  $J$  = Hz, 6.75, 2 H), 7.59 (d,  $J$  = 8.85 Hz, 2 H), 7.70 (d,  $J$  = 8.85 Hz, 2 H), 8.28 (d,  $J$  = 8.85 Hz, 2 H).  $^{13}\text{H}$  NMR (500 MHz,  $\text{CDCl}_3$ )  $\delta$  = 55.42, 114.59, 124.14, 127.07, 128.56, 131.07, 137.48, 147.20, 160.43.



**6o:**  $^1\text{H}$  NMR (500 MHz,  $\text{CDCl}_3$ )  $\delta$  = 3.86 (s, 3 H), 7.01 (d,  $J$  = 7.0 Hz, 2 H), 7.54 (d,  $J$  = 7.0 Hz, 2 H), 7.64 (d,  $J$  = 7.0, Hz, 2 H), 7.69 (d,  $J$  = 7.0 Hz, 2 H).  $^{13}\text{H}$  NMR (500 MHz,  $\text{CDCl}_3$ )  $\delta$  = 55.40, 110.10, 114.55, 119.09, 127.11, 128.35, 131.51, 132.56, 145.22, 160.20.



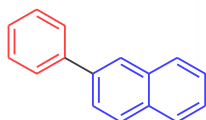
**6p:**  $^1\text{H}$  NMR (500 MHz,  $\text{CDCl}_3$ )  $\delta$  = 3.84 (s, 6 H), 6.96 (dd,  $J$  = 8.65 Hz, 4 H), 7.48 (dd,  $J$  = 8.60 Hz, 4 H).  $^{13}\text{C}$  NMR (125 MHz,  $\text{CDCl}_3$ )  $\delta$  = 55.32, 114.13, 127.12, 133.46, 158.66.



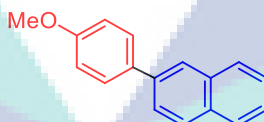
**6q:**  $^1\text{H}$  NMR (500 MHz,  $\text{CDCl}_3$ )  $\delta$  = 2.66 (s, 3 H), 7.51-7.54 (m 2 H), 7.76-7.93 (m, 6 H), 8.08 (d,  $J$  = 8.45 Hz, 3 H).  $^{13}\text{C}$  NMR (125 MHz,  $\text{CDCl}_3$ )  $\delta$  = 26.68, 125.15, 126.37, 126.55, 127.67, 128.33, 128.69, 128.98, 132.99, 133.52, 137.12, 145.69, 197.83.



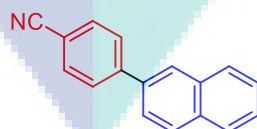
**6r:**  $^1\text{H}$  NMR (500 MHz,  $\text{CDCl}_3$ )  $\delta$  = 7.54-7.56 (m, 2 H), 7.57 (d,  $J$  = 8.5 Hz, 1 H), 7.71-7.9 (m, 5 H), 8.10 (s, 1 H), 8.33 (d,  $J$  = 8.5 Hz, 2 H).  $^{13}\text{C}$  NMR (125 MHz,  $\text{CDCl}_3$ )  $\delta$  = 124.21, 124.92, 126.86, 127.76, 128.04, 128.46, 129.03, 133.26, 136.03, 147.60.



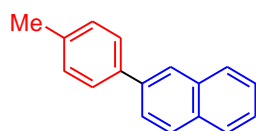
**6s:**  $^1\text{H}$  NMR (500 MHz,  $\text{CDCl}_3$ )  $\delta$  = 7.42 (m, 1 H), 7.45-7.53 (m, 4 H), 7.72-7.75 (m, 3 H), 7.78-7.94 (m, 3 H), 8.07 (s, 1 H);  $^{13}\text{C}$  NMR (125 MHz,  $\text{CDCl}_3$ )  $\delta$  = 120.36, 125.6, 125.8, 125.9, 126.3, 127.4, 128.86, 138.57.



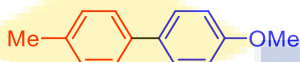
**6t:**  $^1\text{H}$  NMR (500 MHz,  $\text{CDCl}_3$ )  $\delta$  = 3.91 (s, 3 H), 7.07 (d,  $J$  = 8.75 Hz, 2 H), 7.48-7.51 (m, 2 H), 7.53-7.71 (m, 3 H), 7.75-7.79 (m, 3 H), 8.02 (s, 1 H).  $^{13}\text{C}$  NMR (125 MHz,  $\text{CDCl}_3$ )  $\delta$  = 55.35, 114.30, 125.00, 125.41, 125.62, 126.20, 127.59, 128.02, 133.29, 133.61, 138.12, 159.22.



**6u:**  $^1\text{H}$  NMR (500 MHz,  $\text{CDCl}_3$ )  $\delta$  = 7.55-7.59 (2 H), 7.73-7.99 (m, 8 H), 8.08 (s, 1 H).  $^{13}\text{C}$  NMR (125 MHz,  $\text{CDCl}_3$ )  $\delta$  = 110.9, 124.85, 126.55, 126.74, 127.71, 128.37, 132.65. MS-EI,  $m/z$  229 ( $\text{M}^+$ ).



**6v:**  $^1\text{H}$  NMR (500 MHz,  $\text{CDCl}_3$ )  $\delta$  = 2.43 (s, 3 H), 7.29 (d,  $J$  = 7.5 Hz, 2 H), 7.47-7.53 (m, 2 H), 7.64 (d,  $J$  = 8.0 Hz, 2 H), 7.75 (d,  $J$  = 8.5 Hz, 1 H), 7.85-7.90 (m, 3 H), 8.03 (s, 1 H);  $^{13}\text{C}$  NMR (125 MHz,  $\text{CDCl}_3$ )  $\delta$  = 21.26, 125.40, 125.53, 125.75, 126.20, 127.23, 127.61, 128.11, 128.32, 129.57, 132.47, 133.72, 137.14, 138.20.



**6w:**  $^1\text{H}$  NMR (500 MHz,  $\text{CDCl}_3$ )  $\delta$  = 2.40 (s, 3 H), 3.84 (s, 3 H), 6.97 (dd,  $J$  = 8.5 Hz, 2 H), 7.11 (d,  $J$  = 8.5 Hz, 1 H), 7.25-7.36 (m, 3 H), 7.52 (d,  $J$  = 8.5 Hz, 2 H).  $^{13}\text{C}$  NMR (125 MHz,  $\text{CDCl}_3$ )  $\delta$  = 21.01, 55.27, 114.11, 126.54, 127.90, 129.40, 133.69, 136.30, 137.92, 158.89.

UMP

## CHAPTER 5

### CONCLUSIONS AND RECOMMENDATIONS

#### 5.1 Conclusions

Bio-waste corn-cob cellulose was modified through the polymerization and subsequent amidoximation. The polyamidoxime ligand was treated with Cu/Pd salts to give the corresponding metal complexes. The complexes were reduced by hydrazine to provide cellulose supported metal nanoparticles (**CuNs@PA/PdNs@PA**) which were well characterized by using several spectroscopic methods.

The corn-cob cellulose supported poly(amidoxime) copper nanoparticles (**CuNs@PA**) efficiently promoted the chemoselective Aza-Michael reaction of aliphatic amines with  $\alpha,\beta$ -unsaturated carbonyl compounds in methanol at room temperature. The **CuN@PA** showed high catalytic efficiency (0.5 mol%) toward Aza-Michael reaction to give the corresponding addition products in up to 96% yield moreover **CuN@PA** was reused eight cycles without significant loss of its catalytic activity.

On the other hand **PdNs@PA** was successfully (0.03 to 0.2 mol%) used towards Suzuki-Miyaura cross-coupling reactions of both electron-rich and electron-poor aryl halides with a variety of phenylboronic acids in aqueous ethanol under mild reaction conditions. The **PdNs@PA** was efficiently afforded corresponding biaryl products in up to 97% yield. The highest catalytic activity of **PdNs@PA** was also determined which provided high TON and TOF number when 0.0056 mol% of **PdNs@PA** was used as a catalyst. Furthermore, **PdNs@PA** was separated from the reaction mixture and reused six times without significant loss of its catalytic activity.

## 5.2 Future Directions

The cross coupling reactions play vital role in chemical synthesis. So, other cross-coupling reactions can be investigated using these cellulose supported metal catalysts as well as can be explored to hetero atomic compounds to open a new dimension of this research area. In addition, introduction of new functional groups in the cellulose/bulky molecule to prepare new catalyst can also be a wonderful way to advance this field.

The bio-waste corn-cob cellulose supported poly(amidoxime) metal complexes were prepared and successfully applied to the C-C and C-N bond formation reactions through Suzuki-Miyaura and Aza-Michael reactions. However, from this research, it was realized that the isolation of corn-cob cellulose process followed several steps and provided only 25-30% yields of the cellulose. Additionally, it was hard to determine the the molecular weight of the polymer. Gel Permeation Chromatography (GPC) may be useful to determine the molecular weight of the polymer. Also in this research the analysis the effect of base on reaction progression was not on focus. These obstacles should be addressed in the future study.



UMP

## REFERENCES

- Ai, X., Wang, X., Liu, J.-M., Ge, Z.-M., Cheng, T.-M., & Li, R.-T. (2010). An effective aza-Michael addition of aromatic amines to electron-deficient alkenes in alkaline Al<sub>2</sub>O<sub>3</sub>. *Tetrahedron*, 66(29), 5373-5377.
- Ardizzioia, G. A., Brenna, S., & Therrien, B. (2012). Ni (II) and Pd (II) pyridinyloxazolidine-compounds: synthesis, X-ray characterisation and catalytic activities in the aza-Michael reaction. *Dalton Transactions*, 41(3), 783-790.
- Baig, R. N., & Varma, R. S. (2012). A highly active and magnetically retrievable nanoferrite-DOPA-copper catalyst for the coupling of thiophenols with aryl halides. *Chemical Communications*, 48(20), 2582-2584.
- Bartoli, G., Bartolacci, M., Giuliani, A., Marcantoni, E., Massaccesi, M., & Torregiani, E. (2005). Improved heteroatom nucleophilic addition to electron-poor alkenes promoted by CeCl<sub>3</sub>·7H<sub>2</sub>O/NaI system supported on alumina in solvent-free conditions. *The Journal of Organic Chemistry*, 70(1), 169-174.
- Bartoli, G., Cimarelli, C., & Palmieri, G. (1994). Convenient procedure for the reduction of β-enamino ketones: synthesis of γ-amino alcohols and tetrahydro-1,3-oxazines. *Journal of the Chemical Society, Perkin Transactions 1*(5), 537-543.
- Baruah, D., Das, R. N., Hazarika, S., & Konwar, D. (2015). Biogenic synthesis of cellulose supported Pd (0) nanoparticles using hearth wood extract of *Artocarpus lakoocha* Roxb-A green, efficient and versatile catalyst for Suzuki and Heck coupling in water under microwave heating. *Catalysis Communications*, 72, 73-80.
- Bergbreiter, D. E. (1999). Alternative polymer supports for organic chemistry. *Medicinal Research Reviews*, 19(5), 439-450.
- Bhadra, S., Sreedhar, B., & Ranu, B. C. (2009). Recyclable heterogeneous supported copper-catalyzed coupling of thiols with aryl halides: base-controlled differential arylthiolation of bromiodobenzenes. *Advanced Synthesis & Catalysis*, 351(14-15), 2369-2378.
- Blaser, H.-U., Indolese, A., Schnyder, A., Steiner, H., & Studer, M. (2001). Supported palladium catalysts for fine chemicals synthesis. *Journal of Molecular Catalysis A: Chemical*, 173(1), 3-18.
- Boudart, M., & Djéga-Mariadassou, G. (2014). *Kinetics of heterogeneous catalytic reactions*: Princeton University Press.
- Calo, V., Nacci, A., Monopoli, A., & Montingelli, F. (2005). Pd nanoparticles as efficient catalysts for Suzuki and Stille coupling reactions of aryl halides in ionic liquids. *The Journal of Organic Chemistry*, 70(15), 6040-6044.

- Camara, F., Benyahya, S., Besse, V., Boutevin, G., Auvergne, R., Boutevin, B., & Caillol, S. (2014). Reactivity of secondary amines for the synthesis of non-isocyanate polyurethanes. *European Polymer Journal*, *55*, 17-26.
- Chaudhuri, M. K., Hussain, S., Kantam, M. L., & Neelima, B. (2005). Boric acid: a novel and safe catalyst for aza-Michael reactions in water. *Tetrahedron Letters*, *46*(48), 8329-8331.
- Cheng, J., Sun, Y., Wang, F., Guo, M., Xu, J.-H., Pan, Y., & Zhang, Z. (2004). A copper-and amine-free Sonogashira reaction employing aminophosphines as ligands. *The Journal of Organic Chemistry*, *69*(16), 5428-5432.
- Chow, W. K., So, C. M., Lau, C. P., & Kwong, F. Y. (2011). Palladium-catalyzed borylation of aryl mesylates and tosylates and their applications in one-pot sequential Suzuki–Miyaura biaryl synthesis. *Chemistry—A European Journal*, *17*(25), 6913-6917.
- Dai, L., Zhang, Y., Dou, Q., Wang, X., & Chen, Y. (2013). Chemo/regioselective Aza-Michael additions of amines to conjugate alkenes catalyzed by polystyrene-supported AlCl<sub>3</sub>. *Tetrahedron*, *69*(6), 1712-1716.
- Das, B., & Chowdhury, N. (2007). Amberlyst-15: An efficient reusable heterogeneous catalyst for aza-Michael reactions under solvent-free conditions. *Journal of Molecular Catalysis A: Chemical*, *263*(1), 212-215.
- Das, P., Bora, U., Tairai, A., & Sharma, C. (2010). Triphenylphosphine chalcogenides as efficient ligands for room temperature palladium (II)-catalyzed Suzuki–Miyaura reaction. *Tetrahedron Letters*, *51*(11), 1479-1482.
- Del Pozo, C., Corma, A., Iglesias, M., & Sánchez, F. (2011). Recyclable mesoporous silica-supported chiral ruthenium-(NHC) NN-pincer catalysts for asymmetric reactions. *Green Chemistry*, *13*(9), 2471-2481.
- Demchuk, O. M., Yoruk, B., Blackburn, T., & Snieckus, V. (2006). A mixed naphthyl-phenyl phosphine ligand motif for Suzuki, Heck, and hydrodehalogenation reactions. *Synlett*, *2006*(18), 2908-2913.
- Dewan, A., Bora, U., & Borah, G. (2014). A simple and efficient tetradentate Schiff base derived palladium complex for Suzuki-Miyaura reaction in water. *Tetrahedron Letters*, *55*(10), 1689-1692.
- Dey, R., Sreedhar, B., & Ranu, B. C. (2010). Molecular sieves-supported palladium (II) catalyst: Suzuki coupling of chloroarenes and an easy access to useful intermediates for the synthesis of irbesartan, losartan and boscalid. *Tetrahedron*, *66*(13), 2301-2305.
- Dhake, K. P., Tambade, P. J., Singhal, R. S., & Bhanage, B. M. (2010). Promiscuous *Candida antarctica* lipase B-catalyzed synthesis of  $\beta$ -amino esters via aza-Michael addition of amines to acrylates. *Tetrahedron Letters*, *51*(33), 4455-4458.

- Didier, D., Meddour, A., Bezenine-Lafollée, S., & Collin, J. (2011). Samarium Iodobinaphtholate: An efficient catalyst for enantioselective aza-michael additions of O-Benzylhydroxylamine to N-alkenoyloxazolidinones. *European Journal of Organic Chemistry*, (14), 2678-2684.
- Fadini, L., & Togni, A. (2003). Ni (II) Complexes containing chiral tridentate phosphines as new catalysts for the hydroamination of activated olefins. *Chemical Communications*(1), 30-31.
- Fedotova, A. I., Komarova, T. A., Romanov, A. R., Ushakov, I. A., Legros, J., Maddaluno, J., & Rulev, A. Y. (2017). Adamantyl aziridines via aza-Michael initiated ring closure (aza-MIRC) reaction. *Tetrahedron*, 73(8), 1120-1126.
- Fu, G.-T., Wu, R., Liu, C., Lin, J., Sun, D.-M., & Tang, Y.-W. (2015). Arginine-assisted synthesis of palladium nanochain networks and their enhanced electrocatalytic activity for borohydride oxidation. *RSC Advances*, 5(23), 18111-18115.
- Gates, B. (1995). Supported metal clusters: synthesis, structure, and catalysis. *Chemical Reviews*, 95(3), 511-522.
- Geelhaar, T. (1998). Liquid crystals for display applications. *Liquid Crystals*, 24(1), 91-98.
- Gelman, D., & Buchwald, S. L. (2003). Efficient palladium-catalyzed coupling of aryl chlorides and tosylates with terminal alkynes: Use of a Copper Cocatalyst Inhibits the Reaction. *Angewandte Chemie International Edition*, 42(48), 5993-5996.
- Ghaderi, A., Gholinejad, M., & Firouzabadi, H. (2016). Palladium deposited on naturally occurring supports as a powerful catalyst for carbon-carbon bond formation reactions. *Current Organic Chemistry*, 20(4), 327-348.
- Gholinejad, M., & Jeddi, N. (2014). Copper nanoparticles supported on agarose as a bioorganic and degradable polymer for multicomponent click synthesis of 1,2,3-triazoles under low copper loading in water. *ACS Sustainable Chemistry and Engineering*, 2(12), 2658-2665.
- Hahn, W., Szalecki, W., & Boszczyk, W. (1978). Ethaneanthracenes. 3. attempts to simplify the synthesis of 9, 12-methaneiminomethane-9, 10-ethane-9, 10-dihydroanthracene (Vol. 52, pp. 2497-2499): Polish chemical society C/O Polish acad sciences, Inst Physical Chemistry, UL Kasprzaka 44/52, 01-224 Warsaw, Poland.
- Halima, T. B., Zhang, W., Yalaoui, I., Hong, X., Yang, Y.-F., Houk, K. N., & Newman, S. G. (2017). Palladium-catalyzed Suzuki-Miyaura coupling of aryl esters. *Journal of American Chemical Society*, 139(3), 1311-1318.



- Hatakeyama, T., Kondo, Y., Fujiwara, Y.-i., Takaya, H., Ito, S., Nakamura, E., & Nakamura, M. (2009). Iron-catalysed fluoroaromatic coupling reactions under catalytic modulation with 1, 2-bis (diphenylphosphino) benzene. *Chemical Communications*(10), 1216-1218.
- Horton, D. A., Bourne, G. T., & Smythe, M. L. (2003). The combinatorial synthesis of bicyclic privileged structures or privileged substructures. *Chemical Reviews*, 103(3), 893-930.
- Huang, Y. L., Weng, C. M., & Hong, F. E. (2008). Density functional studies on palladium-catalyzed suzuki-miyaura cross-coupling reactions assisted by N-or P-chelating ligands. *Chemistry—A European Journal*, 14(14), 4426-4434.
- Huang, Z., Li, F., Chen, B., Xue, F., Chen, G., & Yuan, G. (2011). Nitrogen-rich copolymeric microsheets supporting copper nanoparticles for catalyzing arylation of N-heterocycles. *Applied Catalysis A: General*, 403(1), 104-111.
- Islam, S., Mandal, B. H., Biswas, T. K., Rahman, M. L., Rashid, S. S., Tan, S., & Sarkar, M. S. (2016). Poly (hydroxamic acid) functionalized copper catalyzed CN bond formation reactions. *RSC Advances*, 6, 56450-56457
- Islam, S., Mondal, P., Roy, A. S., Mondal, S., & Hossain, D. (2010). Heterogeneous Suzuki and copper-free Sonogashira cross-coupling reactions catalyzed by a reusable palladium (II) complex in water medium. *Tetrahedron Letters*, 51(15), 2067-2070.
- Jadhav, S., Jagdale, A., Kamble, S., Kumbhar, A., & Salunkhe, R. (2016). Palladium nanoparticles supported on a titanium dioxide cellulose composite (PdNPs@ TiO<sub>2</sub>-Cell) for ligand-free carbon-carbon cross coupling reactions. *RSC Advances*, 6(5), 3406-3420.
- Kang, Q., & Zhang, Y. (2011). N-Heterocyclic carbene-catalyzed aza-Michael addition. *Organic & Biomolecular Chemistry*, 9(19), 6715-6720.
- Kang, T., Feng, Q., & Luo, M. (2005). An active and recyclable polystyrene-supported N-heterocyclic carbene-palladium catalyst for the suzuki reaction of arylbromides with arylboronic acids under mild conditions. *Synlett*, (15), 2305-2308.
- Keipour, H., Khalilzadeh, M. A., Hosseini, A., Pilevar, A., & Zareyee, D. (2012). An active and selective heterogeneous catalytic system for Michael addition. *Chinese Chemical Letters*, 23(5), 537-540.
- Kim, J.-H., Lee, D.-H., Jun, B.-H., & Lee, Y.-S. (2007). Copper-free Sonogashira cross-coupling reaction catalyzed by polymer-supported N-heterocyclic carbene palladium complex. *Tetrahedron Letters*, 48(40), 7079-7084.
- Kobayashi, S., Kakumoto, K., & Sugiura, M. (2002). Transition metal salts-catalyzed aza-Michael reactions of enones with carbamates. *Organic Letters*, 4(8), 1319-1322.

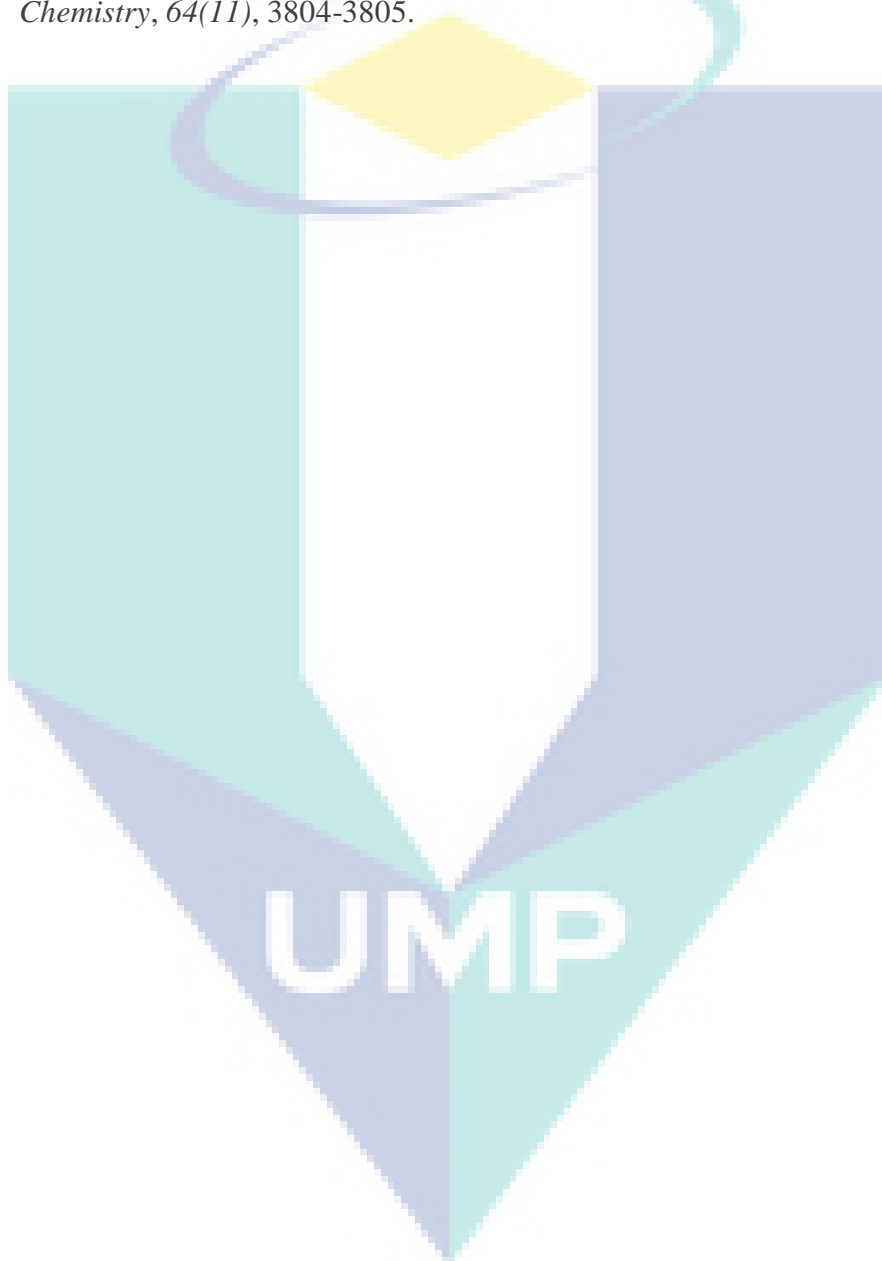
- Larsen, R. D., King, A. O., Chen, C. Y., Corley, E. G., Foster, B. S., Roberts, F. E., Tschäen, D. M. (1994). Efficient synthesis of losartan, a nonpeptide angiotensin II receptor antagonist. *The Journal of Organic Chemistry*, 59(21), 6391-6394.
- Leek, J., Carr, I., Bell, S., Markham, A., & Lench, N. (1997). Assignment of the DNA fragmentation factor gene (DFFA) to human chromosome bands 1p36. 3→p36. 2 by in situ hybridization. *Cytogenetic and Genome Research*, 79(3-4), 212-213.
- Li, C.-J. (2008). Cross-dehydrogenative coupling (CDC): Exploring C–C bond formations beyond functional group transformations. *Accounts of Chemical Research*, 42(2), 335-344.
- Liu, C., Zhang, H., Shi, W., & Lei, A. (2011). Bond formations between two nucleophiles: transition metal catalyzed oxidative cross-coupling reactions. *Chemical Reviews*, 111(3), 1780-1824.
- Liu, F., Feng, G., Lin, M., Wang, C., Hu, B., & Qi, C. (2014). Superoleophilic nanoporous polymeric ionic liquids loaded with palladium acetate: Reactants enrichment and efficient heterogeneous catalysts for Suzuki–Miyaura coupling reaction. *Journal of Colloid and Interface Science*, 435, 83-90.
- Mao, P., Yang, L., Xiao, Y., Yuan, J., Liu, X., & Song, M. (2012). Suzuki cross-coupling catalyzed by palladium (II) complexes bearing 1-aryl-3, 4, 5, 6-tetrahydropyrimidine ligands. *Journal of Organometallic Chemistry*, 705, 39-43.
- Matheron, M. E., & Porchas, M. (2005). *Comparative performance and preservation of chemical management tools for powdery mildew on muskmelon*. Paper presented at the III International Symposium on Cucurbits 731.
- Miyaura, N., Yamada, K., & Suzuki, A. (1979). A new stereospecific cross-coupling by the palladium-catalyzed reaction of 1-alkenylboranes with 1-alkenyl or 1-alkynyl halides. *Tetrahedron Letters*, 20(36), 3437-3440.
- Molnár, Á., & Papp, A. (2014). The use of polysaccharides and derivatives in palladium-catalyzed coupling reactions. *Catalysis Science & Technology*, 4(2), 295-310.
- Monsalve, L. N., Gillanders, F., & Baldessari, A. (2012). Promiscuous Behavior of *Rhizomucor miehei* Lipase in the Synthesis of N-Substituted  $\beta$ -Amino Esters. *European Journal of Organic Chemistry*, 2012(6), 1164-1170.
- Mukherjee, C., & Misra, A. K. (2007). Aza-Michael addition of amines to activated alkenes catalyzed by silica supported perchloric acid under a solvent-free condition. *Letters in Organic Chemistry*, 4(1), 54-59.
- Polshettiwar, V., & Varma, R. S. (2010). Nano-organocatalyst: magnetically retrievable ferrite-anchored glutathione for microwave-assisted Paal-Knorr reaction, aza-Michael addition, and pyrazole synthesis. *Tetrahedron*, 66(5), 1091-1097.

- Prenești, E., & Berto, S. (2002). Interaction of copper (II) with imidazole pyridine nitrogen-containing ligands in aqueous medium: a spectroscopic study. *Journal of Inorganic Biochemistry*, 88(1), 37-43.
- Rahman, M. L., Rohani, N., Mustapa, N., & Yusoff, M. M. (2014). Synthesis of polyamidoxime chelating ligand from polymer-grafted corn-cob cellulose for metal extraction. *Journal of Applied Polymer Science*, 131(19).
- Reddy, K. R., & Kumar, N. S. (2006). Cellulose-supported copper (0) catalyst for aza-Michael addition. *Synlett*, 2006(14), 2246-2250.
- Reetz, M. T., & Westermann, E. (2000). Phosphane-free palladium-catalyzed coupling reactions: the decisive role of Pd nanoparticles. *Angewandte Chemie International Edition*, 39(1), 165-168.
- Rout, L., Sen, T. K., & Punniyamurthy, T. (2007). Efficient CuO-nanoparticle-catalyzed C-S cross-coupling of thiols with iodobenzene. *Angewandte Chemie International Edition*, 46(29), 5583-5586.
- Roy, S. R., & Chakraborti, A. K. (2010). Supramolecular assemblies in ionic liquid catalysis for aza-Michael reaction. *Organic Letters*, 12(17), 3866-3869.
- Sarkar, S. M., Rahman M. L. (2017) Cellulose supported poly(amidoxime) copper complex for Click reaction. *Journal of Cleaner Production* 141, 683-692.
- Sarkar, S., Guibal, E., Quignard, F., & SenGupta, A. (2012). Polymer-supported metals and metal oxide nanoparticles: synthesis, characterization, and applications. *Journal of Nanoparticle Research*, 14(2), 1-24.
- Schmidt, U., Leitenberger, V., Griesser, H., Schmidt, J., & Meyer, R. (1992). Total synthesis of the biphenomycins; V. 1 synthesis of biphenomycin A. *Synthesis*, 1992(12), 1248-1254.
- Siemsen, P., Livingston, R. C., & Diederich, F. (2000). Acetylenic coupling: a powerful tool in molecular construction. *Angewandte Chemie International Edition*, 39(15), 2632-2657.
- Song, J., Zhao, H., Liu, Y., Han, H., Li, Z., Chu, W., & Sun, Z. (2017). Efficient symmetrical bidentate dioxime ligand-accelerated homogeneous palladium-catalyzed Suzuki–Miyaura coupling reactions of aryl chlorides. *New Journal of Chemistry*, 41(1), 372-376.
- Sreedhar, B., Yada, D., & Reddy, P. S. (2011). Nanocrystalline titania-supported palladium (0) nanoparticles for Suzuki–Miyaura cross-coupling of aryl and heteroaryl halides. *Advanced Synthesis & Catalysis*, 353(14-15), 2823-2836.
- Srivastava, N., & Banik, B. K. (2003). Bismuth nitrate-catalyzed versatile Michael reactions. *The Journal of Organic Chemistry*, 68(6), 2109-2114.

- Surendra, K., Krishnaveni, N. S., Sridhar, R., & Rao, K. R. (2006).  $\beta$ -Cyclodextrin promoted aza-Michael addition of amines to conjugated alkenes in water. *Tetrahedron Letters*, 47(13), 2125-2127.
- Ulusal, F., Darendeli, B., Erünal, E., Egitmen, A., & Guzel, B. (2017). Supercritical carbon dioxide deposition of  $\gamma$ -Alumina supported Pd nanocatalysts with new precursors and using on Suzuki-Miyaura coupling reactions. *The Journal of Supercritical Fluids*, 127, 111-120.
- Valente, C., Çalimsiz, S., Hoi, K. H., Mallik, D., Sayah, M., & Organ, M. G. (2012). The development of bulky palladium NHC complexes for the most-challenging cross-coupling reactions. *Angewandte Chemie International Edition*, 51(14), 3314-3332.
- Wang, J., He, H., Cooper, R. C., & Yang, H. (2017). In situ-forming polyamidoamine dendrimer hydrogels with tunable properties prepared via Aza-Michael addition reaction. *ACS Applied Materials & Interfaces*, 9(12), 10494-10503.
- Wang, X., Hu, P., Xue, F., & Wei, Y. (2014). Cellulose-supported N-heterocyclic carbene-palladium catalyst: Synthesis and its applications in the Suzuki cross-coupling reaction. *Carbohydrate Polymers*, 114, 476-483.
- Wang, Y., Yuan, Y.-Q., & Guo, S.-R. (2009). Silica sulfuric acid promotes aza-Michael addition reactions under solvent-free condition as a heterogeneous and reusable catalyst. *Molecules*, 14(11), 4779-4789.
- Wen, Y., Siew, S., Rahman, M. L., Arshad, S. E., Surugau, N., & Musta, B. (2012). Synthesis and characterization of poly (hydroxamic acid)-poly (amidoxime) chelating ligands from polymer-grafted acacia cellulose. *Journal of Applied Polymer Science*, 124(6), 4443-4451.
- White, R. J., Luque, R., Budarin, V. L., Clark, J. H., & Macquarrie, D. J. (2009). Supported metal nanoparticles on porous materials. Methods and applications. *Chemical Society Reviews*, 38(2), 481-494.
- Yamada, Y. M., Sarkar, S. M., & Uozumi, Y. (2012). Amphiphilic self-assembled polymeric copper catalyst to parts per million levels: click chemistry. *Journal of the American Chemical Society*, 134(22), 9285-9290.
- Yang, L., Xu, L.-W., & Xia, C.-G. (2007). Efficient catalytic aza-Michael additions of carbamates to enones: revisited dual activation of hard nucleophiles and soft electrophiles by InCl<sub>3</sub>/TMSCl catalyst system. *Tetrahedron Letters*, 48(9), 1599-1603.
- Yang, L., Xu, L.-W., Zhou, W., Li, L., & Xia, C.-G. (2006). Highly efficient aza-Michael reactions of aromatic amines and N-heterocycles catalyzed by a basic ionic liquid under solvent-free conditions. *Tetrahedron Letters*, 47(44), 7723-7726.

Ying, A.-G., Wang, L.-M., Deng, H.-X., Chen, J.-H., Chen, X.-Z., & Ye, W.-D. (2009). Green and efficient aza-Michael additions of aromatic amines to  $\alpha$ ,  $\beta$ -unsaturated ketones catalyzed by DBU based task-specific ionic liquids without solvent. *Arkivoc*, 11, 288-298.

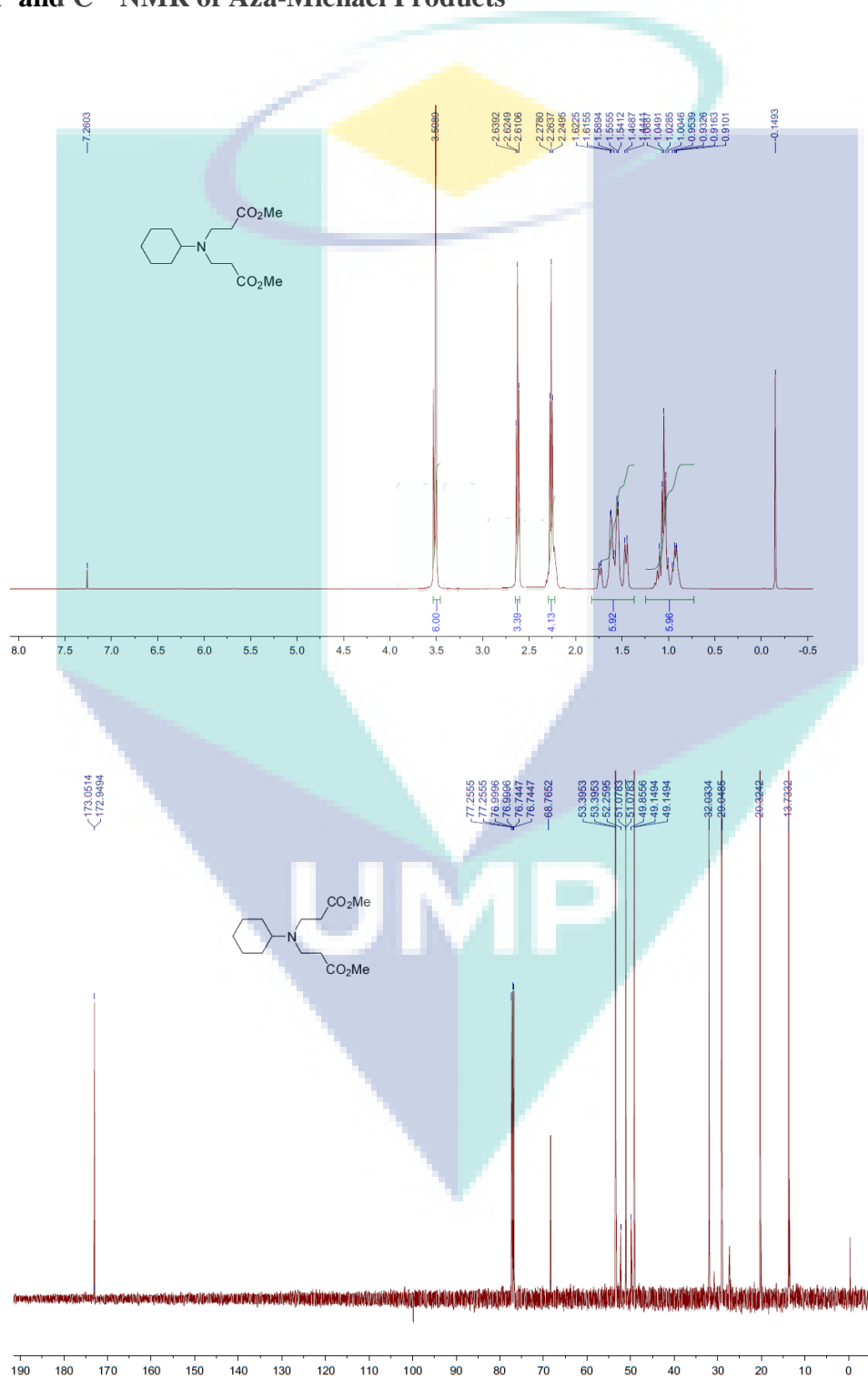
Zhang, C., Huang, J., Trudell, M. L., & Nolan, S. P. (1999). Palladium–imidazol-2-ylidene complexes as catalysts for facile and efficient Suzuki cross-coupling reactions of aryl chlorides with arylboronic Acids. *The Journal of Organic Chemistry*, 64(11), 3804-3805.

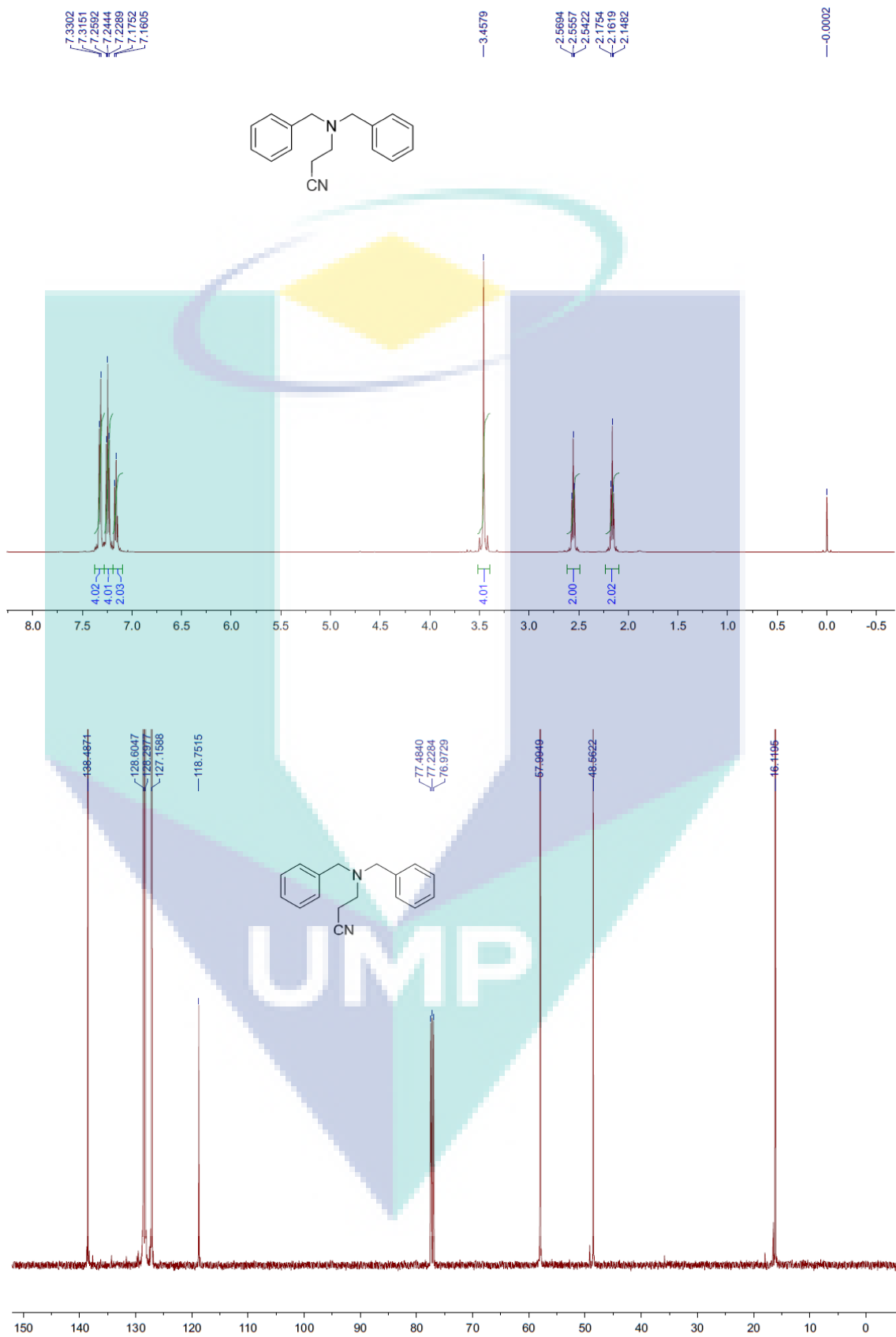


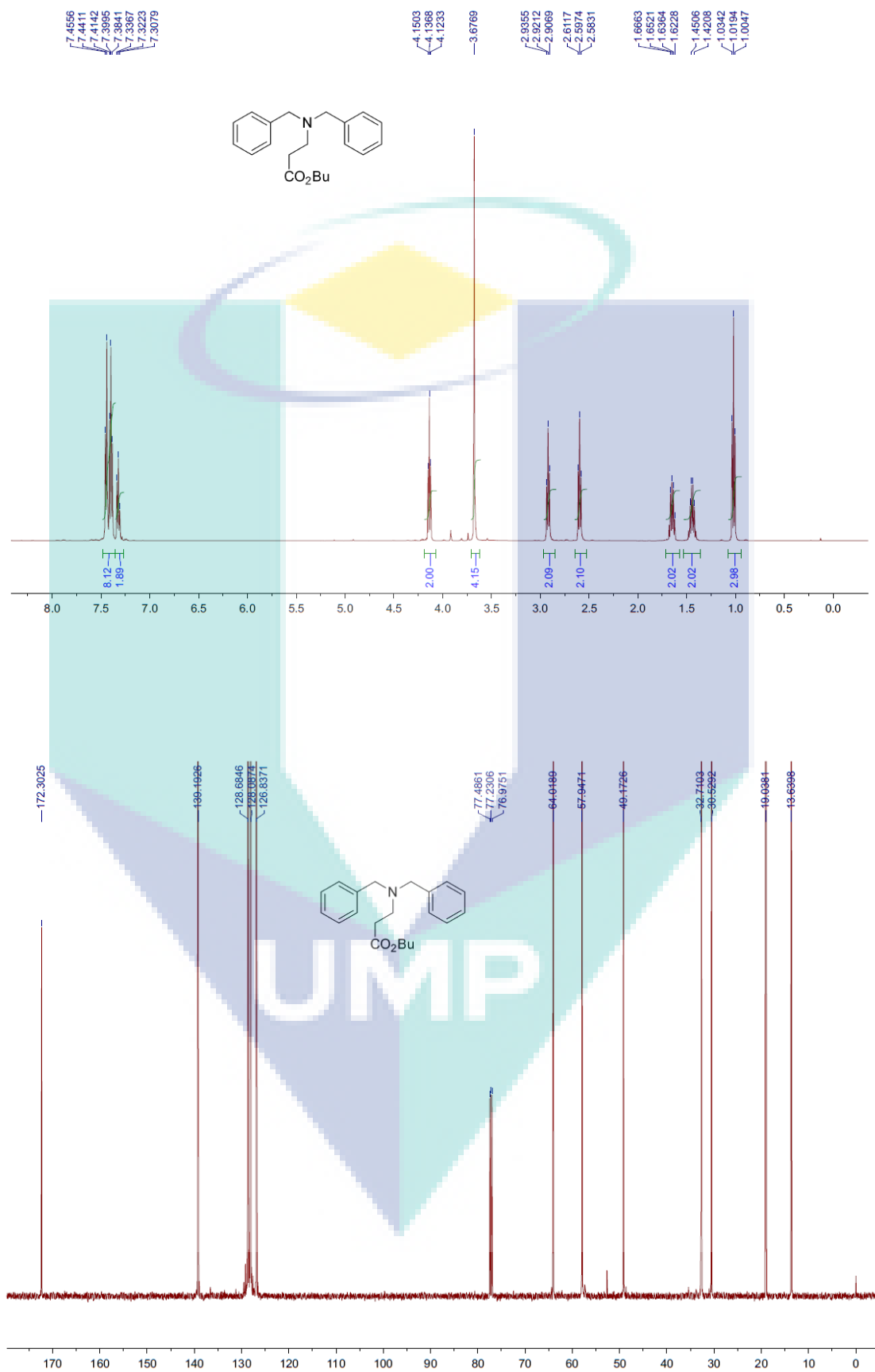
# APPENDICES

## Appendix A1

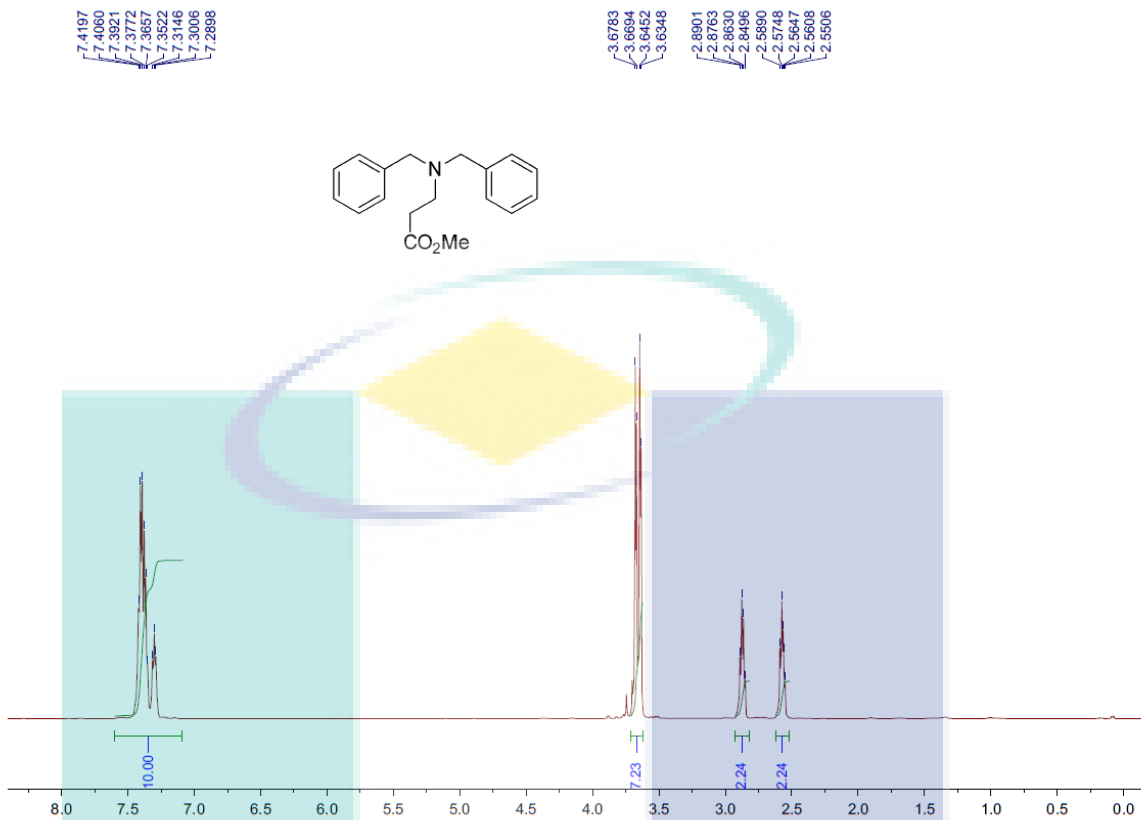
### $H^1$ and $C^{13}$ NMR of Aza-Michael Products

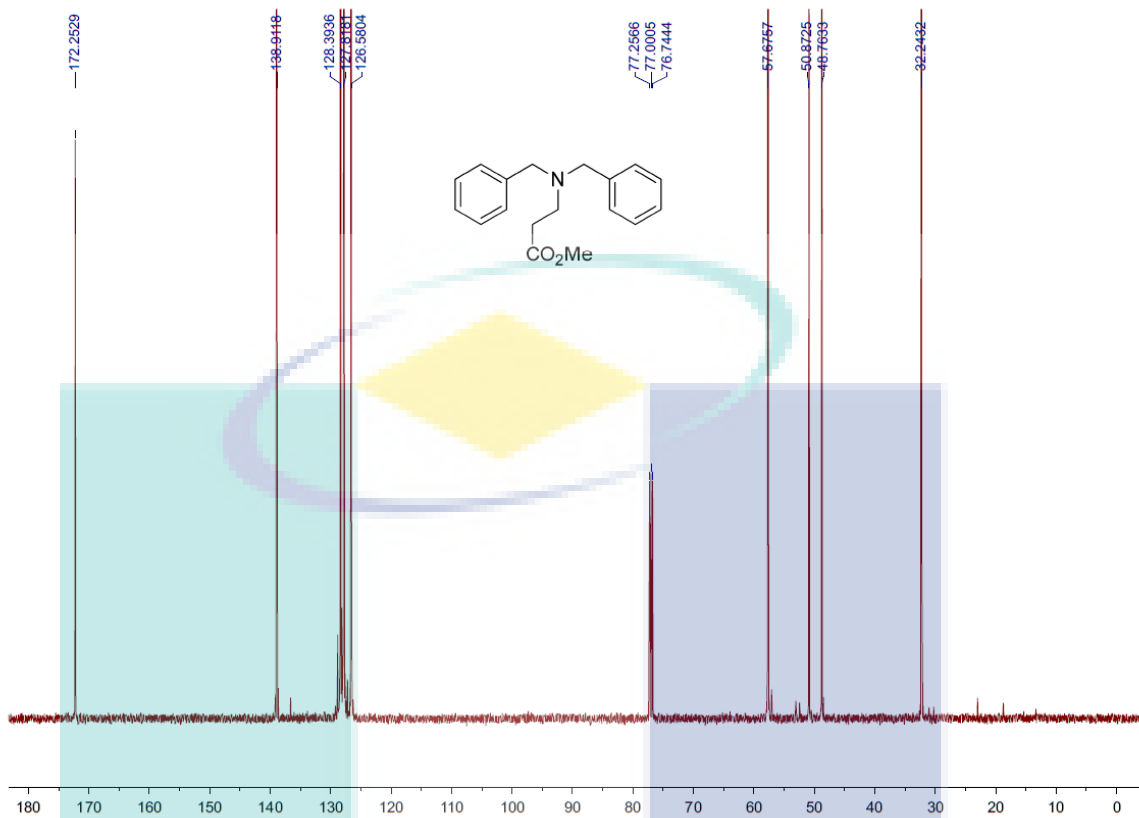




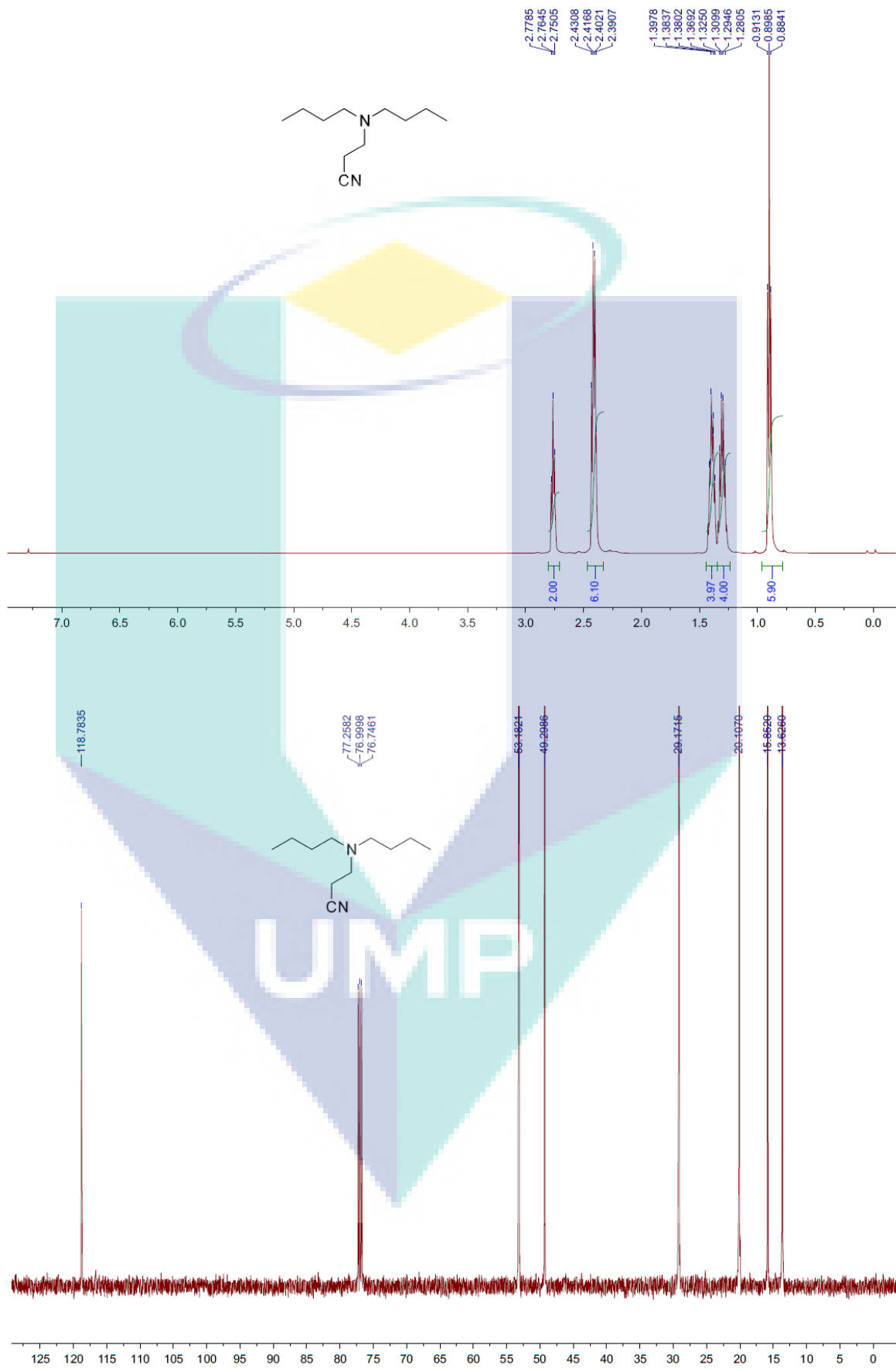


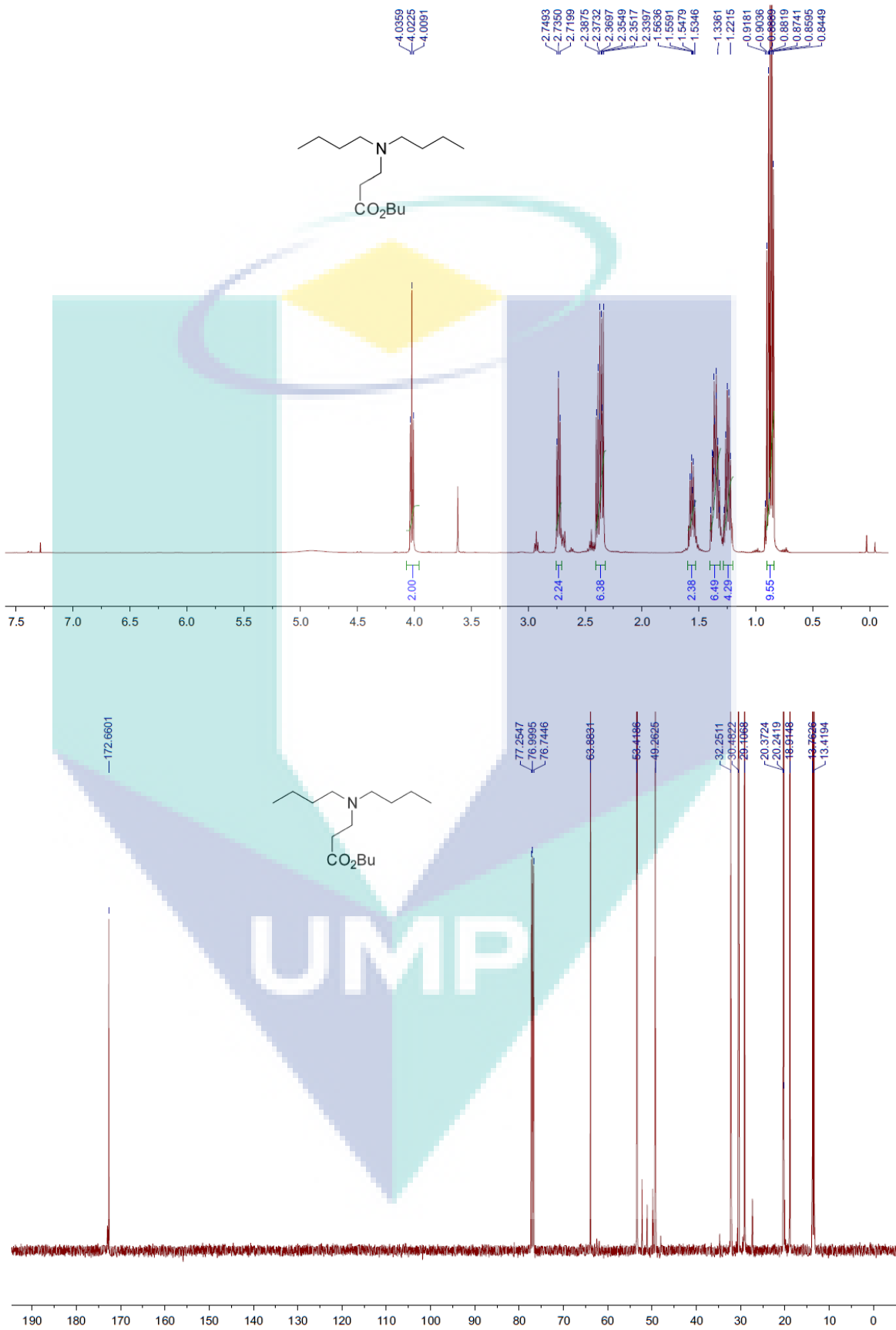


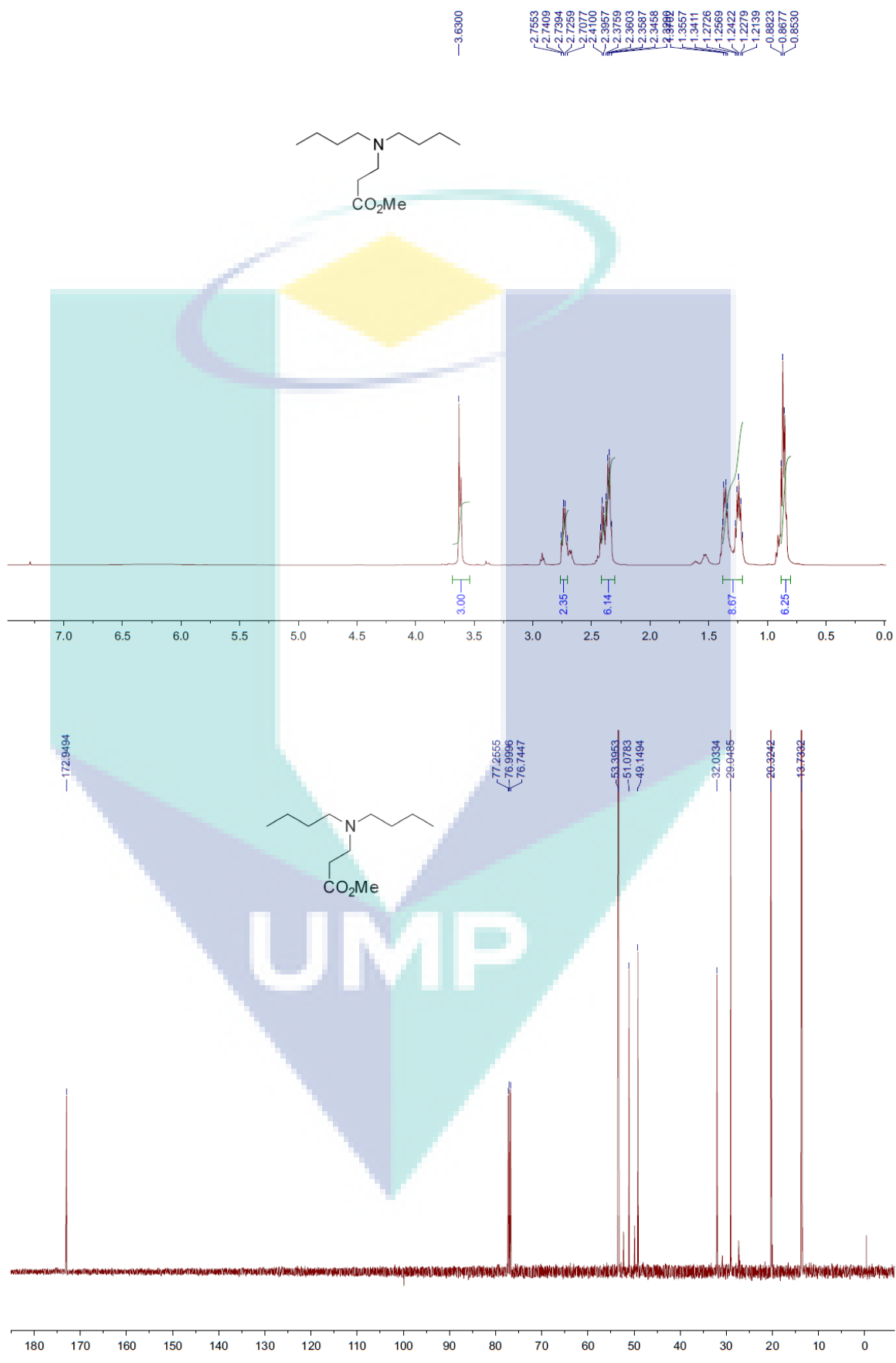


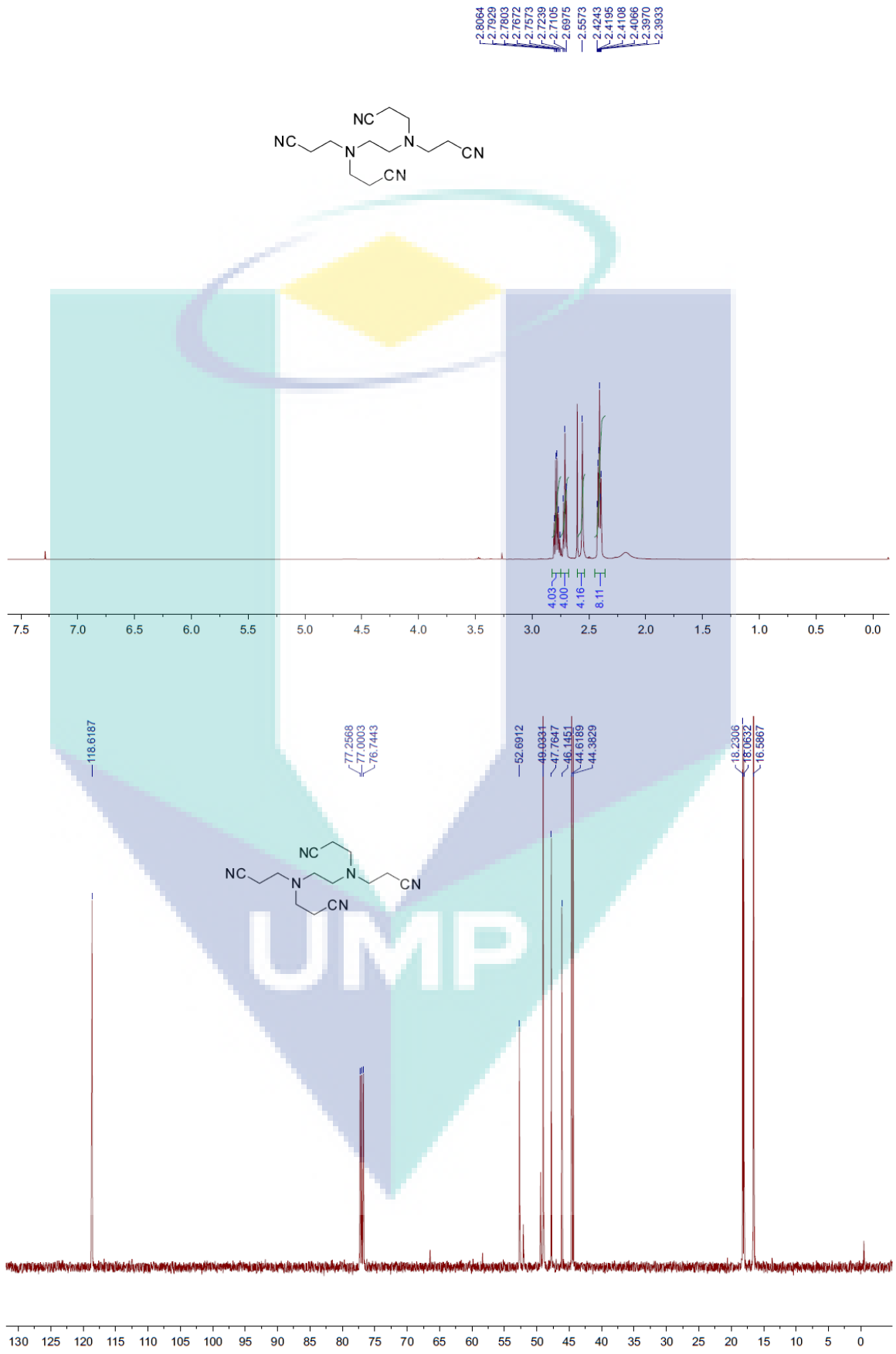


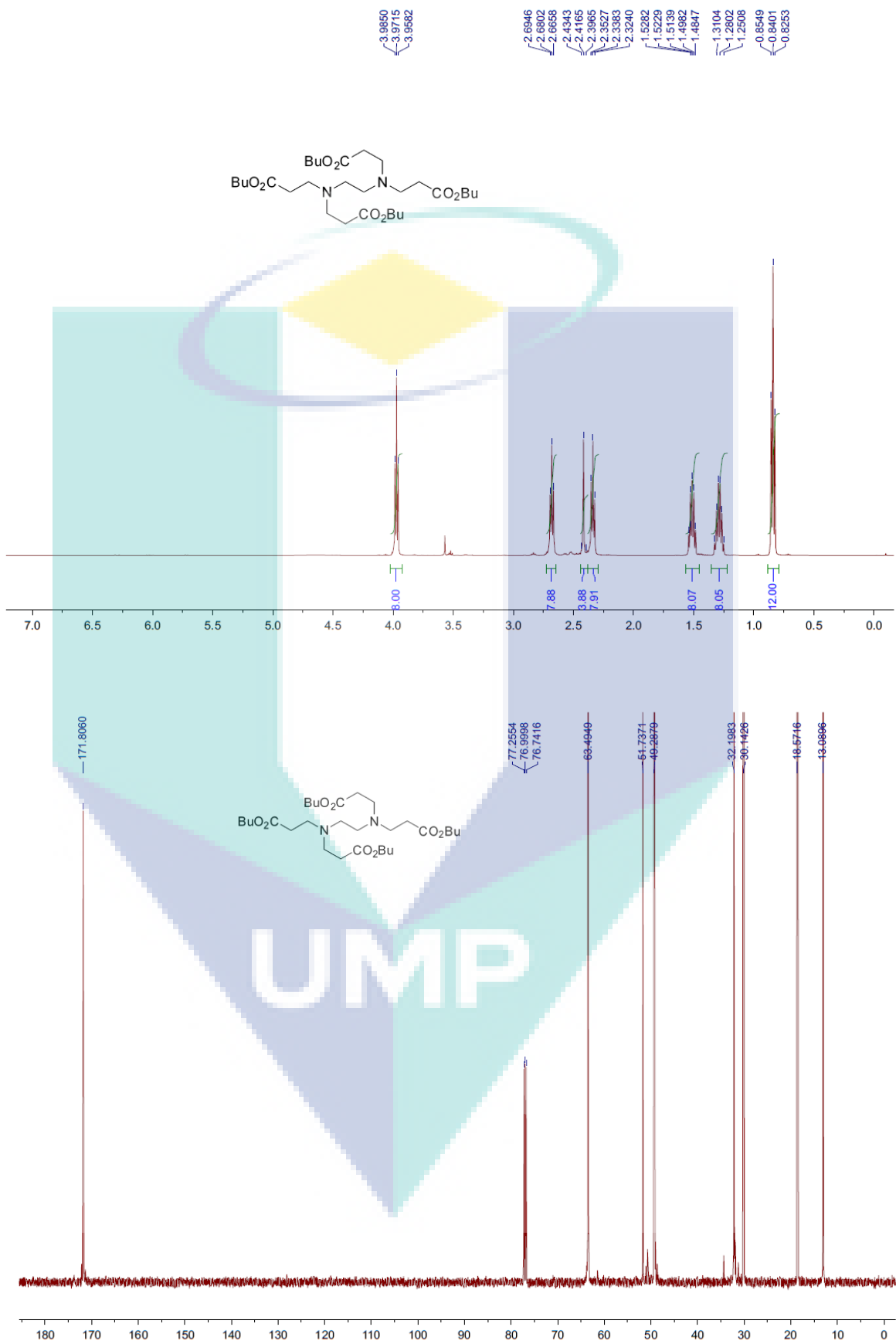
UMP

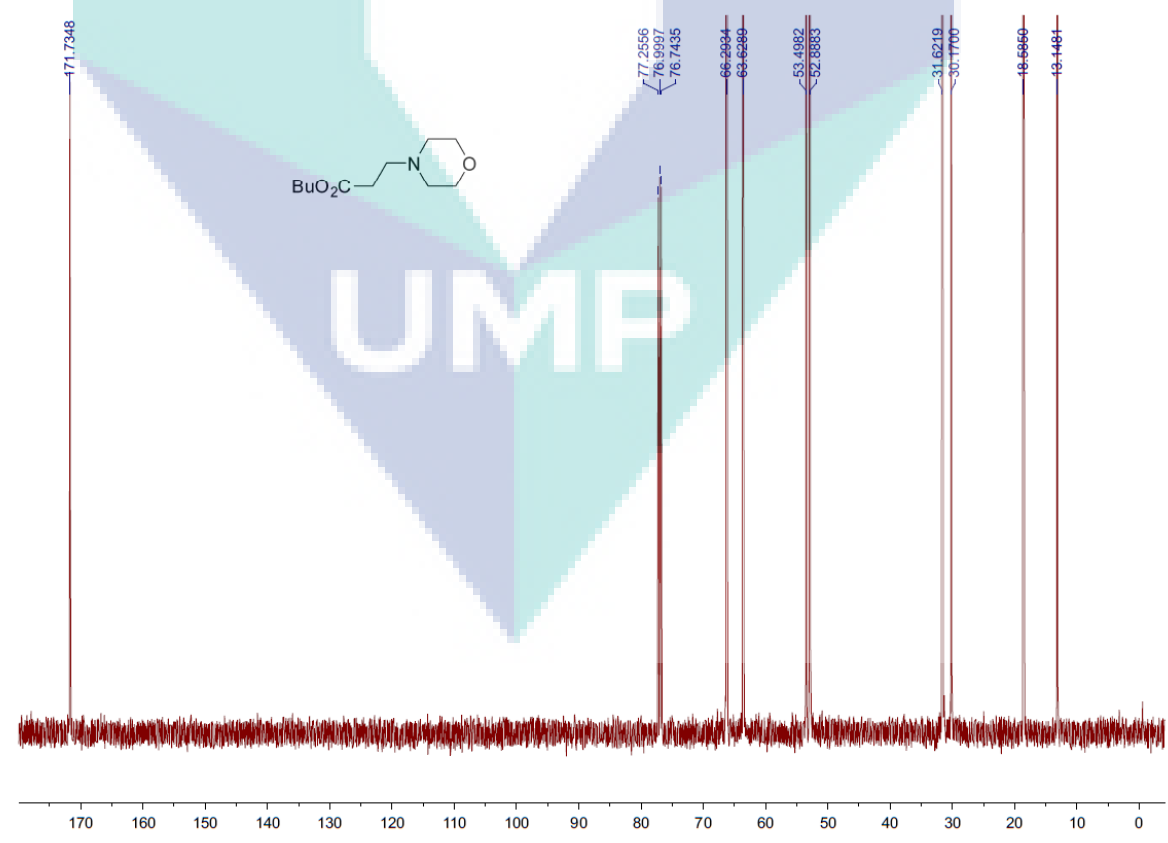
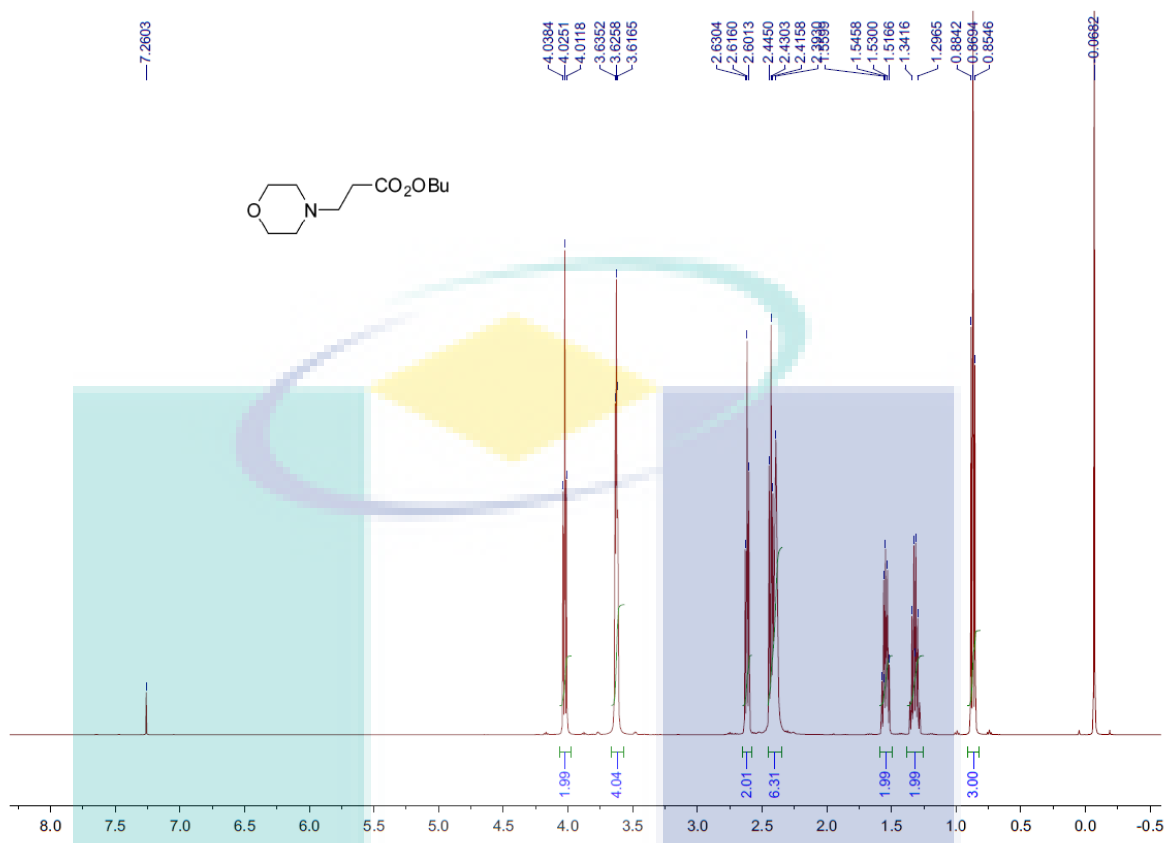




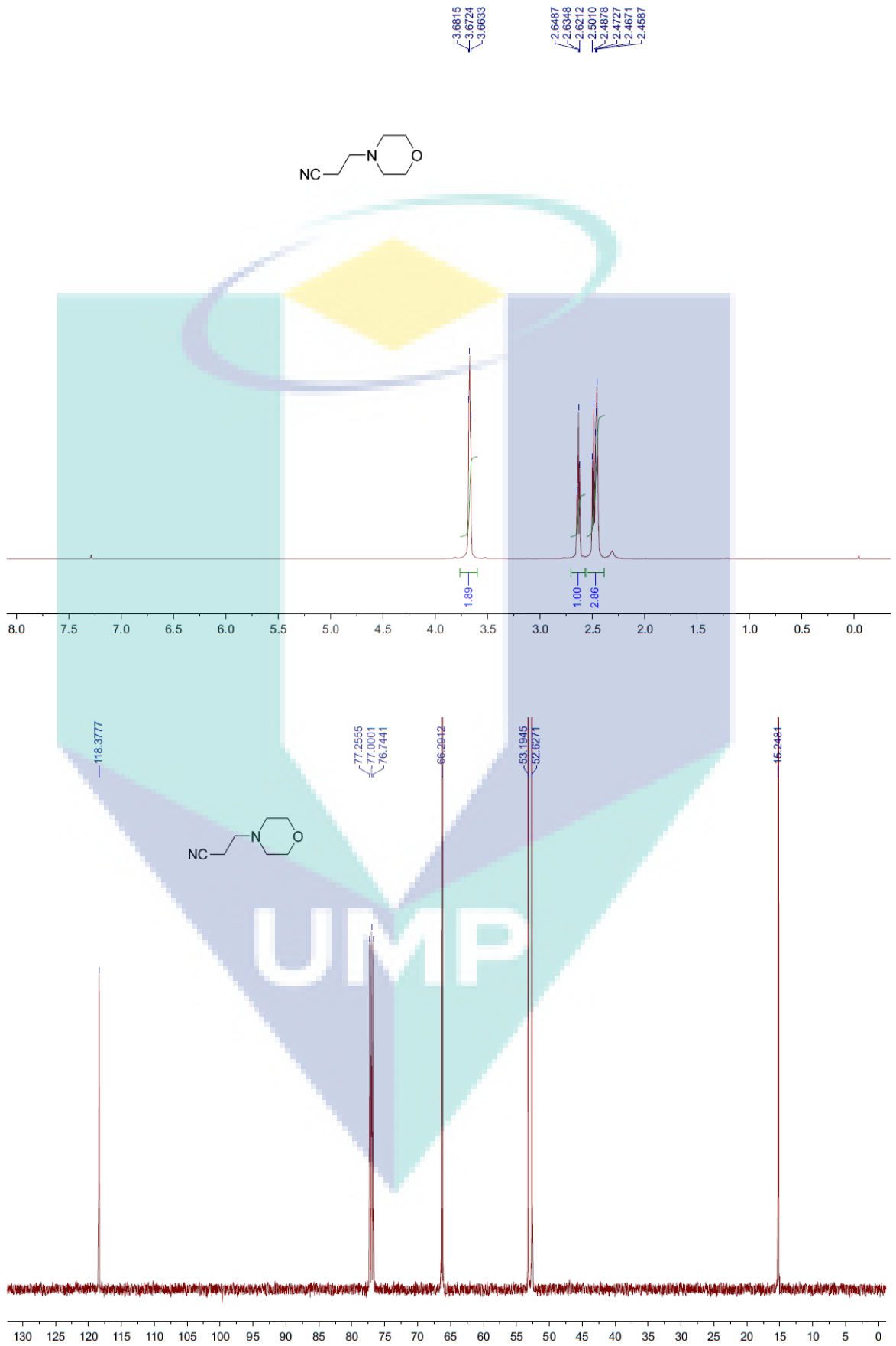


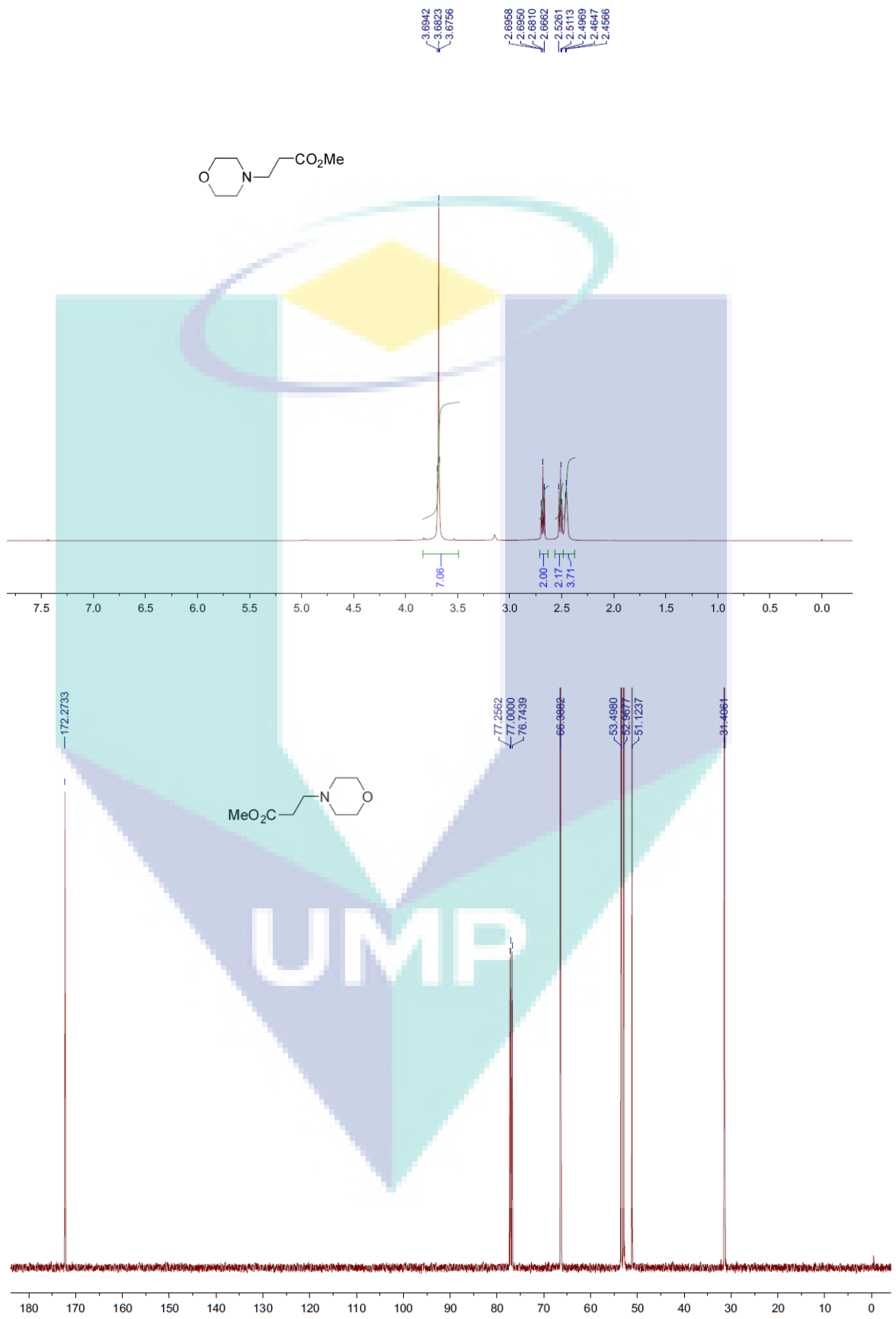


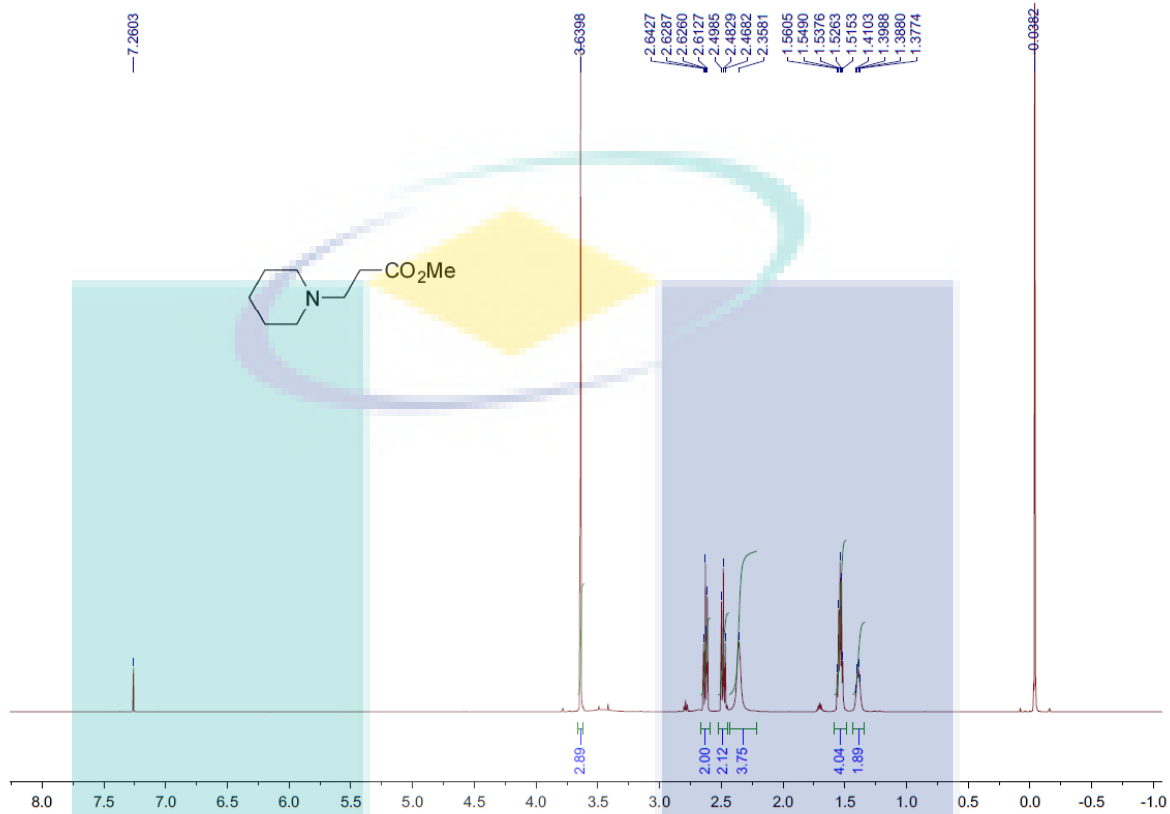




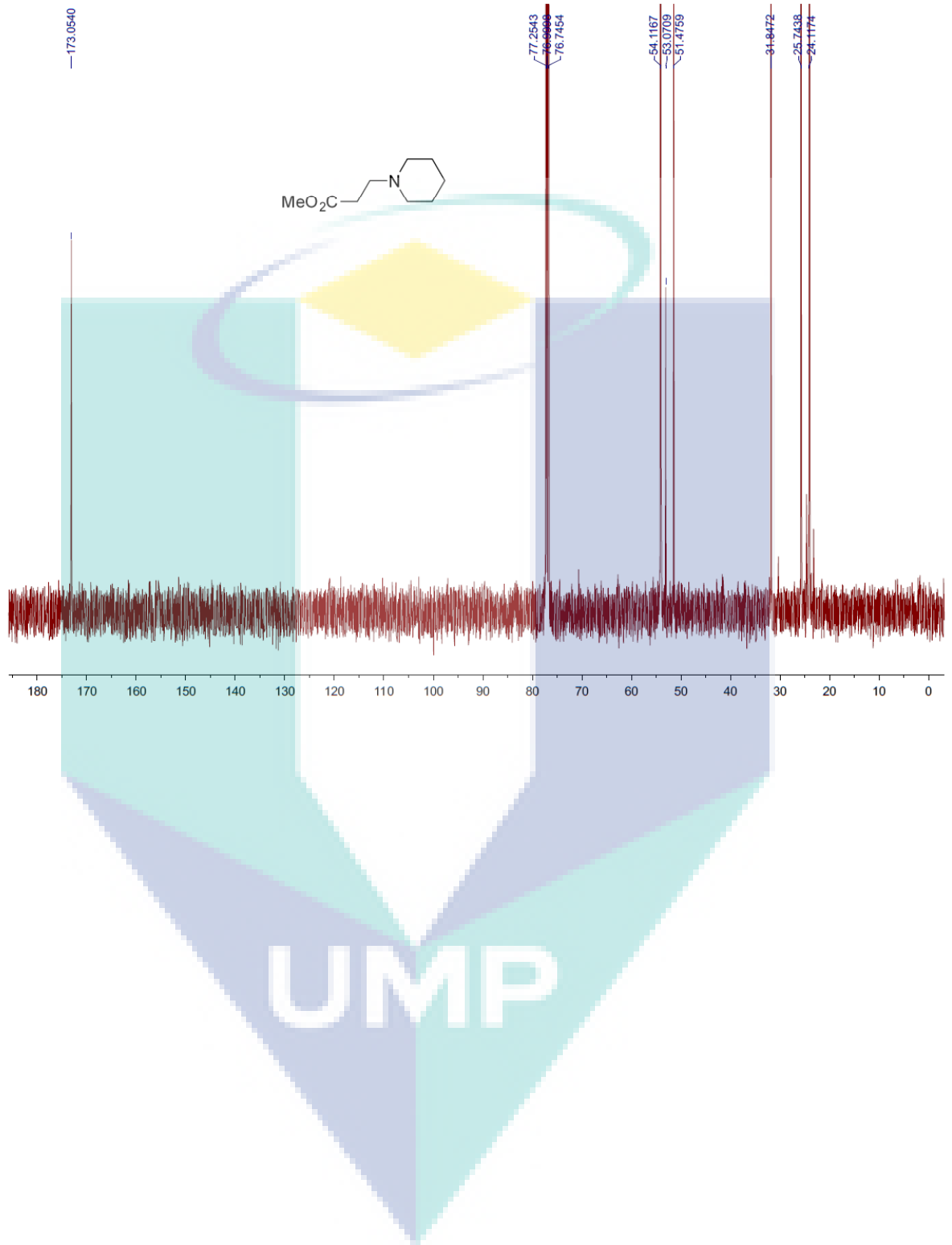


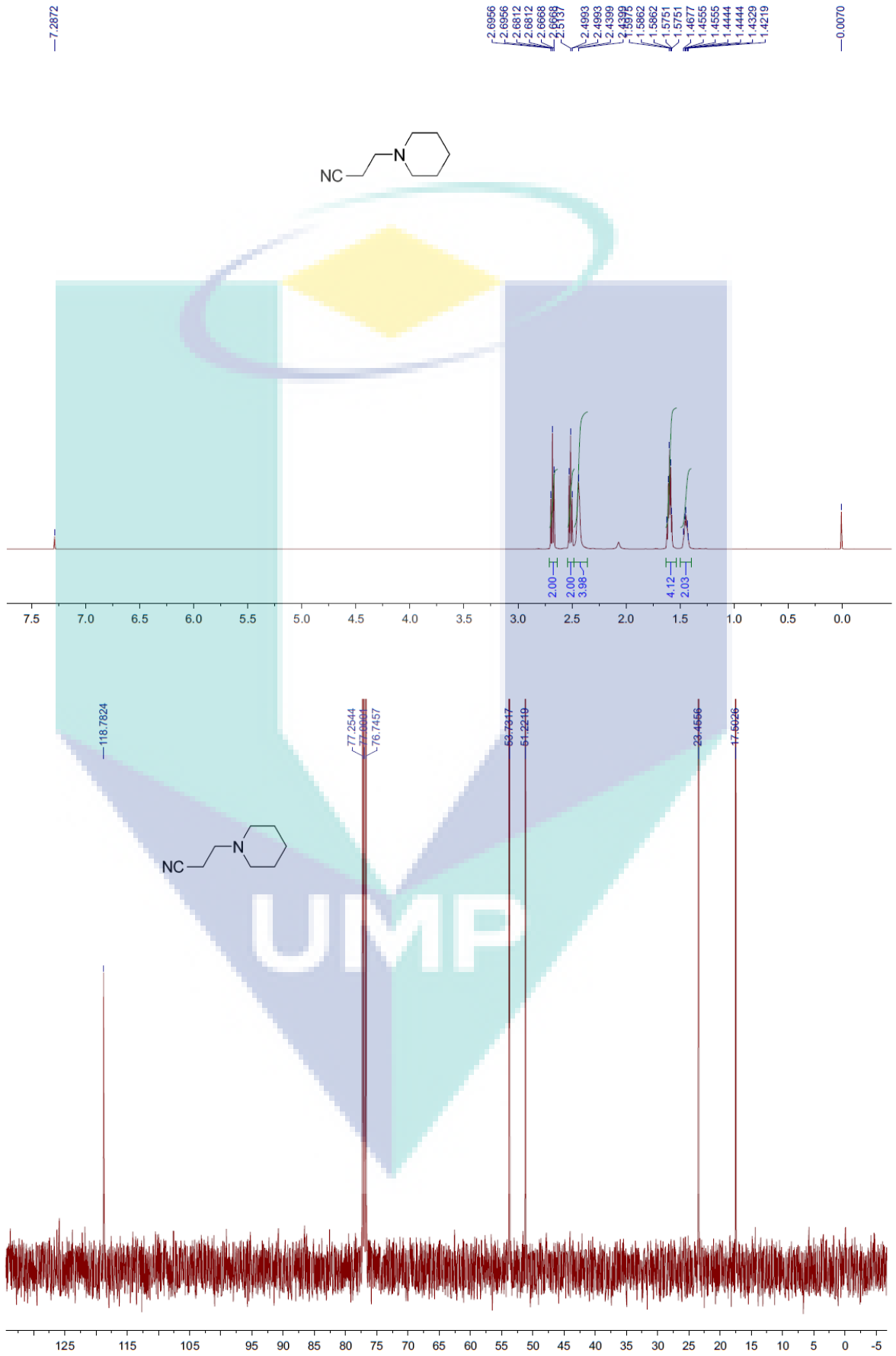


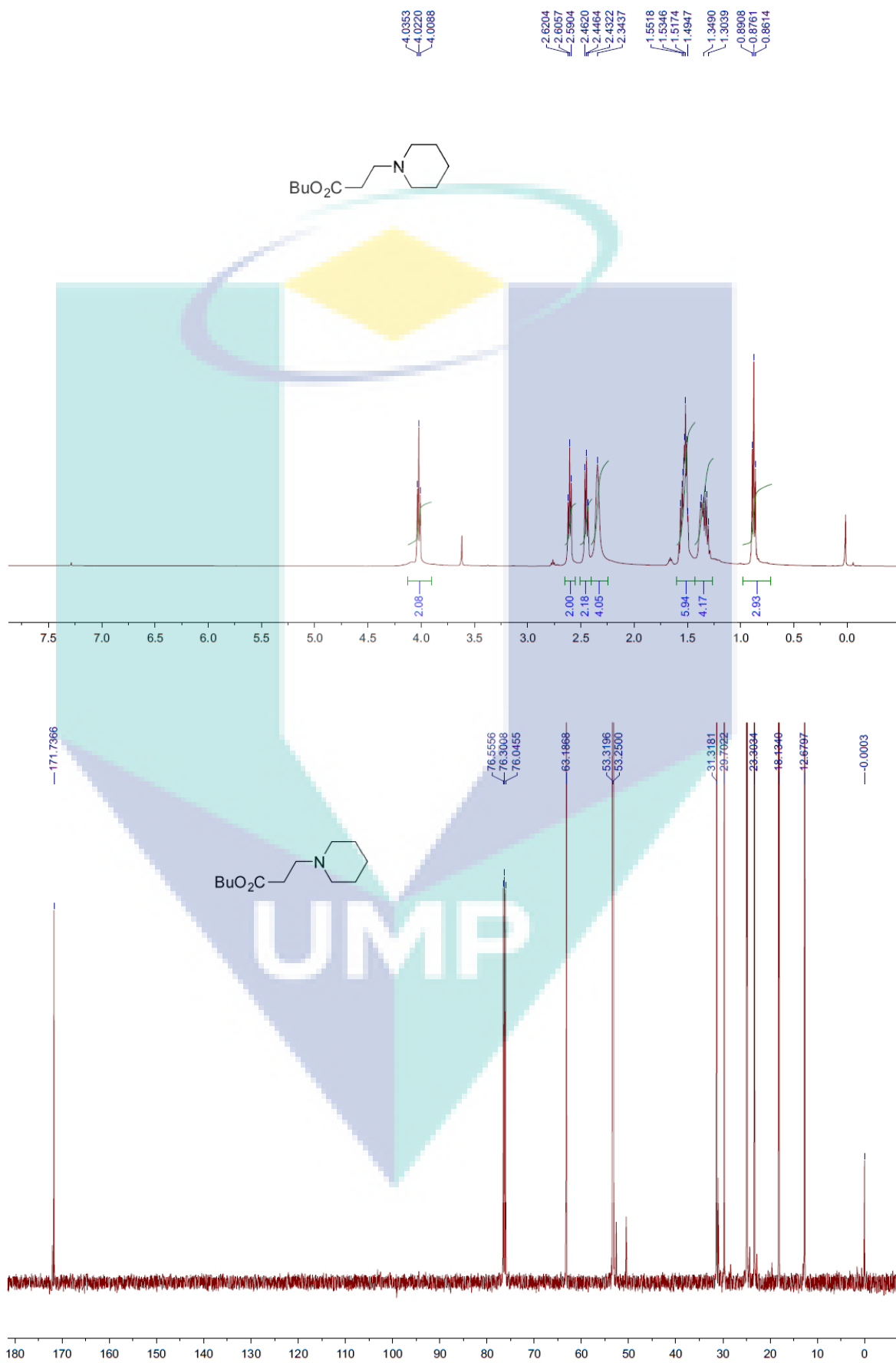




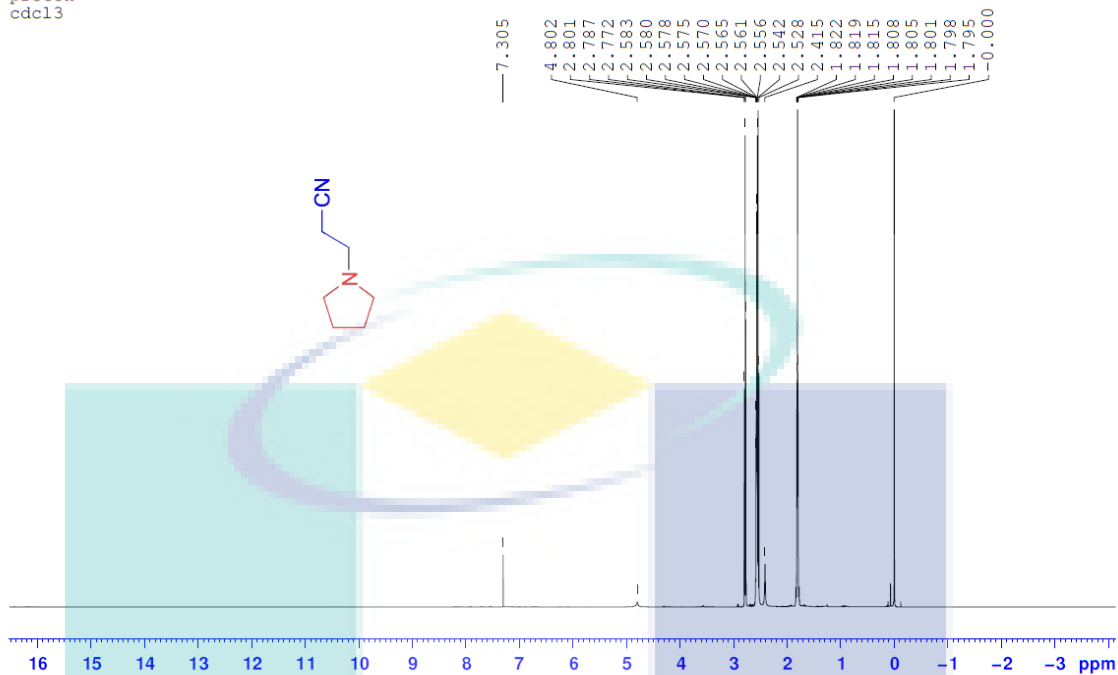
UMP



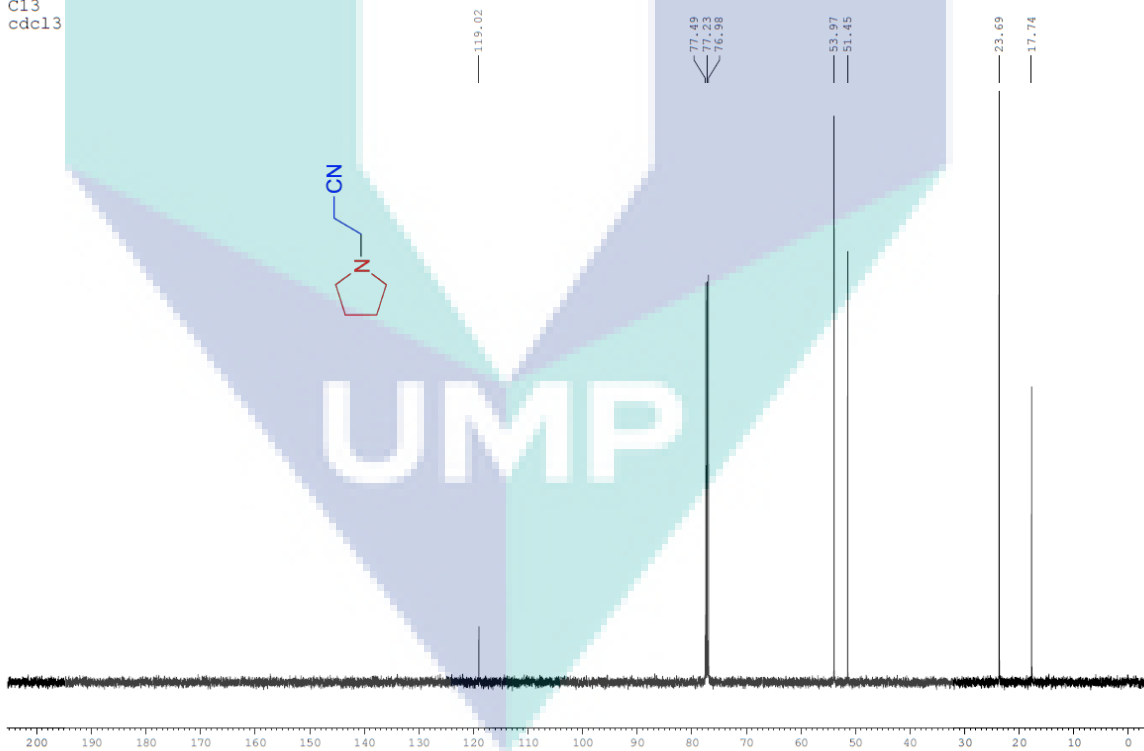


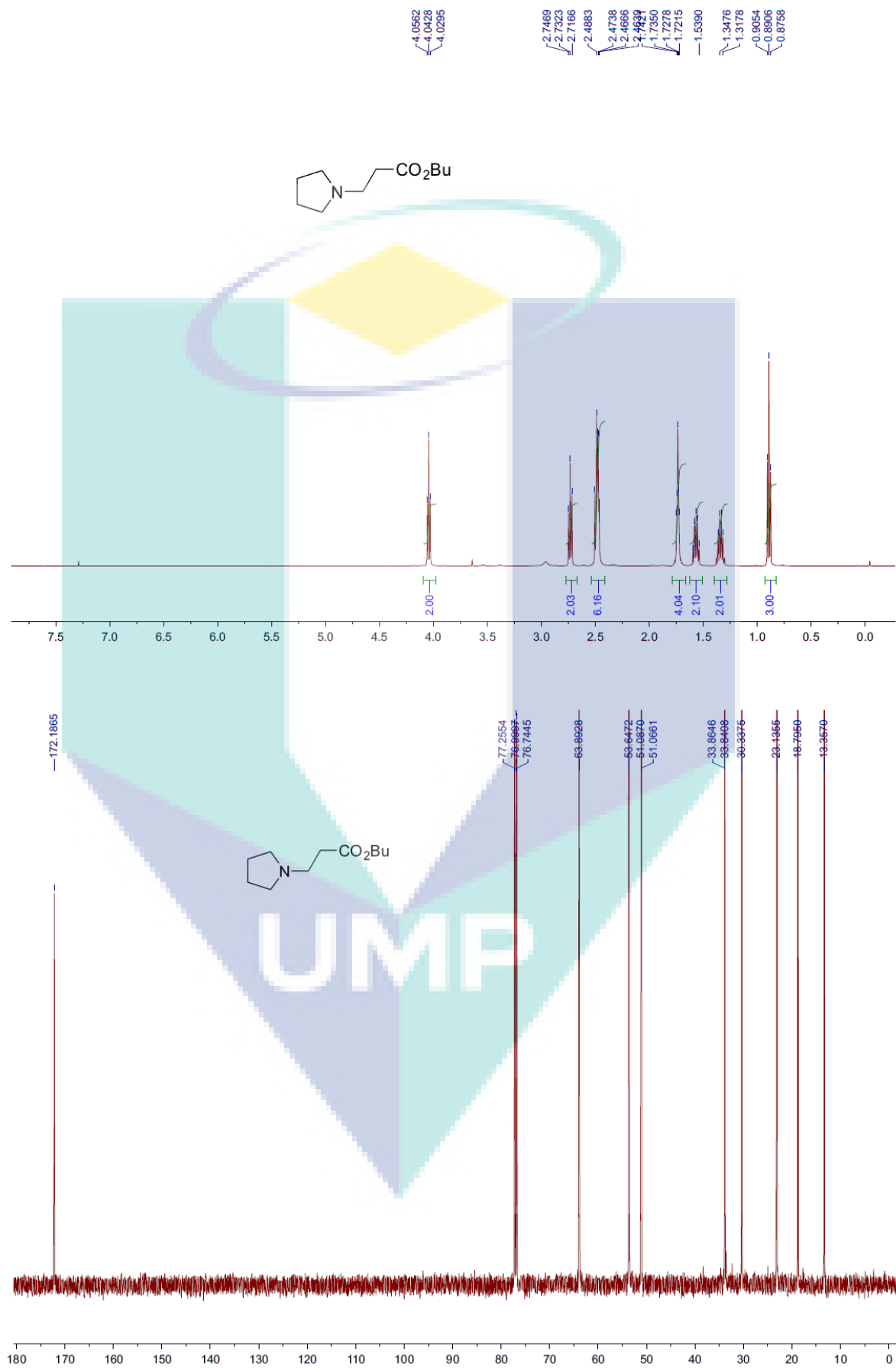


sample 20  
proton  
cdcl3



sample 20  
C13  
cdcl3

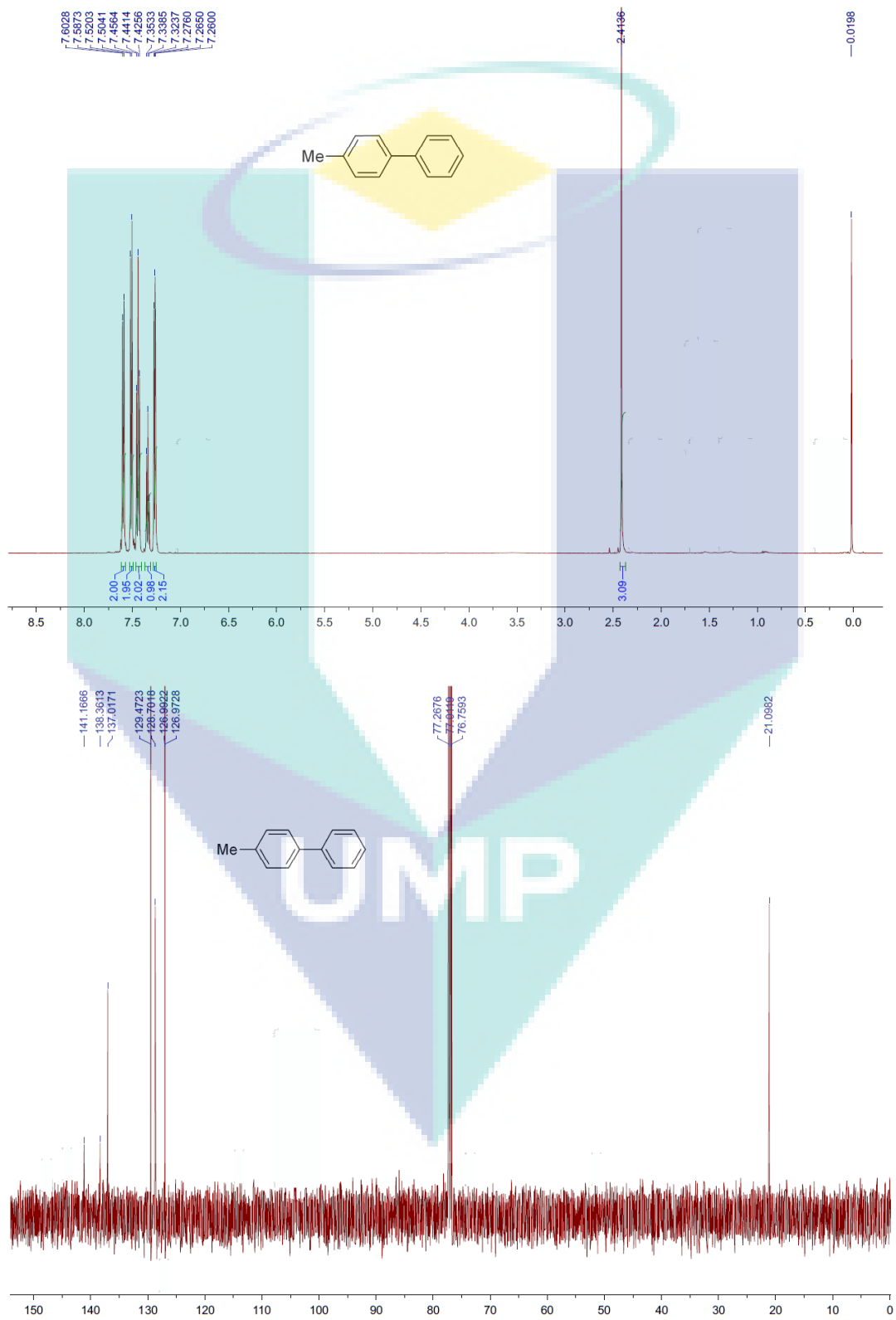


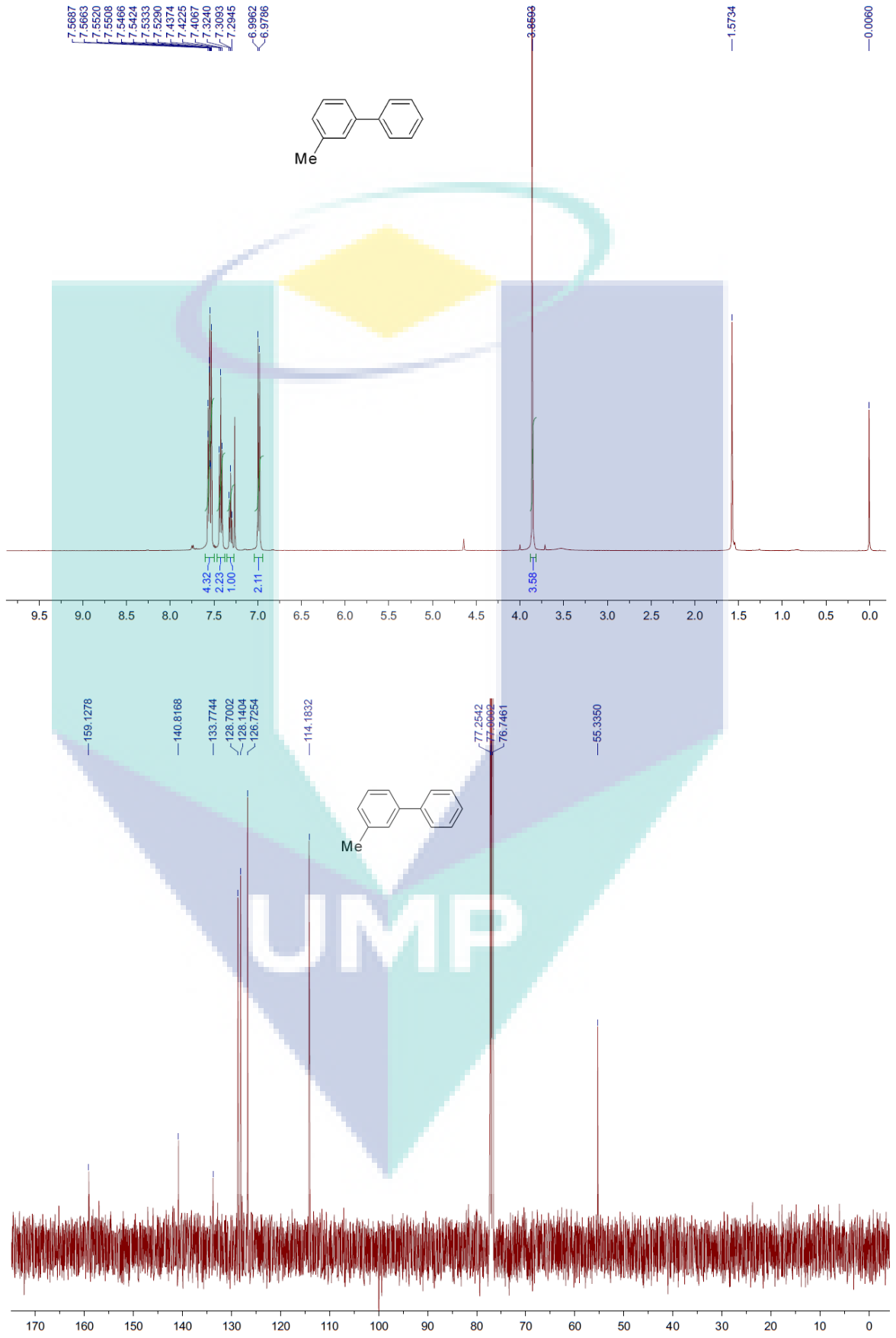


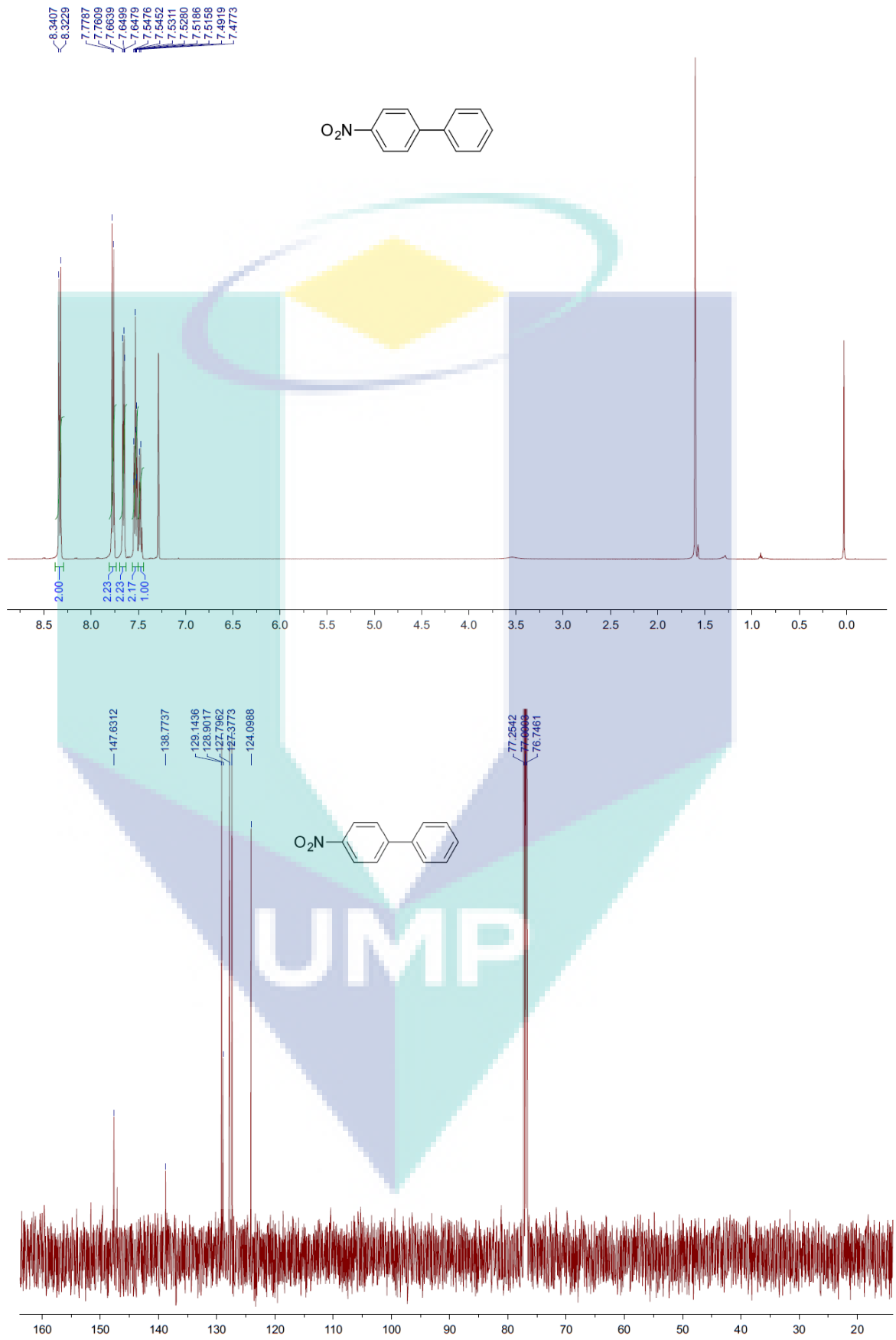


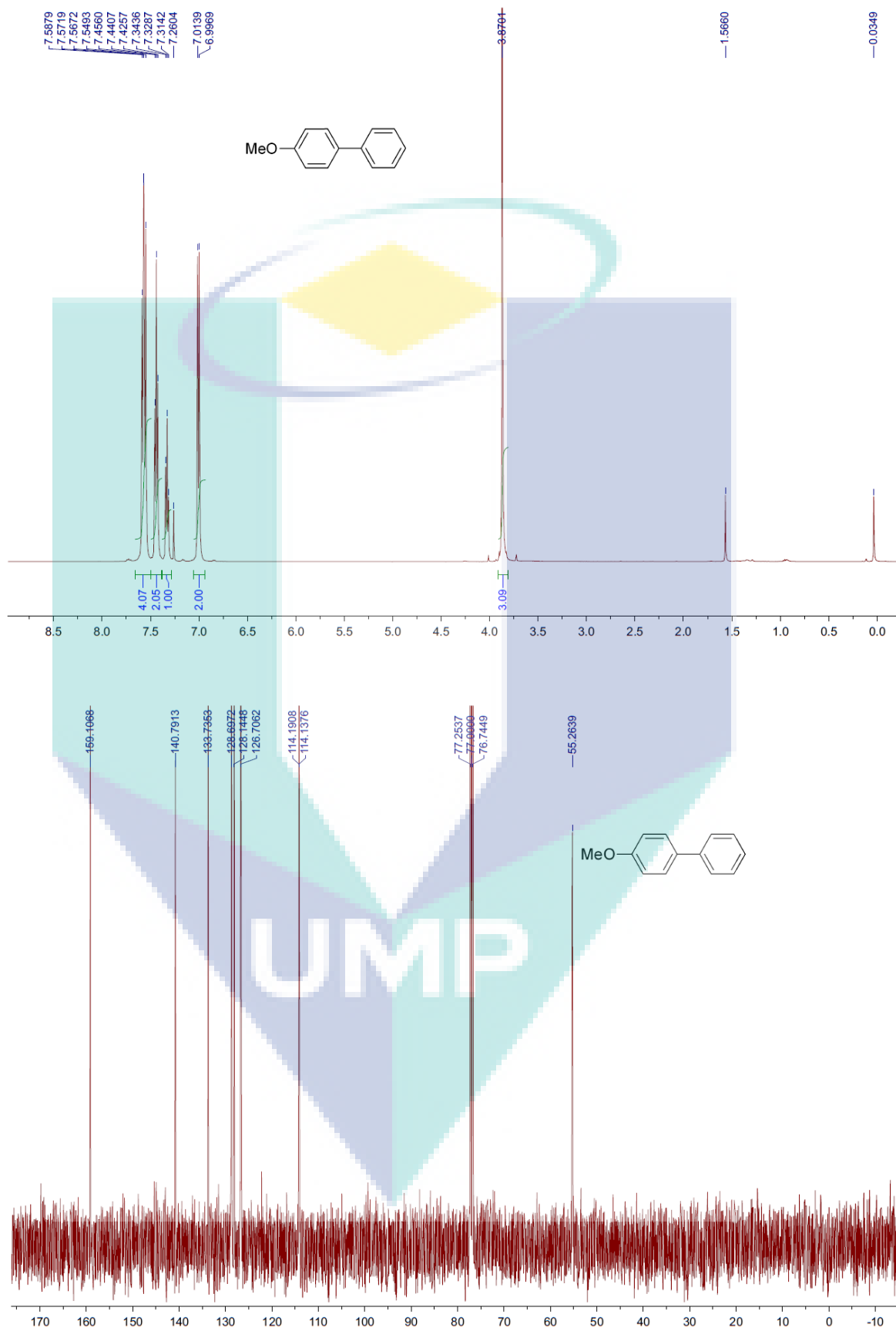
## Appendix A2

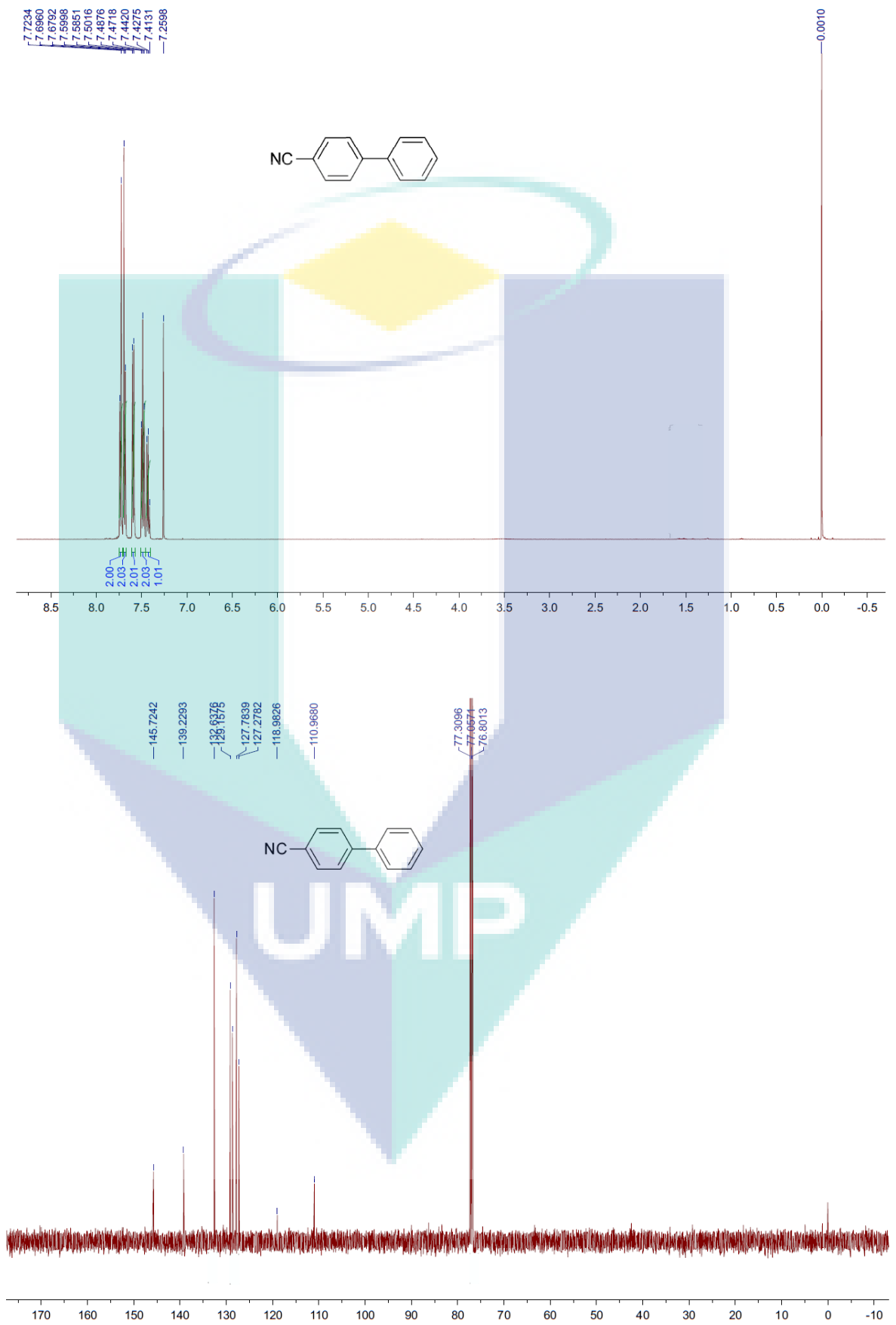
### $^1\text{H}$ and $^{13}\text{C}$ NMR results for Suzuki-Miyaura Products

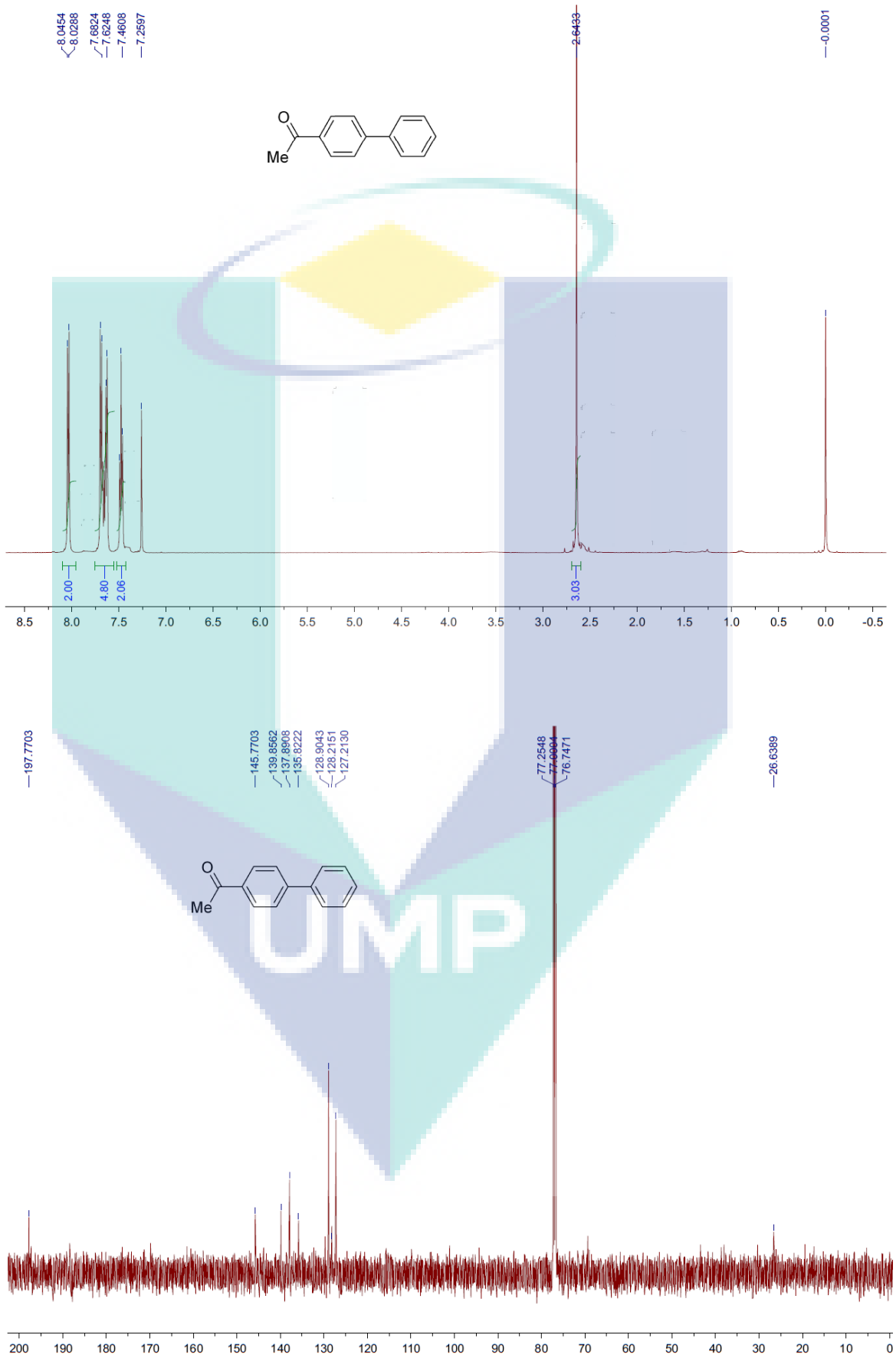


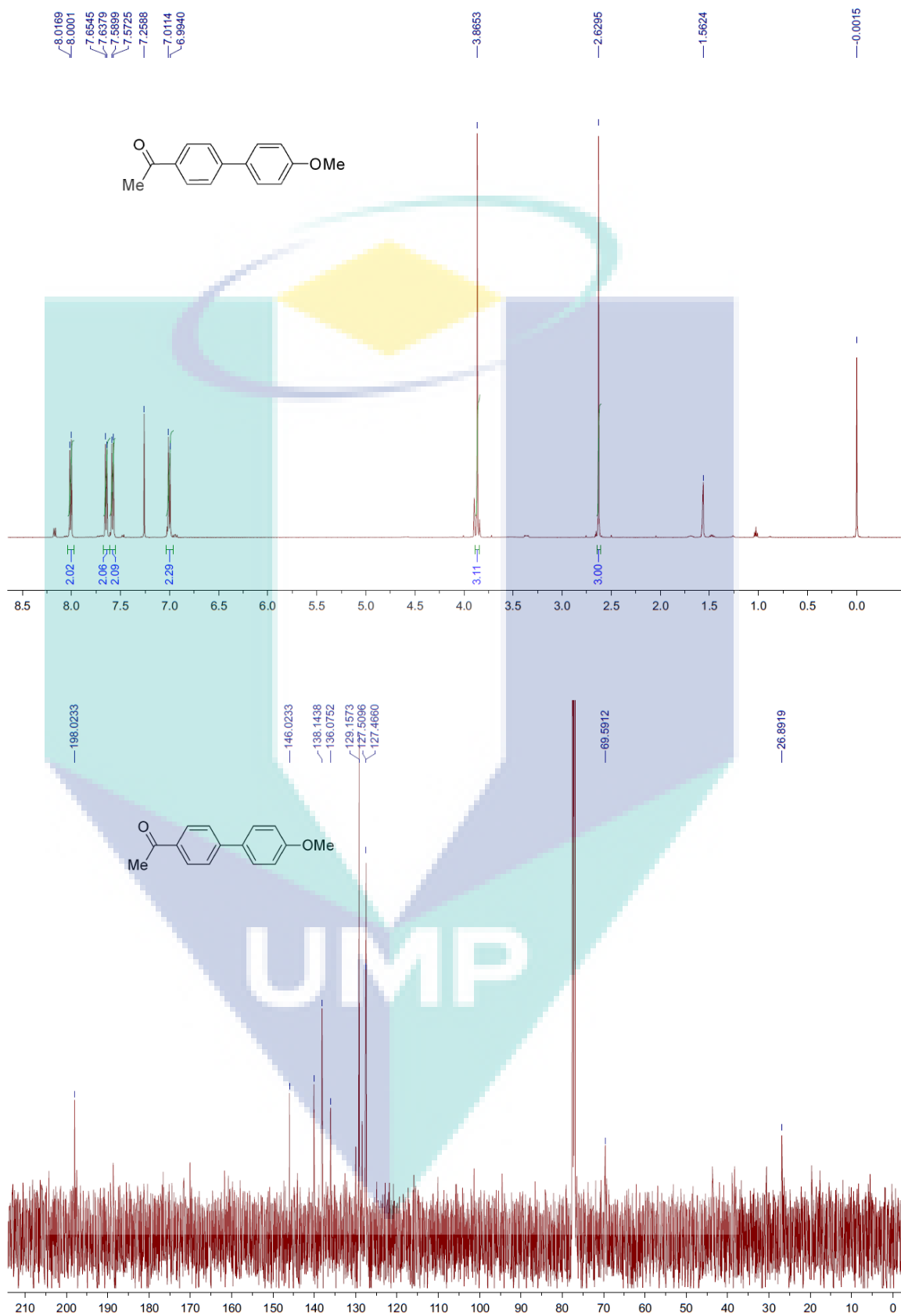


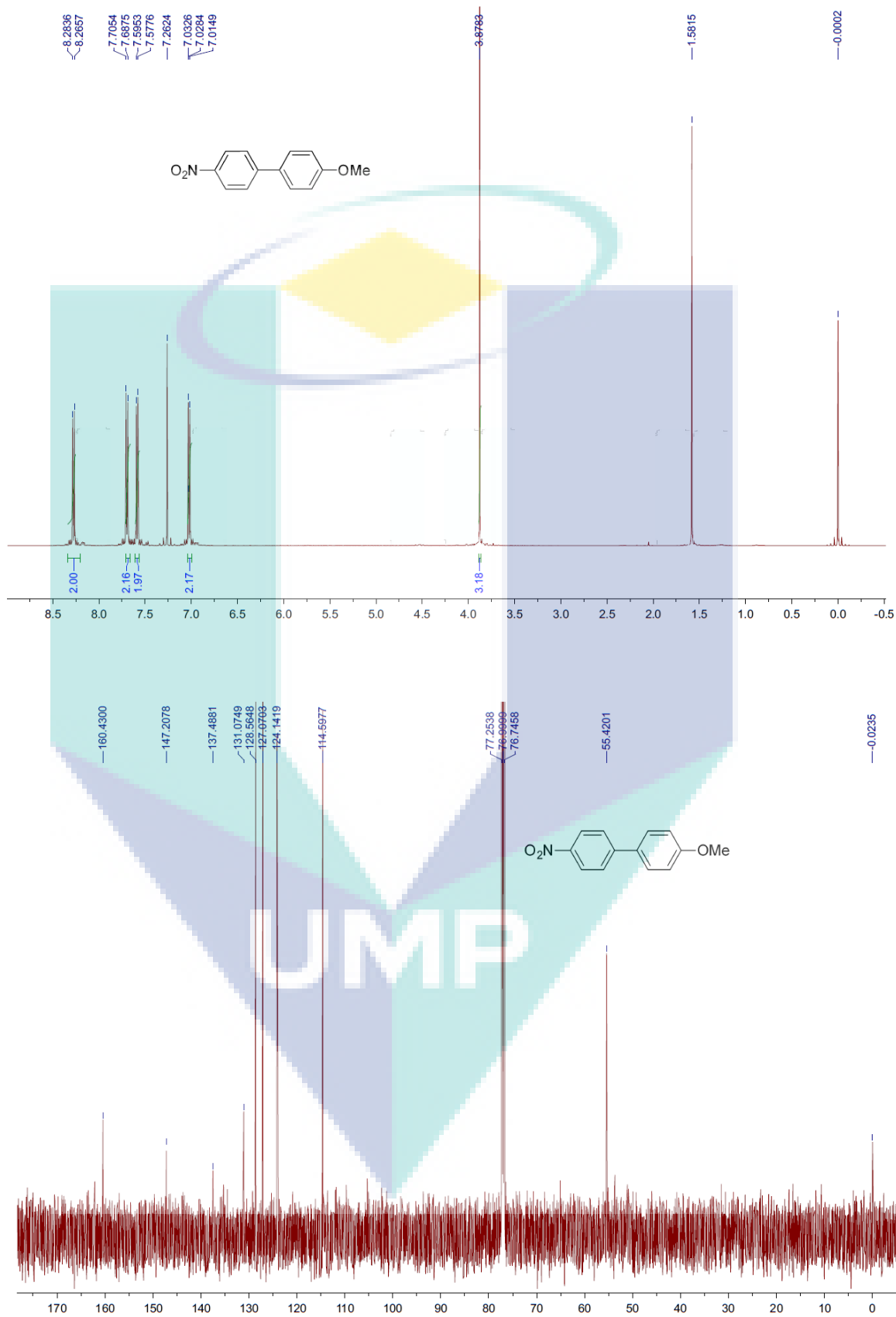




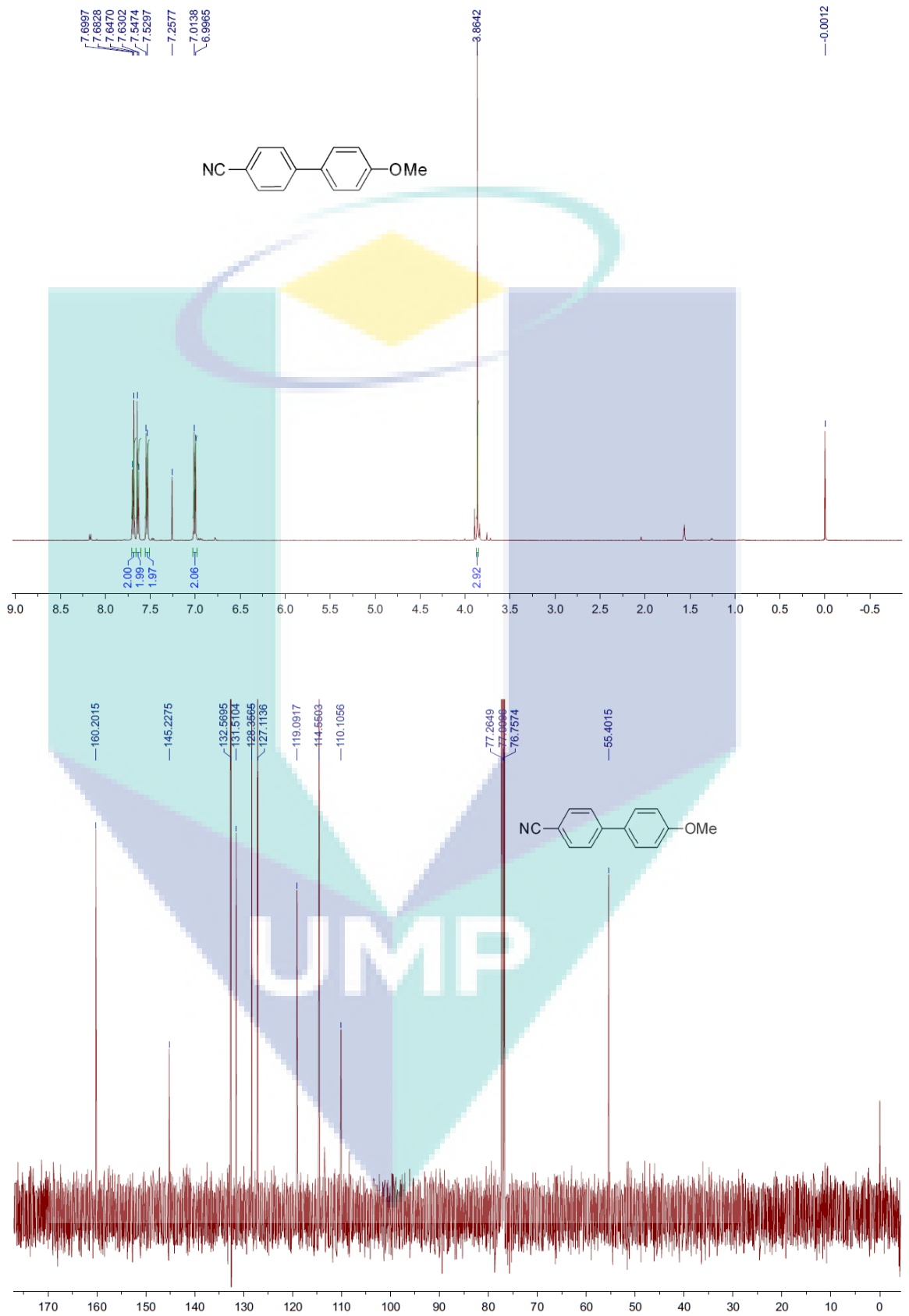












## PUBLICATIONS

- Sarkar, S. M., Sultana, T., Biswas, T. K., Rahman, M. L., & Yusoff, M. M. (2016). Waste corn-cob cellulose supported bio-heterogeneous copper nanoparticles for aza-Michael reactions. *New Journal of Chemistry*, 40(1), 497-502.
- Sultana, T., Mandal, B. H., Rahman, M. L., & Sarkar, S. M. (2016). Bio-waste corn-cob cellulose supported poly(amidoxime) palladium nanoparticles for suzuki-miyaura cross-coupling reactions. *Chemistry Select*, 1, 4108 – 4112.

